PROTEIN SENSORS FOR MEMBRANE CHOLESTEROL

APPROVED BY SUPERVISORY COMMITTEE

_____

Arun Radhakrishnan, Ph.D.

_____

Russell DeBose-Boyd, Ph.D.

_____

Daniel Siegwart, PhD.

_____

Daniel Rosenbaum, Ph.D.

DEDICATION

This work is dedicated to David Turner.

You are a man of true character.

PROTEIN SENSORS FOR MEMBRANE CHOLESTEROL

by

AUSTIN TYLER GAY

DISSERTATION

Presented to the Faculty of the Graduate School of Biomedical Sciences

The University of Texas Southwestern Medical Center at Dallas

In Partial Fulfillment of the Requirements

For the Degree of

DOCTOR OF PHILOSOPHY

The University of Texas Southwestern Medical Center at Dallas

Dallas, Texas

May, 2016

PROTEIN SENSORS FOR MEMBRANE CHOLESTEROL

AUSTIN TYLER GAY, Ph.D.

The University of Texas Southwestern Medical Center at Dallas, 2016

ARUN RADHAKRISHNAN, Ph.D.

The cholesterol content of animal cells is maintained within narrow limits. This regulation applies not only to the overall cholesterol level in the cell, but also to the concentration of cholesterol in the membrane of each organelle. Maintaining the proper level and distribution of cholesterol, which is virtually insoluble, requires an efficient network of proteins that can measure cholesterol levels in membranes and transport cholesterol. Despite much interest, our understanding of how cholesterol sensors accurately measure cholesterol levels in membranes and how cholesterol is transferred between membranes remains limited. A recently discovered class of cholesterol-sensing bacterial toxins share the same specificity and sensitivity for cholesterol as mammalian cholesterol sensors. Using two members of this large family, perfringolysin O and anthrolysin O, I showed that sigmoidal responses of cholesterol sensors can

arise primarily from membrane effects due to sharp changes in the chemical activity of cholesterol. The nonlinear response emerges because interactions between bilayer lipids control cholesterol accessibility to sensors in a threshold-like fashion. Around these thresholds, the affinity of sensors for membrane cholesterol varies by >100-fold, generating highly cooperative lipid-dependent responses independently of protein-protein interactions. I then used supported bilayer technology and fluorescently labeled anthrolysin O to devise an ultrasensitive method to measure protein-mediated cholesterol transport between fluid membranes. Using this method, I showed that human Niemann Pick Type C2 disease protein and yeast oxysterol-binding protein homolog transport cholesterol between membranes. I also showed that two point mutations in Niemann Pick Type C2 disease protein that cause cholesterol storage disease also render the protein defective in transporting cholesterol between membranes. I then characterized the lipid binding properties of a fungal toxin ostreolysin A, and showed that it binds membranes only when they contain cholesterol and sphingomyelin. I developed fluorescently labeled ostreolysin A as a tool to probe for sphingomyelin-cholesterol complexes in the plasma membranes of mammalian cells. In ongoing work, I am screening for compounds that bind anthrolysin O, as candidates for inhibitors of the human cholesterol sensor, Scap. The tools that I have developed will improve our understanding of cholesterol regulation in animal cells.

AKNOWLEDGEMENTS

Here, I wish to thank the people who have helped me on my path towards completing this body of work. To my mom and dad, thank you for sacrificing so much to help get me where I am today. We've all done a lot of growing over the last few years, and I'm so grateful for your support. Laiken, thank you for knocking down my block castles when we were kids so that I had to rebuild them; repetition is an important part of learning.

I've had amazing teachers throughout the years who were not only wonderful educators, but great friends. I specifically wish to acknowledge Lee Ferguson and Dr. Dena Leggett, my high school biology and chemistry teachers. Lee, thank you for teaching with such passion, and for constantly championing science education. I know I'm not the first person you inspired, and I'm far from the last. Dena, Allen High should count its lucky stars every day that you're teaching there. I was a bright kid growing up, but you showed me what I was truly capable of through work and focus.

Mary Hestand, thank you for believing in me and helping me find my first research position. More than that, thank you for being a continual source of support as I've gone from being an intern to now finishing my PhD. Dr. Michael Brown, you showed me that even a Nobel laureate can laugh about a project; finding the humor in a problem requires great understanding. Dr. Joseph Goldstein, thank you for demonstrating that science can also be art. Ceci n'est pas une pipe; images are treacherous. Nancy Street, thank you everything you do for me and all the other students on campus; you're an essential piece of UT Southwestern and do so much good every day. Melanie Cobb, I want to thank you for running our NIH Cell and Molecular Biology

training grant. More than that though, thank you for taking science seriously enough to be rigorous, but not so seriously that it stops being a joyful endeavor.

Dr. Brown once told me that the second most important thing for a scientist is developing hands you can trust to give good experimental results (the most important thing is picking the right spouse). Bray Denard, we only worked together for one short summer, but I somehow learned more about proper lab technique, rigor and experimental design from you than anyone. That summer after my junior year, I was vacillating between different options of what to do after graduation. I remember a specific conversation we had at your bench that made me decide to go to graduate school. I would not be the researcher I am today without your good advice.

The help of several talented technicians was absolutely critical to this work. Daphne Rye, not only do you have the best hands on the floor, not only do you brighten everyone's day, you've done it for the last quarter of a century! I'm lucky and humbled to have worked alongside you. Donna Frias, I'm constantly amazed by how quickly you pick things up and how many of my mistakes you catch before they become problems. I want to thank Cameron Fazeli, Linda Donnelly, Lisa Beatty, Muleya Kapaale, Ijeoma Dukes, Lucie Batte for additional technical work.

I also want to thank the many students and postdoctoral fellows who were always ready to provide help, advice or reagents. Thank you Dr. Feiran Lu, Dr. Donald Anderson, Dr. Akash Das, Dr. Matthew Mitsche, Shreya Endapally, Brittany Johnson, Sarah Bayless, Rima Shah-Chakrabarti, and the entire Department of Molecular Genetics.

My dissertation committee has been a valuable resource throughout this process. Thank you to Dr. Russell DeBose-Boyd, Dr. Daniel Rosenbaum and Dr. Daniel Siegwart. I'd also like to acknowledge Dr. Daniel Siegwart and his lab members, Hu Xiong and Kejin Zhou, for their

contributions to our continued collaborative project. To my mentor, Dr. Arun Radhakrishnan, thank you for your continued advice and mentorship. We first met in 2008 when I was an undergraduate intern and you were a postdoctoral fellow; we've both learned a lot in the last eight years.

Katherine Blakely, thank you for your patience and support throughout my time in college and graduate school. Soon, it will be November.

TABLE OF CONTENTS

PRIOR PUBLICATIONS

Gay A, Rye D, Radhakrishnan A. (2015). Switch-like responses of two cholesterol sensors do not require protein oligomerization in membranes. *Biophys J*. 108(6), 1459-69

Denard B, Seemann J, Chen Q, **Gay A**, Huang H, Chen Y, Ye J. (2011). The membrane-bound transcription factor CREB3L1 is activated in response to virus infection to inhibit proliferation of virus-infected cells. *Cell Host Microbe*. 10(1), 65-74

LIST OF FIGURES

INTRODUCTION

CHAPTER 1

CHAPTER 2

CHAPTER 3

CONCLUSION AND PERSPECTIVE

LIST OF ABBREVIATIONS

ACAT, acyl coenzyme A:cholesterol acyltransferace

ALO, anthrolysin O

BSA, bovine serum albumin

CDC, cholesterol-dependant cytolysin

CHO, Chinese hamster ovary

COPII, coat protein complex II

D4, domain 4

DMSO, dimethyl sulfoxide

DOPC, 1,2-dioleoyl-sn-glycero-3-phosphocholine

DPhyPC, 1,2-diphytanoyl-sn-glycero-3-phosphocholine

DTT, dithiothreitol

ER, endoplasmic reticulum

FCS, fetal calf serum

FL, full-length

HMG CoA, 3-hydroxy-3-methylglutarate coenzyme A

HPCD, hydroxypropyl beta-cyclodextrin

LDL, low density lipoprotein

LLO, listeriolysin O

LPDS, lipoprotein-deficient serum

LPL, lipoprotein lipase

MWCO, molecular weight cut-off

Ni-NTA, nickel-nitrilotiacetic acid

NPC, Niemann-Pick Type C disease

NPC1, Niemann-Pick Type C1 disease protein

NPC2, Niemann-Pick Type C2 disease protein

OlyA, ostreolysin

ORP, oxysterol-binding protein related protein

OSBP, oxysterol-binding protein

Osh4, oxysterol-binding protein homolog

PFO, perfringolysin O

PM, plasma membrane

S1P, site-1 protease

S2P, site-2 protease

SCAP, SREBP cleavage-activating protein

SDS-PAGE, sodium dodecyl sulfate polyacrylamide gel electrophoresis

SM, sphingomyelin

SMase, sphingomyelinase

SREBP, sterol regulatory element-binding protein

SREBP-2, sterol regulatory element-binding protein 2

TCEP, tris(2-carboxyethyl)phosphine hydrochloride

TR-DHPE, Texas Red 1,2-dihexadecanoyl-sn-glycero-3-phosphoethanolamine

VLDL, very low-density lipoprotein

WT, wild type

INTRODUCTION

In 1933, Rudolf Schoenheimer and Fritz Breusch found that mice fed a cholesterol-free diet synthesize their own cholesterol, while mice fed sufficient cholesterol do not [132]. This simple observation revealed two important features of cholesterol homeostasis; mammals are able to synthesize cholesterol, and this synthesis rate is subject to negative feedback [14]. In fact, this was possibly the first published example of end-product feedback inhibition in biology [48]. Further studies in other organisms revealed that cholesterol synthesis is a heavily regulated and conserved process across species [6, 50, 83]. Any process subject to such careful control begs the obvious questions, "Why?" and "How?"

Why cholesterol is regulated became clear as researchers probed the physiological roles of cholesterol, and discovered the damaging results of an animal having too much, too little, or poorly-distributed cholesterol. One of the most critical roles for cholesterol is as a component of cellular membranes, where it serves to maintain membrane fluidity, integrity, and selective permeability [23, 97, 157]. Cholesterol is also an important precursor molecule in other synthesis pathways, including steroid hormones and digestive bile acids [55, 129]. Peripheral membrane proteins can be anchored to bilayers by covalent attachment to hydrophobic lipid molecules, a modification that is often essential to the protein's function [18, 139]. Sometimes, this lipid molecule is cholesterol, and perturbations of cholesterol homeostasis can disrupt the function of cholesterol-anchored proteins [71, 114, 117, 169]. Transmembrane proteins are often sensitive to membrane cholesterol, which affects protein folding and organization into distinct membrane microdomains [146]. Perturbations of cholesterol regulation can lead to aberrant protein folding, as seen in amyloidogenic diseases such as Alzheimer's disease and prion-related disorders [54,

112]. Membrane cholesterol also plays an important role in membrane modifications during endocytosis, both for normal cellular function and pathogen infection [53, 57, 91]. Regulating the distribution of cholesterol is also critical. Why cholesterol requires precise regulation is perhaps most clearly illustrated by the cause of death for one-quarter of all adults, heart disease [1, 58]. When cholesterol is overproduced, poorly packaged, or ineffectively cleared from the bloodstream, arterial deposits of cholesterol are formed that eventually lead to inflammation, atherosclerosis and occluded blood flow [48, 147, 148]. All of these and more are reasons why cholesterol is regulated, and lead to the more complicated question of how.

How does a cell or organism determine how much cholesterol it needs to synthesize, and how does dietary cholesterol shut down synthesis? Schoenheimer's mice consumed dietary cholesterol, which along with triglycerides and other lipids was then solubilized into micelles in the digestive tract and absorbed through the intestinal epithelium [21, 28, 61]. Intestinal enterocytes packaged the cholesterol along with triglycerides into lipoproteins such as chylomicrons and very low-density lipoprotein (VLDL). These lipoproteins entered the lymphatic system, and then the bloodstream [52, 92, 93, 153]. The chylomicrons supplied free fatty acids derived from triglycerides to peripheral tissue after their release by lipoprotein lipase (LPL), and were eventually reduced to chylomicron remnants [24, 44, 52, 127]. The remnants were cleared from circulation by the liver through receptor-mediated endocytosis, which then esterified and repackaged residual cholesterol into additional VLDL [4, 11, 31, 137]. Like the chylomicron, VLDL also supplied free fatty acids to peripheral tissue, becoming progressively smaller and more dense to form cholesterol-rich low-density lipoprotein (LDL) [5]. While LDL is not the only means of delivering cholesterol to peripheral cells, it is arguably the most important particle in the cholesterol homeostasis pathway in terms of human disease because of

its atherosclerotic properties [46, 48, 80]. Schoenheimer's cholesterol-fed mouse now had a bloodstream rich with LDL particles, but this information needs to reach the nucleus of a peripheral cell before it can halt its own cholesterol synthesis [64].

Transmission of this information begins when LDL binds to its receptor in coated pits on the cell surface, and the entire complex is internalized through receptor-mediated endocytosis [47]. The internalized LDL is transported through the endosomal pathway to the lysosome, where LDL's cholesterol esters are hydrolyzed by lysosomal acid lipase to generate free cholesterol [32, 90]. The cell is now presented with another challenge—how to transport hydrophobic cholesterol from the aqueous interior of the lysosome, across the lysosomal membrane, and then to the rest of the cell? Insight into this step has come from studies of Niemann-Pick disease, a condition where lipids are trapped inside lysosomes [144]. Niemann-Pick disease type C (NPC) is a rare autosomal-recessive disorder that results from a mutation in the gene encoding one of two proteins, NPC1 or NPC2 [158]. NPC1 is a transmembrane protein that spans the bilayers of late endosomes and lysosomes, while NPC2 is a soluble protein enriched in lysosomes [17, 101]. These two proteins engage in a "hydrophobic handoff," working together to move cholesterol out of the lysosome [81, 161]. In normal cells, cholesterol delivered to the lysosome through LDL eventually arrives in both the plasma membrane (PM) and endoplasmic reticulum (ER) and leads to the inhibition of cholesterol synthesis by the cell, but cells harboring mutations in NPC1 or NPC2 are unable to shut down cholesterol biosynthesis even when LDL levels are high. [68, 90, 115]. Precisely how cholesterol moves from lysosomes to PM and ER remains a mystery [26, 156]. Some groups have proposed that LDL-derived cholesterol moves from the lysosome to the PM and then to the ER, others have suggested that the ER receives all incoming cholesterol before it is transported to the PM [89, 103, 156].

Regardless, LDL-derived cholesterol eventually arrives in the ER, where it binds to sterol regulatory element-binding protein cleavage activating protein (Scap), the cholesterol sensor.

Scap, a polytopic membrane protein, forms hetero-oligomers with another membrane protein called sterol regulatory element-binding proteins (SREBPs) (Figure 1) [14]. SREBPs contain a basic helix-loop-helix transcription factor domain that binds to sterol regulatory elements in the upstream promoter regions of more than 30 genes that encode for all the cholesterol biosynthetic enzymes, including 3-hydroxy-3-methylglutarate coenzyme A (HMG CoA) reductase and the LDL receptor (Figure 1B) [142, 143]. Activation of SREBP's transcriptional regulatory activity requires its cleavage by two Golgi proteases, site-1 and site-2 protease (S1P and S2P) [15, 125]. When Scap is bound to cholesterol, it adopts a conformation that allows for binding to Insig, an ER-resident membrane protein, and prevents binding to coat protein complex II (COPII) proteins, incorporation into transport vesicles, and movement to the Golgi [122, 142, 143]. As a result, SREBPs are not activated, cholesterol biosynthetic genes are not upregulated, and cholesterol synthesis declines [9]. Schoenheimer's cholesterol-fed mouse thus halts its cholesterol synthesis.

In the mice fed the cholesterol-free diet in Schoenheimer's experiments, the level of cholesterol in the ER remains low, and Scap is not bound to cholesterol [14]. This form of Scap is unable to bind Insig, but instead binds to COPII proteins, and along with SREBPs is packaged into transport vesicles and moved to the Golgi [9, 64, 149]. In the Golgi, SREBPs are sequentially cleaved by S1P and S2P, and the soluble, transcriptionally active fragment of SREBP is released to travel to the nucleus, where it upregulates cholesterol biosynthesis and LDL receptor genes (Figure 1A) [49]. As a result, Schoenheimer's cholesterol-starved mice increase their own synthesis of cholesterol.

Scap is the key protein in this regulatory network that acts as a cholesterol sensor [49]. How does Scap physically detect cholesterol in the membrane, and how does cholesterol detection lead to ER retention? Though a "sterol-sensing domain" has been proposed, the exact molecular mechanism by which Scap binds to cholesterol in the ER membrane remains poorly understood [14]. What is known is that the conformational change in Scap induced by cholesterol binding promotes its binding to another ER transmembrane protein, Insig [166]. Without sufficient Insig, Scap constitutively transports SREBP to the Golgi, where it is cleaved and activated regardless of cholesterol content in the ER [164]. Additional layers of cholesterol regulation through negative feedback exist, including sterols promoting the Insig-mediated degradation of HMG CoA reductase, and sterol binding to liver X receptor regulating cholesterol efflux regulatory protein and SREBP expression [19, 42, 100, 113, 135, 136, 152, 155].

The studies to date have provided valuable insights into cholesterol homeostasis, and have led to several important therapies to lower LDL cholesterol in humans [48]. Yet, our understanding of how Scap detects cholesterol remains limited. In cells, Scap is presumably binding to membrane cholesterol, but previous experiments testing the affinity of Scap for sterols have relied on detergent solubilization of both protein and ligand [122]. In the context of the ER membrane, what is Scap's sensitivity to cholesterol? Answering this question required monitoring the cholesterol content of the ER while at the same time assaying for the activation of SREBP-2. After much effort, a method to purify ER membranes was developed. Using this method, an experiment was carried out where the cholesterol content of cells was depleted with cyclodextrin, or enriched with VLDL treatment. The cholesterol concentration of the purified ER membranes was then measured by mass spectrometry, and the extent of SREBP-2 cleavage was assayed by Western blot. Surprisingly, the response to cholesterol was distinctly non-linear and

sigmoidal. When ER cholesterol was just above 5 mole %, SREBP-2 was completely inactivated, while it was completely activated at just below 5 mole % (Figure 2A) [118].

How is Scap able to detect cholesterol in an all-or-none manner as concentration rises only slightly? One obvious explanation would be protein-protein oligomerization leading to positive cooperativity, as seen between hemoglobin subunits [25, 95]. Indeed, Scap exists in a complex with other proteins such as SREBPs, Insig and COPII proteins, and has been shown to self-oligomerize under certain conditions, though the stoichiometry or function of such complexes in membranes of living cells is currently unknown [122, 167]. Alternatively, the accessibility of membrane cholesterol itself may be switch like, meaning that a certain threshold must be exceeded before it can be sensed by proteins [145]. Proteins such as perfringolysin O (PFO) (a soluble cholesterol-binding toxin from *Clostridium perfringens*) and even small molecules such as hydroxypropyl beta-cyclodextrin (HPCD) bind membrane cholesterol only after a certain concentration (Figure 2B) [59, 121]. How is this threshold determined? Is it the same for all sterol sensors? What can this phenomenon tell us about the organization of cholesterol within the membrane?

As described above, there are several black boxes that need to be addressed if a full understanding of cholesterol regulation is to be achieved. What is the molecular mechanism behind the switch-like sensitivity of cholesterol sensors such as Scap? How is cholesterol transported from the lysosome to the PM and ER, and in what order does it arrive? How do the other components of lipid bilayers contribute to cholesterol regulation? A primary hurdle to answering these questions is the lack of quantitative tools. Here, I present my work in developing and utilizing new methods to study cholesterol homeostasis.

FIGURE 1

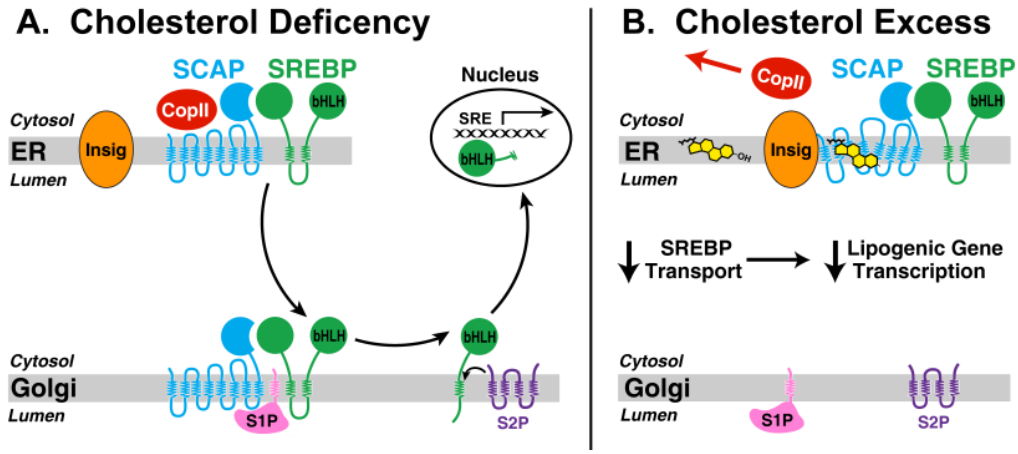

Figure 1. Model of the Scap/SREBP pathway. (A) When ER cholesterol is low, Scap binds COPII proteins. Scap and SREBP are then transported from the ER to the Golgi by COPII-coated vesicles. In the Golgi, SREBP is sequentially cleaved by two membrane-bound proteases, site-1 and site-2 protease, releasing a soluble, transcriptionally active fragment of SREBP-2. This active fragment travels to the nucleus, where it transcriptionally activates genes involved in lipid synthesis and uptake of lipoproteins. (B) When ER cholesterol rises above a threshold concentration (5 mole %), Scap binds to membrane cholesterol and undergoes a conformational change. This causes Insig to bind to Scap, and blocks COPII coat protein binding to Scap. Scap and SREBP are not transported to the Golgi, SREBP is not cleaved, and this leads to the downregulation of genes involved in lipid synthesis and uptake of lipoproteins. Figure adapted from [14].

FIGURE 2

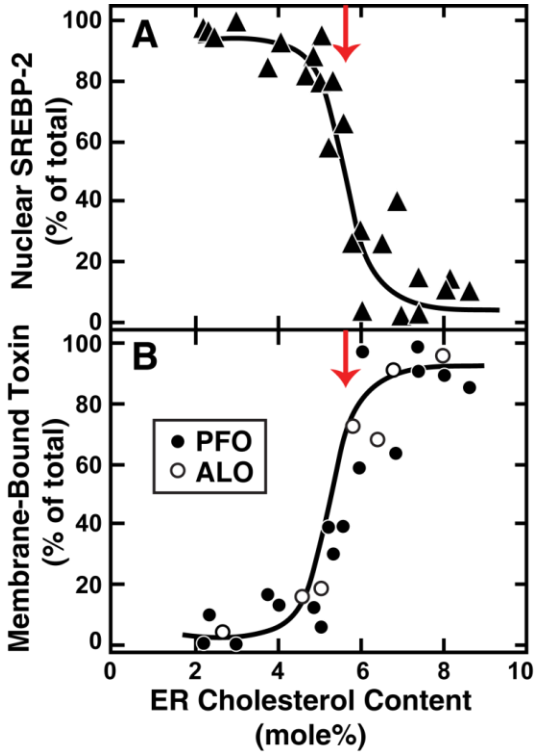

Figure 2. Correlation between SREBP-2 activation in CHO-K1 cells and binding of PFO and ALO to purified ER membranes. Cells were treated with HPCD to deplete cholesterol or VLDL or cholesterol:HPCD complexes to increase cholesterol. (A) A portion of cell homogenate was subjected to SDS-PAGE, and immunoblot analysis for SREBP-2. Nuclear SREBP-2 is expressed as the percentage of activated, nuclear SREBP-2 relative to total SREBP-2. (B) The remaining homogenate was used to purify ER membranes, which were then incubated with 5 µg of either PFO or ALO for 1 h at 37°C. Reactions were subjected to SDS-PAGE, transferred to nitrocellulose membrane, and His-tagged PFO and ALO were visualized and quantified by densitometry after α-His immunoblot. Membrane bound toxin is expressed as the percentage of

toxin in the membrane-bound, oligomeric form relative to total toxin. Red arrows indicate the narrow concentration range where a switch-like response occurs. Figure adapted from [145] with ALO data provided by Das, A., Rye, D., and Radhakrishnan, A. (unpublished).

CHAPTER ONE

SWITCH-LIKE RESPONSES OF TWO CHOLESTEROL-SENSING BACTERIAL TOXINS DO NOT REQUIRE PROTEIN OLIGOMERIZATION IN MEMBRANES

SUMMARY

Many cellular processes are sensitive to levels of cholesterol in specific membranes, and show strongly sigmoidal dependences on membrane composition. The sigmoidal responses of cholesterol sensors involved in these processes could arise from several mechanisms, including positive cooperativity (protein effects) and limited cholesterol accessibility (membrane effects). Here, we describe a sigmoidal response that arises primarily from membrane effects, due to sharp changes in the chemical activity of cholesterol. Our models for eukaryotic membrane-bound cholesterol sensors are soluble bacterial toxins that show identical switch-like specificity for endoplasmic reticulum membrane cholesterol. We show that truncated versions of these toxins fail to form oligomers but still show sigmoidal binding to cholesterol-containing membranes. The non-linear response emerges because interactions between bilayer lipids control cholesterol accessibility to toxins in a threshold-like fashion. Around these thresholds, affinity of toxins for membrane cholesterol varies by >100-fold, generating highly cooperative lipid-dependent responses independent of protein-protein interactions. Such lipid-driven cooperativity may control the sensitivity of many cholesterol-dependent processes.

INTRODUCTION

Cholesterol-sensing proteins respond to small changes in the concentration of cholesterol in mammalian cell membranes with sharp, switch-like sensitivity [27, 118, 145]. In one example, a small increase in endoplasmic reticulum (ER) membrane cholesterol from 5 mole% to 8 mole% of total ER lipids triggers an all-or-none response from Scap, a cholesterol-sensing oligomeric membrane protein that controls the activation of sterol-regulatory element binding proteins (SREBPs), transcription factors that stimulate lipid synthesis and uptake [13, 118]. Another example of such a sensor is perfringolysin O (PFO), a soluble bacterial toxin that specifically binds to cholesterol-containing membranes, and forms large oligomeric pores [154]. Binding of PFO to purified ER membranes occurs only after the concentration of cholesterol exceeds a threshold of 5 mole%, precisely the same concentration at which Scap is activated (Figure 2B) [145]. Binding of PFO to purified plasma membranes (PM) also shows a threshold response, except that the threshold cholesterol concentration is shifted to 35 mole% [27]. Binding of PFO to much simpler model membranes composed of just two components, cholesterol and a phospholipid, also occurs only after the cholesterol concentration exceeds a threshold – ranging from 20 mole% to 50 mole% depending on the phospholipid headgroup and acyl chain structure [36, 102, 145].

The molecular basis for these thresholds remains poorly understood. It is not known whether such highly sigmoidal responses arise due to allosteric changes in the binding of cholesterol to Scap or PFO oligomers, or due to properties of the membrane that affect the chemical activity of cholesterol, and thus its accessibility to Scap or PFO. Determining the relative contribution of either mechanism is crucial for understanding the sensitivity of

cholesterol sensors and for guiding their use as probes for cholesterol in the membranes of living cells.

Scap is a polytopic membrane protein and studying its interaction with membrane cholesterol is technically challenging [122]. Unlike Scap, PFO is a soluble protein that does not require detergents for stability and can be easily produced in large quantities. Moreover, there are two remarkable similarities in how Scap and PFO detect membrane cholesterol. The first similarity is their common threshold sensitivity for ER membrane cholesterol. Both Scap and PFO bind to ER cholesterol only after the cholesterol concentration exceeds a threshold of 5 mole% of total lipids [118, 145]. The second similarity is their identical sterol structural specificity. Both Scap and PFO bind to cholesterol, dihydrocholesterol, desmosterol, and β-sitosterol, but not to epicholesterol, lanosterol, 19-hydroxy-cholesterol, or 25-hydroxy-cholesterol [119, 145]. Their common ability to distinguish between cholesterol and epicholesterol, a diastereomer differing only in the orientation of the sterol 3-hydroxyl group, is especially striking. PFO is thus a convenient model for investigating the sensitivity of cholesterol sensors for membrane cholesterol.

PFO is the best-studied member of a large family of cholesterol-dependent cytolysins (CDCs) that are produced by more than 25 bacterial species and share a high degree (greater than 45%) of sequence similarity [60, 154]. To date, high-resolution crystal structures of the soluble forms of six members of this family – PFO [128], intermedilysin [116], anthrolysin O (ALO) [7], suilysin [162], listeriolysin O [77], and streptolysin O [34] – have been solved. There are no high-resolution crystal structures of the cholesterol-bound or oligomeric forms of any member of the CDC family. Nevertheless, extensive biophysical studies of PFO [33, 36, 123, 130], combined with a cryo-electron microscopy study of oligomers of another CDC, pneumolysin

[151], have revealed many details of CDC pore formation, as illustrated in the Figure 1-1A schematic diagram. CDCs are elongated proteins that can be divided into four domains [128]. The carboxy-terminal domain, referred to as domain 4 (D4) and shaded yellow in Figure 1-1A, is necessary and sufficient for binding to membrane cholesterol [33]. This initial binding event is followed by oligomerization into a circular pre-pore complex. Dramatic restructuring involving all four domains eventually leads to formation of a transmembrane β-barrel pore comprised of 35-50 monomers with an inner diameter of 250-300 Å. Unfortunately, these elegant studies do not explain PFO's threshold sensitivity for membrane cholesterol. None of the studies to date have decoupled the contributions by PFO oligomerization from those by membrane effects in determining PFO's sharp sigmoidal binding to cholesterol-containing membranes.

Here, we provide an answer to this problem through a detailed study of the threshold cholesterol sensitivities of two members of the CDC family, PFO and ALO. Using truncated forms of PFO and ALO that do not form oligomers, we isolate the role of membrane cholesterol accessibility in defining the threshold-like sensitivity of these toxins. We find that the primary trigger for their switch-like responses is encoded by the lipid composition of the membrane. Interactions of cholesterol with membrane phospholipids can modulate affinities of PFO and ALO for membrane cholesterol by more than 100-fold, resulting in sharp, switch-like responses. Toxin oligomerization is not necessary, but can further sensitize this response.

EXPERIMENTAL PROCEDURES

Materials – We obtained 1,2-dioleoyl-sn-glycero-3-phosphocholine (DOPC) and 1,2-diphytanoyl-sn-glycero-3-phosphocholine (DPhyPC) from Avanti Polar Lipids; Dulbecco's phosphate buffered saline (DPBS) from Corning; Alexa Fluor 594 C_5 maleimide, dimethyl sulfoxide (DMSO), Texas Red 1,2-dihexadecanoyl-sn-glycero-3-phosphoethanolamine (TR-DHPE), Marina Blue 1,2-dihexadecanoyl-sn-glycero-3-phosphoethanolamine (MB-DHPE), and isopropyl-1-thio-β-d-galactopyranoside (IPTG) from Invitrogen; cholesterol and tris (2-carboxyethyl) phosphine (TCEP) from Sigma-Aldrich; epicholesterol from Steraloids; and bovine serum albumin (BSA) from Thermo Scientific. Newborn calf lipoprotein-deficient serum (LPDS, $d < 1.215$ g/mL) was prepared by ultracentrifugation, as described previously [45].

Buffers – Buffer A contains 50 mM Tris-HCl (pH 7.5) and 150 mM NaCl. Buffer B is buffer A supplemented with 1 mM dithiothreitol (DTT). Buffer C is buffer A supplemented with 1 mM TCEP. Buffer D is DPBS supplemented with 2% (v/v) LPDS and 1 mM EDTA.

Expression Plasmids – All genetic constructs were cloned into the pRSET B expression vector. A plasmid containing the gene encoding the signal-peptide deficient PFO from Clostridium Perfringens (amino acids 29-500) where the sole cysteine was mutated to alanine (C459A) was a gift from Art Johnson (Texas A&M University). This construct has been described previously [36] and is hereafter referred to as PFO-FL. A plasmid containing the gene encoding a truncated fragment of PFO-FL (amino acids 391-500) was kindly provided to us by Akash Das (University of Texas Southwestern Medical Center). This fragment was defined as the fourth of four distinct structural domains of the soluble form of PFO [128] and has been shown to bind to cholesterol-containing membranes without causing membrane lysis [70, 138].

This construct is hereafter referred to as PFO-D4. The gene encoding signal-peptide deficient ALO from *Bacillus Anthracis* (amino acids 35-512) with flanking BamHI and EcoRI restriction sites was synthesized by GenScript, Inc. with a codon sequence optimized for efficient bacterial overexpression, and provided to us in the pUC57 cloning vector. This ALO gene was excised and ligated into the pRSET B expression vector, and this construct is hereafter referred to as ALO-FL. Using ALO-FL as template, a plasmid encoding a truncated fragment of ALO (amino acids 404-512) was generated by site-directed mutagenesis (QuikChange II XL Site Directed Mutagenesis Kit, Agilent). This fragment of ALO was defined as domain 4 of ALO in a study comparing the structures of the soluble forms of ALO and PFO [7], and is hereafter referred to as ALO-D4. The PFO-FL, ALO-FL, and ALO-D4 constructs have an NH_2-terminal hexahistidine tag followed by an enterokinase cleavage site. The PFO-D4 construct has an NH_2-terminal octahistidine tag. Mutations in all four constructs were generated by site-directed mutagenesis. The integrity of each plasmid was verified by DNA sequencing of its entire open reading frame.

Overexpression and Purification of Recombinant Proteins – Expression plasmids were transformed into BL21 (DE3) pLysS E. coli competent cells (Invitrogen) and protein overexpression was carried out as described [36] with the following modifications: PFO-FL and derivatives were induced with 1 mM IPTG at 37°C for 3.5 hours; ALO-FL and derivatives were induced with 0.5 mM IPTG at 30°C for 16 hours; and PFO-D4, ALO-D4 and derivatives were induced with 1 mM IPTG at 18°C for 16 hours. A cell pellet from a 6L bacterial culture was resuspended in 120 ml of buffer B containing 1 mg/ml lysozyme, 0.4 mg/ml phenylmethanesulfonyl fluoride, and 6 protease inhibitor cocktail tablets (Complete Mini, EDTA-free, Roche) and incubated at 4°C for 30 min. The lysozyme-disrupted cells were lysed using a Dounce homogenizer followed by a tip sonicator (Branson, Inc) and then subjected to

220,000 x g centrifugation for 1h. The resulting supernatant was loaded on a column packed with Ni-NTA (nickel-nitrilotriacetic acid) agarose beads (Qiagen). The column was washed with 10 column volumes of buffer B containing 50 mM imidazole, and bound proteins were eluted with either buffer B containing 300 mM imidazole (PFO-FL, ALO-FL, and derivatives) or with buffer B containing a linear gradient of 50-300 mM imidazole (PFO-D4, ALO-D4, and derivatives). The eluted fractions with the desired proteins were pooled and concentrated using an Amicon Ultra centrifugal filter (Millipore; 30,000 MWCO for PFO-FL and ALO-FL, and 10,000 MWCO for PFO-D4 and ALO-D4) and further purified by gel filtration chromatography on a Tricon 10/300 Superdex 200 column (GE Healthcare) equilibrated with buffer B. Protein-rich fractions were pooled, concentrated to 1-10 mg/ml, and stored at 4°C until use. Protein concentrations were measured using a Nanodrop instrument (Thermo Fisher Scientific) or by using a bicinchoninic acid kit (Pierce).

Preparation of Liposomes – All lipids were used without further purification. Mixtures containing the indicated proportions of phospholipids and sterols (from chloroform stock solutions) were evaporated to dryness under a steady stream of nitrogen gas and stored under vacuum for at least 16 hours. A trace amount (< 0.2 mole%) of a fluorescently labeled phospholipid (TR-DHPE for assays with unlabeled proteins, MB-DHPE for assays with Alexa-594 labeled proteins) was included for detection and quantification of liposomes. The dried lipid mixtures were hydrated by adding 500 µL of buffer A (final lipid concentration, 800 µM), agitated on a vortexer for 1 hour, and subjected to 3 freeze-thaw cycles (1 cycle = 60 seconds in a liquid nitrogen bath, 3 minutes in a room temperature water bath). The resulting lipid dispersions were placed in a water bath at 37°C and subjected to sonication for 15 min followed by a 15 min pause for cooling (2 cycles). Finally, the lipid mixtures were extruded through a

polycarbonate filter (100 nm pore size) 11 times to yield homogeneous unilamellar liposomes. Liposomes were stored at 4°C and used within 5 days. Spot checks were carried out to verify cholesterol concentrations in liposomes, as described previously [145]. In all cases, the measured concentration of cholesterol in liposomes was within 5 mole% of the expected values.

Assays for interaction of purified proteins with liposomes – Reaction mixtures (200 µL) containing 600 µM liposomes (total lipid) and 4.4 µM protein in buffer B were set up in 1.5 mL tubes (Phenix Research Products). After incubation for 1 h at room temperature, a portion of each reaction mixture (100 µl) was transferred to a 96-well plate (black, flat-bottom, non-binding; Greiner Bio-One), and intrinsic tryptophan fluorescence was measured using a micro-plate reader (Tecan) (excitation wavelength, 290 nm; emission wavelength, 340 nm; band pass, 5 nm for each). A portion of each reaction mixture (20 µL) was mixed with SDS loading buffer, heated for 10 min at 37°C, and subjected to SDS-PAGE. Proteins were visualized with Coomassie Brilliant Blue R-250 stain (Bio-Rad). In assays measuring the affinity of PFO for membrane cholesterol, reaction mixtures (1 mL) containing 100 nM PFO and 0-500 µM liposomes, all in buffer B, were set up in 1.5 mL tubes. Following incubation for 2 h at room temperature, 40 µL of Ni-NTA agarose bead slurry that had been washed twice and resuspended in 100 µL of buffer B was added to each reaction. Following additional incubation for 1h at room temperature, the His_6-tagged PFO was pelleted by centrifugation at 16,000 x g for 5 min. The supernatant was discarded, and the Ni-bound PFO was eluted by the addition of 20 µL of buffer B supplemented with 500 mM imidazole. After addition of 4 µL of 5x SDS loading buffer and heating for 10 min at 37°C, samples were centrifuged at 16,000 x g for 5 min and the resulting supernatant was subjected to SDS-PAGE. Proteins were visualized with Coomassie Brilliant Blue R-250 stain. Densitometry analysis was carried out using ImageJ software (NIH,

version 1.36B). In assays where fluorescently labeled proteins were used, reaction mixtures (120 µL) containing 67 µM liposomes (total lipid), 0.5 µM fluorescently labeled protein, and 0-10 µM unlabeled protein in buffer B were set up in 1.5 mL tubes. After incubation for 1 h at room temperature, a portion of each reaction mixture (100 µl) was transferred to a 96-well plate (Greiner Bio-One), and fluorescence was measured using a micro-plate reader (excitation wavelength, 590 nm; emission wavelength, 617 nm; band pass, 2.5 nm for each).

Hemolysis assays – For a typical assay, 4 mL of fresh rabbit blood was centrifuged at 120 x g for 10 min, and the erythrocyte pellet was resuspended in 4 mL of ice-cold buffer D. After gentle mixing by hand, the mixture was centrifuged at 500 x g for 10 min, and the resulting pellet was again resuspended in 4 mL of ice-cold buffer D. After gentle mixing by hand, the mixture was centrifuged at 1000 x g for 20 min, and the resulting pellet was resuspended in 36 mL of ice-cold buffer D. Standard hemolysis reaction mixtures (500 µL) containing 450 µL of erythrocytes, washed and diluted as described above, and 50 µL of buffer A containing protein (0-300 nM final concentration) were set up in 1.5 mL tubes. In some hemolysis assays, proteins were preincubated with cholesterol or epicholesterol dissolved in DMSO (4% (v/v) final concentration) for 1 h at room temperature before addition of erythrocytes. After incubation for 10 min at 37°C, the mixtures were centrifuged at 380 x g for 15 min, and a portion of the supernatant (100 µl) was transferred to a 96-well plate (clear, flat-bottom; Evergreen Scientific). The extent of hemolysis was quantified using a micro-plate reader by measuring absorbance of released hemoglobin at 540 nm.

Data analysis – The data points in all plots represent the mean of three independent assays (except for Figure 1-3B which shows the average of two independent assays). Error bars represent the standard error of the mean. When not visible, error bars are smaller than the size of

the data symbols. In Figure 1-4, the binding curves represent a weighted least-squares fit of a sigmoidal function to the data points. Best-fit values of switch-points (cholesterol mole percentages where the normalized Trp fluorescence equals 0.5) for the various protein/phospholipid pairs are: 41 mole% for PFO-FL/DOPC; 31 mole% for PFO-FL/DPhyPC; 26 mole% for ALO-FL/DOPC; 17 mole% for ALO-FL/DPhyPC; 45 mole% for PFO-D4/DOPC; 27 mole% for PFO-D4/DPhyPC; 45 mole% for ALO-D4/DOPC; and 27 mole% for ALO-D4/DPhyPC). In Figure 1-5B and 1-5D, the curves for PFO-FL oligomerization and inhibition of PFO-FL and ALO-FL hemolysis by cholesterol represent fits to a one-site receptor-ligand binding model. Best-fit values for half-maximal oligomerization in Figure 1-5B are 11 μM and 16 μM for 40 mole% cholesterol and 50 mole% cholesterol, respectively, and are >1000 μM for 20 mole% and 30 mole% cholesterol. Best fit values for 50% inhibition in Figure 1-5D are 108 nM for ALO-FL and 97 nM for PFO-FL.

RESULTS

Cholesterol switch-points of PFO and ALO: identical for domain 4s, but different for full-length versions – The crystal structures of PFO and ALO monomers are shown in Figure 1-1B with their carboxy-terminal D4s shaded yellow. These proteins share ~70% sequence identity and a common elongated, β-sheet rich architecture. D4s from PFO and ALO were shown to be sufficient for binding to membrane cholesterol but unable to form oligomers or membrane pores [20, 138]. These earlier studies suggested that a comparative study of full-length (FL) versus D4 fragments of CDCs might shed light on the role of oligomerization in determining the threshold cholesterol sensitivity of CDCs. To this end, we expressed FL and D4 versions of both PFO and ALO, all with amino-terminal His-tags, in bacteria. The resulting recombinant proteins, hereafter referred to as PFO-FL, PFO-D4, ALO-FL, and ALO-D4, were purified to homogeneity using nickel chromatography followed by gel filtration chromatography. We then adapted many of the assays established by the Johnson and Tweten groups for PFO-FL, and extended them here to study the various domains of PFO and ALO.

PFO-FL contains seven Trp residues, six of which are located in its D4, and binding to membranes results in a 2-3 fold increase in its Trp fluorescence [59, 99, 145]. Since ALO-FL contains six Trp residues (five in its D4) at similar locations as in PFO-FL, we monitored the intrinsic Trp fluorescence of both proteins to measure their binding to cholesterol-containing membranes. Initially, we used model membranes composed of binary mixtures of 1,2-dioleoyl-sn-glycero-3-phosphocholine (DOPC) and cholesterol, and varied the mole fraction of cholesterol while keeping the total amount of membranes constant in each reaction. In this

approach, changes in membrane cholesterol content are accompanied by an opposite change in the content of DOPC.

As shown in Figure 1-1C and previously [36, 102, 145], when incubated with liposomes containing increasing mole fractions of cholesterol, the Trp fluorescence of PFO-FL increased by ~3-fold in a sharp, sigmoidal fashion, with a half-maximum at 41 mole% cholesterol. We hereafter use the term "switch-point" to refer to the cholesterol mole fraction corresponding to the midpoint of the switch-like increase in Trp fluorescence, an indicator of CDC binding to membranes (see *Experimental Procedures* for details on curve fitting). The Trp fluorescence of ALO-FL, when incubated with DOPC-cholesterol membranes, increased by ~2-fold in a sharp, sigmoidal fashion as well, except its switch-point was shifted to 26 mole% cholesterol. PFO-FL and ALO-FL showed no binding to membranes containing epicholesterol, even when the mole fraction of this diastereomer of cholesterol reached 60 mole%. Binding was also abolished when a conserved hexapeptide sequence, GTTLYP (shaded red in Figure 1-1B), was mutated to GTAAYP in PFO-FL and to AAAAAA in ALO-FL. The threonine-leucine pair within this hexapeptide region was previously shown to be critical for the binding of PFO and two other CDCs, streptolysin and pneumolysin, to cholesterol-containing membranes [33]. Mutation of just the TL-pair in ALO-FL to AA only partially affected ALO-FL's ability to bind to cholesterol-containing membranes.

We then measured the interaction of truncated D4 fragments of PFO and ALO with DOPC-cholesterol membranes. As shown in Figure 1-1D, the Trp fluorescence of PFO-D4 increased by ~2.5-fold in a sigmoidal fashion, with a switch-point at 45 mole% cholesterol, slightly shifted from the 41 mole% switch-point observed for PFO-FL. The Trp fluorescence of ALO-D4 also increased by ~2.5-fold in a sigmoidal fashion, with a switch-point at 45 mole%

cholesterol, significantly shifted from the 26 mole% switch-point observed for ALO-FL. Remarkably, although the switch-points for PFO-FL and ALO-FL in Figure 1-1C differed dramatically (41 mole% cholesterol versus 26 mole% cholesterol), the switch-points for PFO-D4 and ALO-D4 were identical (45 mole% cholesterol). Like their full-length counterparts, PFO-D4 and ALO-D4 also showed no binding to membranes containing epicholesterol. Introducing the same mutations described above for PFO-FL and ALO-FL into PFO-D4 and ALO-D4 also abolished binding.

Domain 4s of PFO and ALO do not form oligomers – We next sought to determine whether the dramatic difference in cholesterol sensitivity between these proteins was related to differences in their ability to form oligomers. To assay for CDC oligomerization, we took advantage of a previous observation that CDC oligomers are resistant to denaturation by SDS, and can be distinguished from CDC monomers by their slower electrophoretic mobility during SDS-PAGE [36, 145]. As shown in Figure 1-2A (top gel), when mixtures of PFO-FL and DOPC-cholesterol liposomes were subjected to SDS-PAGE, PFO-FL migrated primarily as an ~50 kDa species (calculated molecular weight: 57 kDa) for cholesterol mole fractions up to 40 mole%. At higher mole fractions of cholesterol, the ~50 kDa monomeric form of PFO-FL was significantly diminished, and the majority of PFO-FL was found as a slower migrating species (> 250 kDa), consistent with a large oligomer. Figure 1-2B (top gel) shows similar results for mixtures of ALO-FL and DOPC-cholesterol liposomes. A major fraction of ALO-FL electrophoresed as a slow-migrating oligomer (>250 kDa) rather than an ~50 kDa monomer (calculated molecular weight: 56 kDa), only when membrane cholesterol exceeded 25 mole%. The cholesterol mole fractions at which oligomeric forms became dominant (40-45 mole% for PFO-FL; 25-30 mole% for ALO-FL) exactly matched the switch-points observed using the Trp

fluorescence assay (Figure 1-1C). In contrast, when mixtures of PFO-D4 or ALO-D4 and DOPC-cholesterol liposomes were subjected to SDS-PAGE, we observed only their monomeric forms at ~15 kDa (calculated molecular weights - PFO-D4: 14 kDa; ALO-D4: 16 kDa), even at the highest cholesterol mole fraction of 60 mole% (Figures 1-2A and 1-2B, bottom gels).

Oligomerization of CDCs on the surface of cholesterol-containing membranes eventually leads to formation of a membrane-spanning pore. We used a hemolysis assay to test the ability of FL and D4 fragments of PFO and ALO to form pores in rabbit erythrocytes. As shown in Figure 1-2C, PFO-FL caused complete hemolysis at a concentration of 3 nM, whereas PFO-D4 or a control protein (BSA) caused no hemolysis, even when added at a concentration of 300 nM. Similarly, as shown in Figure 1-2D, ALO-FL caused complete hemolysis at a concentration of 1 nM, whereas ALO-D4 or BSA did not lyse red cells, even when added at a concentration of 300 nM.

Combined, the tryptophan fluorescence, gel-shift, and hemolysis assays show that when membrane cholesterol exceeds a threshold concentration, the FL versions of PFO and ALO undergo a transition from a soluble to a membrane-bound form (State I to State II, Figure 1-1A), and then oligomerize to finally form a membrane-spanning pore (States III and IV, Figure 1-1A). The D4 versions of PFO and ALO also bind to cholesterol-rich membranes, but do not form oligomers or pores. The gel-shift assays used to assess oligomerization are not conclusive since it is possible that D4 oligomers are broken down more readily than FL oligomers by the denaturing conditions of SDS-PAGE. To study the oligomeric properties of CDCs using a different approach, we developed a fluorescence quenching assay for oligomerization of ALO-FL and ALO-D4. We mutated the sole cysteine in ALO (C472) to alanine, and introduced single cysteines near the NH_2-terminii of cysteine-less ALO-FL (K46C) and ALO-D4 (S404C). We

then covalently attached fluorophores (Alexa Fluor 594) to the sulfhydryl groups of these cysteine residues. These fluorescently labeled proteins are hereafter referred to as fALO-FL and fALO-D4. By placing fluorescent reporters near the NH_2-terminus, far from the COOH-terminal tip that is involved in cholesterol binding, we hoped to gain insight into post-binding conformational changes involving oligomerization.

As shown in Figure 1-3A, when fALO-FL was incubated with DOPC-cholesterol liposomes, its Alexa 594 fluorescence was constant until membrane cholesterol reached 25 mole%. At higher cholesterol mole fractions, Alexa 594 fluorescence decreased by >75% in a sharp, sigmoidal fashion. No such reduction in Alexa 594 fluorescence was observed when fALO-FL was incubated with liposomes containing epicholesterol. In contrast to the dramatic, cholesterol-specific quenching observed for fALO-FL, no significant change in Alexa 594 fluorescence was observed when fALO-D4 was incubated with DOPC-cholesterol liposomes, even when the membranes contained 60 mole% cholesterol. The Trp fluorescence assays in Figure 1-3B show that fALO-D4 binds to DOPC-cholesterol membranes with a switch-point of ~45 mole% cholesterol, similar to that observed for unlabeled ALO-D4 (Figure 1-1D), thus confirming the activity of this fluorescently labeled protein. The Trp fluorescence assays also show that fALO-FL binds to DOPC-cholesterol membranes with a switch-point of ~30 mole% cholesterol, and does not bind to membranes containing epicholesterol, properties that are similar to those observed for unlabeled ALO-FL in Figure 1-1C. The correlation between changes in Trp and Alexa 594 fluorescence of fALO-FL, but not of fALO-D4, is consistent with oligomerization of membrane-bound fALO-FL, but not of membrane-bound fALO-D4.

If quenching of fALO-FL fluorescence was due to close proximity of Alexa 594 fluorophores in membrane-bound oligomers, then the addition of unlabeled ALO-FL during the

reaction would be expected to result in mixed oligomers and relieve proximity-based quenching. As shown in Figure 1-3C, when fALO-FL was incubated with DOPC-cholesterol liposomes containing 50 mole% cholesterol, its Alexa 594 fluorescence was quenched by ~60% relative to when incubated with liposomes containing no cholesterol. As increasing amounts of unlabeled ALO-FL were added to the reaction, the Alexa 594 fluorescence gradually increased, with complete recovery to unquenched levels occurring when unlabeled ALO-FL concentrations were four times that of fALO-FL. In contrast, no recovery of quenched Alexa 594 fluorescence was observed when unlabeled ALO-D4 or BSA was added to the reaction. These results suggest that ALO-D4 can neither form self-oligomers after binding to membrane cholesterol nor be incorporated efficiently into oligomers of ALO-FL. The fluorescence of a labeled version of PFO-FL (D30C) is also quenched in a sharp sigmoidal fashion when incubated with DOPC-cholesterol liposomes containing >40 mole% cholesterol. However, we have so far been unable to generate a stable fluorescently labeled version of PFO-D4 to study its oligomeric properties using this quenching assay. Single cysteine residues were introduced at ten locations in cysteine-less PFO-D4 (N395, K417, E418, Y432, Q433, D469, S472, Y474, D475, N481), but in all cases the purified recombinant protein precipitated and was unusable. Nonetheless, the fluorescence quenching studies with ALO support the gel-based results of Figure 1-2 that FL versions of CDCs form oligomers after binding cholesterol-containing membranes whereas D4 fragments do not.

Cholesterol switch-points for domain 4s of PFO and ALO depend on the bilayer phospholipid – Despite not forming oligomers, PFO-D4 and ALO-D4 show a sharp, sigmoidal cholesterol dependence in binding to DOPC-cholesterol membranes, with identical switch-points at 45 mole% cholesterol (Figure 1-1D). To test whether this common switch-point reflects

phospholipid-dependent accessibility of cholesterol in membranes, we changed the bulk phospholipid from DOPC (T_m = -2°C) to 1,2-diphytanoyl-sn-glycero-3-phosphocholine (DPhyPC) (T_m < -120°C). The T_m is a convenient measure of the ordering tendency of phospholipid acyl chains – the lower the T_m, the lower the affinity for cholesterol [73]. As shown by the Trp fluorescence assays of Figure 1-4A, both PFO-D4 and ALO-D4 bound to DPhyPC-cholesterol membranes in a sharp, sigmoidal fashion. Remarkably, their switch-points for DPhyPC-cholesterol membranes were also identical, but at 27 mole% cholesterol, significantly lower than the identical 45 mole% switch-point observed for their binding to DOPC-cholesterol membranes (data for DOPC are replotted here from Figure 1-1D in a normalized form). As shown in Figure 1-4B, when we studied the interaction of PFO-FL and ALO-FL with DPhyPC-cholesterol membranes, we found that the binding of these proteins also showed shifts in switch-points to lower cholesterol mole fractions (31 mole% for PFO-FL, 17 mole% for ALO-FL, data for DOPC are replotted here for reference from Figure 1-1C). While the binding curves for PFO-D4 and ALO-D4 to cholesterol-containing membranes collapse into phospholipid-specific groups, the binding curves for PFO-FL and ALO-FL show a wider distribution of switch-points because oligomerization enhances their cholesterol sensitivity. The variation in switch-points (by <10 mole% cholesterol) observed for mutant versions of PFO-FL [72] is likely due to differences in their oligomerization.

Apparent affinities of PFO and ALO for cholesterol are determined by membrane composition – The experiments described so far show that CDC binding to membrane cholesterol is sensitive to the mole fraction or surface density of cholesterol in membranes. To further understand the affinity of CDCs for membrane cholesterol, we designed a set of experiments where we fixed the surface density (mole fraction) of cholesterol in membranes and

varied the amount of cholesterol in the reaction solution by changing the total amount of membranes. In these experiments, we used the gel-shift assay of Figure 1-2A to monitor the interaction of PFO-FL with DOPC membranes containing cholesterol at levels both above and below the 41 mole% switch-point for this protein-phospholipid pair (Figures 1-1C and 1-2A). The extent of oligomer formation in the Coomassie-stained gels shown in Figure 1-5A was quantified by densitometry and plotted in Figure 1-5B as a function of total cholesterol concentration in the reaction.

When mixtures of PFO-FL and increasing amounts of liposomes containing 20 mole% cholesterol were subjected to SDS-PAGE, we observed that most of PFO-FL (90% of total) migrated as a monomeric species, even at the highest total concentration of cholesterol (100 μM). Similar behavior was observed when the liposomes contained 30 mole% cholesterol. When the mole fraction of cholesterol in liposomes increased to 40 and 50 mole%, significant oligomer formation of PFO-FL occurred when cholesterol concentration rose above 5 μM. At cholesterol concentrations of 100 μM, 30-60% of PFO-FL was found in its slower-migrating oligomeric form. These data show that the apparent affinity of PFO-FL for DOPC-cholesterol membranes depends on the lipid composition, ranging from very little affinity (>1000 μM) when the mole fraction of cholesterol is 20 mole% and 30 mole% to an affinity of 11 μM and 16 μM when the mole fraction of cholesterol is 40 mole% and 50 mole%, respectively. To test whether this context-dependent affinity arose due to kinetic differences, we used the Trp fluorescence assay to measure the time course of PFO-FL binding to DOPC-cholesterol membranes. As shown in Figure 1-5C, PFO-FL rapidly bound to membranes containing 40 and 50 mole% cholesterol with half-maximal binding at ~15 minutes. However, no binding of PFO-FL was observed when incubated with membranes containing 20 and 30 mole% cholesterol, even when the reaction time

exceeded 1000 minutes. Similar kinetics were observed for the binding of PFO-FL to membranes composed of palmitoyl-oleoyl phosphatidylcholine and cholesterol [59].

Our studies so far highlight the role of the lipid bilayer membrane in determining the sensitivity of CDCs for membrane cholesterol. In order to study the affinity of CDCs for cholesterol without competing interactions from phospholipids, we designed a solution binding assay where cholesterol was not immersed in a lipid bilayer. We took advantage of early observations that hemolysis by CDCs can be inhibited by pre-incubation of the toxin with cholesterol in organic solvents [154]. As shown in Figure 1-2C and 1-2D, incubation of rabbit erythrocytes with PFO-FL (3 nM) or ALO-FL (1 nM) results in complete hemolysis. We pre-incubated PFO-FL and ALO-FL with cholesterol dissolved in dimethyl sulfoxide (DMSO) before addition to rabbit erythrocytes, and measured the subsequent inhibition of hemolysis. As shown in Figure 1-5D, hemolysis was completely inhibited by pre-incubation of PFO-FL and ALO-FL with 250 nM cholesterol. No inhibition of hemolysis was observed after pre-incubation with epicholesterol, even at the highest concentration of 3 μM. Half-maximal inhibition of hemolysis, which can be related to a solution affinity of PFO and ALO for cholesterol, occurred at similar concentrations of 97 nM and 108 nM, respectively. These affinities are only a rough estimate since a large fraction of cholesterol added to the aqueous phase likely becomes rapidly insoluble and inaccessible. The varied threshold-like cholesterol sensitivities observed in Figure 1-4 due to differences in cholesterol sequestration by membrane phospholipids or by differences in PFO and ALO oligomerization on membranes were no longer observed when the affinity of PFO and ALO for cholesterol was measured in this non-membrane context.

FIGURE 1-1

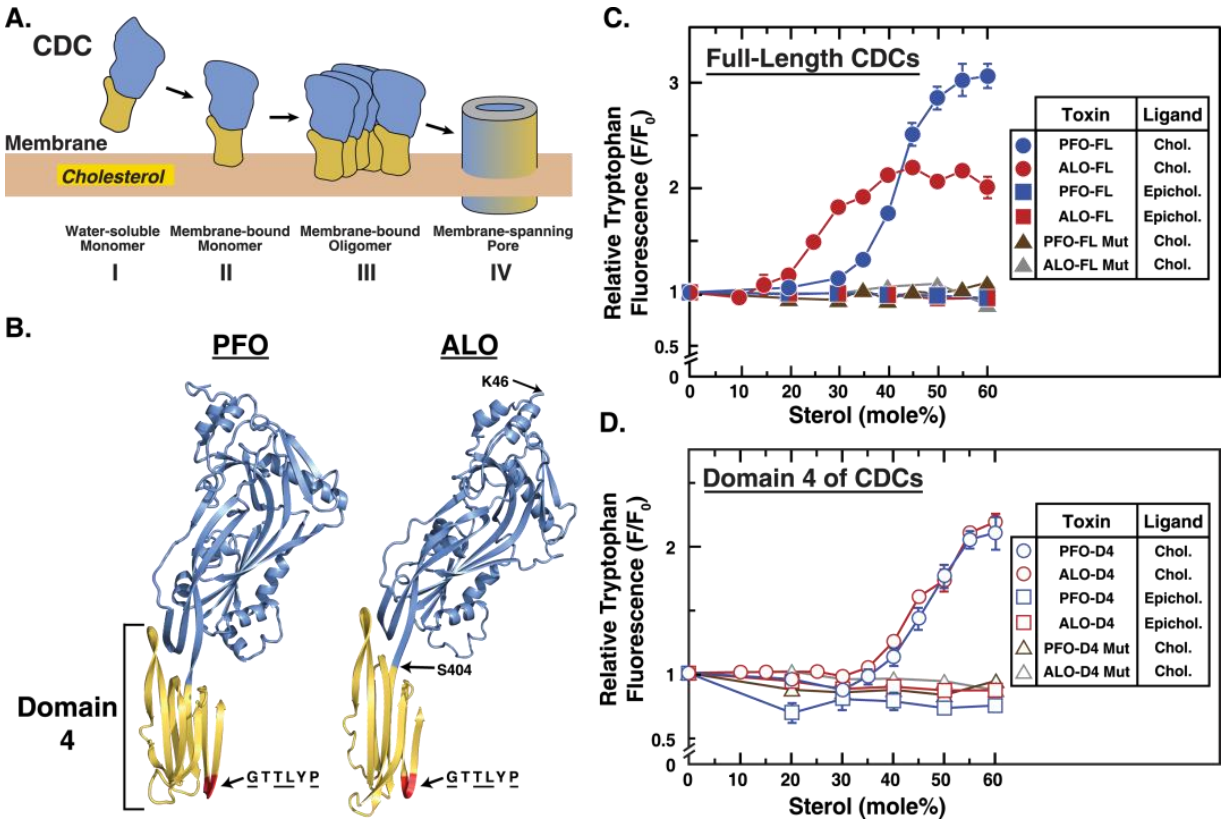

Figure 1-1. Interaction of PFO and ALO with sterol-containing membranes. (A) General model for the interaction of cholesterol-dependent cytolysins (CDCs) with cholesterol-containing membranes. Soluble monomeric CDCs bind to membrane cholesterol, oligomerize on the membrane surface, and undergo large conformational changes to form a membrane-spanning pore. The cholesterol-binding domain is shaded in yellow. (B) Structures of PFO and ALO. A ribbon representation of the α-carbon backbone of the crystal structures of PFO [128] and ALO [7] is shown with domains 1-3 (amino acids 30-390 in PFO; amino acids 46-403 in ALO) in blue and domain 4 (amino acids 391-500 in PFO; amino acids 404-512 in ALO) in yellow. A conserved hexapeptide sequence (GTTLYP) is shaded red. Underlined residues of this

hexapeptide are identical in 26 related CDCs [60]. Also shown are locations of residues in ALO (K46 and S404) that were mutated to cysteines for covalent attachment of fluorescent labels. (C and D) Intrinsic tryptophan fluorescence of PFO and ALO. Recombinant wild-type (WT) and mutant (Mut) versions of full-length PFO and ALO and of domain 4 of PFO and ALO were overexpressed and purified as described in *Experimental Procedures*. Each reaction mixture, in a total volume of 200 µL of buffer B, contained 4.4 µM of the indicated protein and 600 µM liposomes composed of DOPC and varying mole fractions of cholesterol (Chol.) or epicholesterol (Epichol.). After incubation for 1 h at room temperature, intrinsic tryptophan fluorescence from the samples was measured (excitation wavelength, 290 nm; emission wavelength, 340 nm). For each version of PFO or ALO, the fluorescence from mixtures of protein with liposomes containing 0% sterol is normalized to 1.

FIGURE 1-2

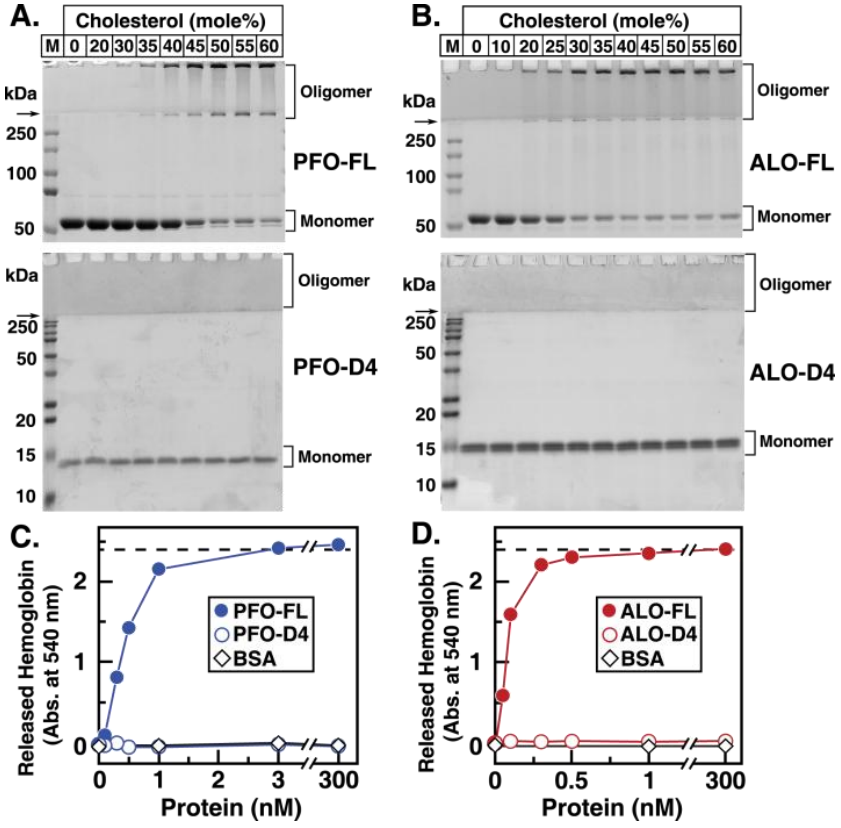

Figure 1-2. Oligomerization and pore formation by PFO and ALO after binding to cholesterol-containing membranes. (A and B). Coomassie staining. Aliquots (10% of total) of the reaction mixtures from Figure 1-1C and 1-1D containing recombinant full-length (FL) or domain 4 (D4) of PFO and ALO with membranes containing DOPC and varying mole fractions of cholesterol were subjected to SDS-PAGE. Proteins were visualized with Coomassie Brilliant Blue R-250 stain. Molecular masses of protein standards are indicated. (C and D) Hemolysis assays. Each reaction mixture, in a final volume of 500 µL, contained varying amounts of the indicated version of PFO, ALO, or bovine serum albumin (BSA), and 450 µL rabbit erythrocytes that had been washed and diluted as described in *Experimental Procedures*. After incubation for

10 min at 37°C, extent of hemolysis was quantified by measuring release of hemoglobin (absorbance at 540 nm). The dashed line represents the amount of hemoglobin released after treatment with 1% (w/v) Triton-X 100 detergent.

FIGURE 1-3

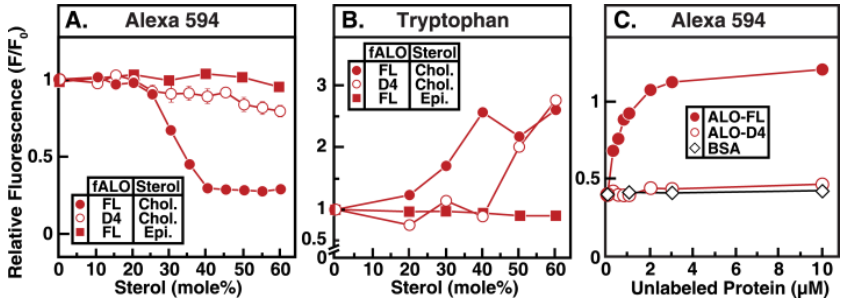

Figure 1-3. Interaction of fluorescently-labeled ALO with sterol-containing membranes. Recombinant full-length ALO (ALO-FL) and domain 4 of ALO (ALO-D4) were overexpressed and purified, and fluorescently-labeled versions (fALO-FL and fALO-D4) were generated as described in *Experimental Procedures*. (A and C) Alexa 594 fluorescence of labeled proteins. Reaction mixtures, in a final volume of 120 µL buffer B, contained 0.5 µM of the indicated fluorescently-labeled protein and 67 µM liposomes comprised of DOPC and varying amounts of cholesterol (Chol.) or epicholesterol (Epi.) (A), or 0.5 µM fALO-FL, 67 µM liposomes comprised of 50 mole% DOPC and 50 mole% cholesterol, and varying amounts of the indicated unlabeled protein (C). (B) Intrinsic tryptophan fluorescence of labeled proteins. Reaction mixtures, in a volume of 100 µL buffer B, contained 3.6 µM of the indicated protein and 600 µM liposomes composed of DOPC and varying mole fractions of cholesterol or epicholesterol. After incubation for 1 h at room temperature, Alexa Fluor 594 fluorescence (A and C) (excitation wavelength, 590 nm; emission wavelength, 617 nm; band pass, 2.5 nm for each), or intrinsic tryptophan fluorescence (B) (excitation wavelength, 290 nm; emission wavelength, 340 nm) was measured. For each protein, fluorescence from mixtures of protein with liposomes containing 0% cholesterol is normalized to 1.

FIGURE 1-4

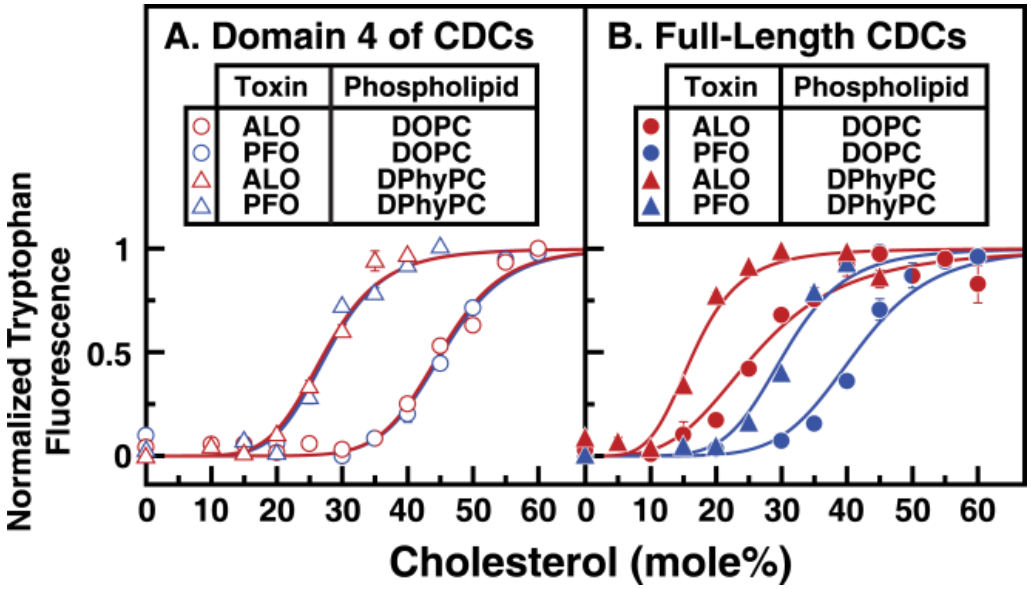

Figure 1-4. Cholesterol thresholds for ALO and PFO are determined by membrane phospholipids. (A and B) Recombinant full-length (FL) and domain 4 (D4) of PFO and ALO were overexpressed and purified as described in *Experimental Procedures*. Each reaction mixture, in a total volume of 200 µL of buffer B, contained 4.4 µM of the indicated protein and 600 µM liposomes composed of DOPC or DPhyPC and varying mole fractions of cholesterol. After incubation for 1 h at room temperature, intrinsic tryptophan fluorescence of the samples was measured (excitation wavelength, 290 nm; emission wavelength, 340 nm). For each combination of protein and phospholipid, fluorescence values were normalized to range from 0 to 1.

FIGURE 1-5

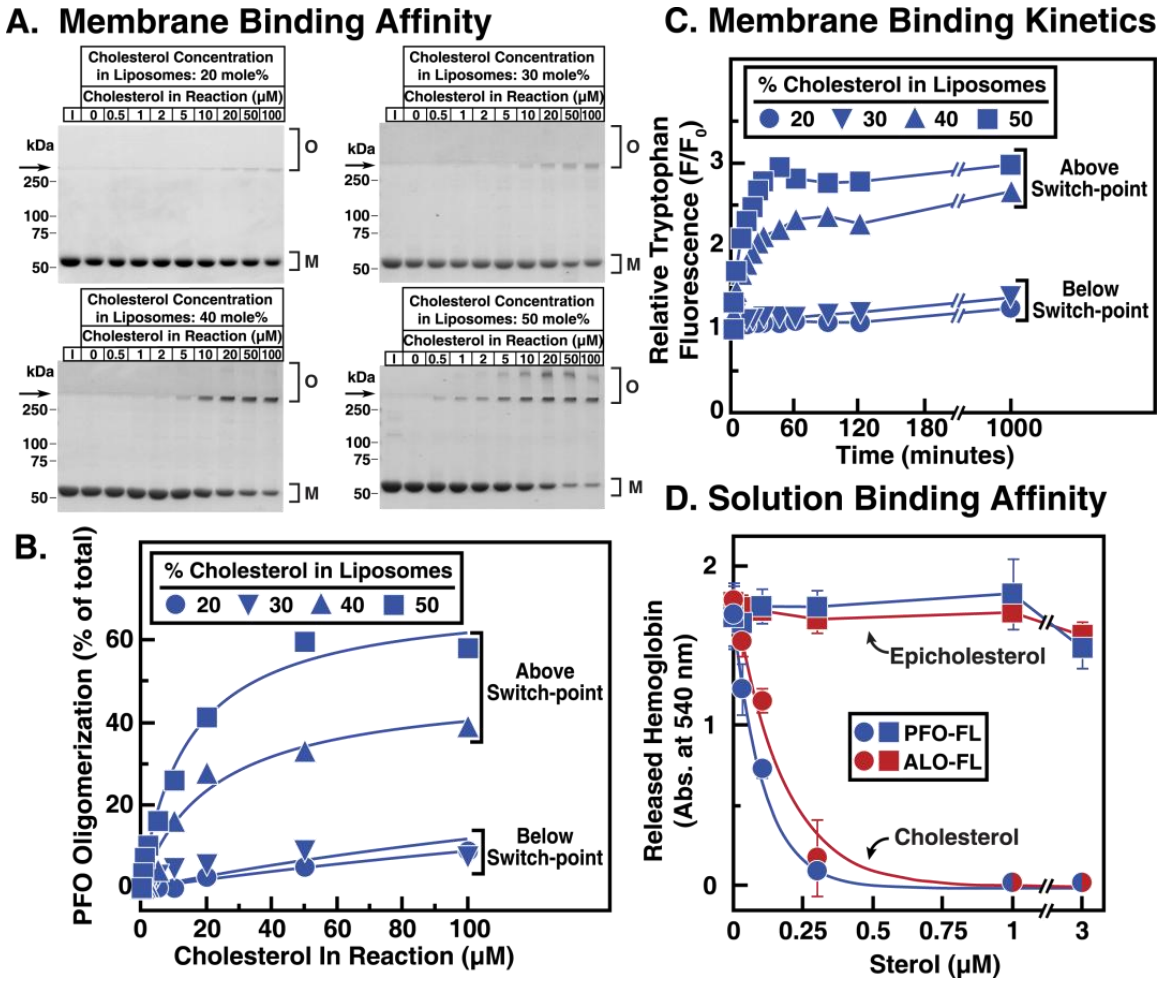

Figure 1-5. Affinity of PFO and ALO for cholesterol is determined by membrane phospholipids. Recombinant PFO-FL and ALO-FL were overexpressed and purified as described in *Experimental Procedures*. (A and B) Affinity of PFO-FL for membrane cholesterol. Each reaction mixture, in a total volume of 1 mL of buffer B, contained 100 nM PFO-FL (5.7 μg) and varying amounts of liposomes composed of DOPC and the indicated amounts of cholesterol. After incubation for 2 h at room temperature, PFO-FL was concentrated to a volume

of 20 µL as described in *Experimental Procedures*, and the entire amount of protein was subjected to SDS-PAGE (A). Lane 1 (I) in each gel contains 5.7 µg of PFO-FL (input amount) as a reference to judge the efficiency of PFO-FL concentration by Ni beads. Proteins were visualized with Coomassie Brilliant Blue R-250 stain. Molecular masses of protein standards are shown. O, membrane-bound oligomeric form of PFO; M, free monomer form of PFO. Gels were scanned, and densitometric analysis (B) was carried out to determine the percentage of oligomeric, membrane-bound form of PFO relative to the total (membrane-bound oligomer plus free monomer). (C) Binding kinetics. Each reaction mixture, in a total volume of 200 µL of buffer B, contained 4.4 µM of PFO-FL and 600 µM liposomes composed of DOPC and the indicated amounts of cholesterol. After incubation at room temperature for the indicated times, intrinsic tryptophan fluorescence from the samples was measured (excitation wavelength, 290 nm; emission wavelength, 340 nm). The fluorescence from mixtures of PFO-FL with liposomes containing 0% sterol is normalized to 1. (D) Binding of DMSO-solubilized sterols to PFO-FL and ALO-FL. Each reaction mixture, in a final volume of 50 µL, contained either ALO-FL (1 nM) or PFO-FL (3 nM), and varying amounts of cholesterol or epicholesterol dissolved in DMSO (4% (v/v) final concentration). After incubation for 1 h at room temperature, 450 µL rabbit erythrocytes, washed and diluted as described in *Experimental Procedures*, was added to each reaction mixture. After incubation for 10 min at 37°C, extent of hemolysis was quantified by measuring release of hemoglobin (absorbance at 540 nm).

DISCUSSION

Our current studies show that the switch-like sensitivity of cholesterol-sensing bacterial toxins for membrane cholesterol arises primarily due to properties of the lipid bilayer. Interactions with membrane phospholipids control the accessibility of membrane cholesterol to soluble sensors like PFO and ALO. After binding to accessible cholesterol at the surface of membranes, the membrane-bound toxins are stabilized by large-scale oligomerization. This complex interplay between lipid-lipid, lipid-protein, and protein-protein interactions results in fine-tuning the final varied sensitivities of PFO and ALO for cholesterol in membranes.

Understanding the initial sensing of membrane cholesterol by PFO and ALO without the complications of protein oligomerization was made possible by engineering non-oligomerizing, truncated versions of these proteins, PFO-D4 and ALO-D4. Figures 1-1 through 1-4 show that despite not forming oligomers, PFO-D4 and ALO-D4 bind to cholesterol-containing membranes in a sharp, sigmoidal manner. The concentration of cholesterol at which this switch-like transition in binding occurs is determined by the phospholipid structure [36, 102, 145]. The absolute specificity for cholesterol over its diastereomer epicholesterol suggests to us a specific binding site in the ~110 amino acid D4 fragments of PFO and ALO. Positive cooperativity between multiple cholesterol binding sites in these non-oligomerizing D4 fragments could be a source of this sigmoidal behavior, however we think this explanation is unlikely as mutation of just a threonine-leucine pair in PFO-D4 to alanines completely abolishes membrane binding (see Figure 1-1). Instead, as outlined above, we propose that the sigmoidal binding of PFO-D4 and ALO-D4 to cholesterol-containing membranes is determined by the accessibility of cholesterol at the surface of membranes.

The binding reaction of PFO-D4 or ALO-D4 to membrane cholesterol can be conceptualized as a two-step reaction. The first step involves an equilibrium between cholesterol dissolved in the lipid bilayer membrane, and cholesterol in the water layer at the surface of a lipid bilayer. Since cholesterol is virtually insoluble in water, this interfacial cholesterol could partially project into the bilayer-associated water layer without fully escaping the bilayer. The fraction of cholesterol molecules that make excursions into this juxtamembranous water layer is controlled by underlying interactions with membrane phospholipids, and is a measure of the chemical activity of cholesterol in the membrane. This first step is purely a feature of the lipid bilayer. The second step occurs in the aqueous phase and involves the binding of water-soluble PFO-D4 or ALO-D4 to cholesterol in the water-layer at the membrane periphery. In this model, the toxin molecules can be considered to be in a competitive binding equilibrium with the phospholipids for bilayer cholesterol (2). In aqueous solution, akin to the second step of this reaction scheme, the apparent binding affinity of PFO for cholesterol in the water phase is high (~100 nM as shown in Figure 1-5D). However, as shown in Figure 1-5B, when cholesterol-phospholipid interactions in bilayers are included, the apparent binding affinity of PFO is much weaker (~10 μM). In the extreme case where membrane cholesterol is below the switch-point concentration, interactions with phospholipids dominate the reaction, and there is very little apparent affinity of PFO for membrane cholesterol (>1000 μM). The sigmoidal dependence for PFO and ALO binding to membranes clearly involves the chemical activity of cholesterol, and this could dominate the reaction even if the binding of toxins to membranes is not reversible, and/or involves toxin oligomerization.

The chemical activity of cholesterol, which controls its surface accessibility to sensor proteins, generally increases as the concentration of cholesterol increases, but can be severely

suppressed at lower concentrations in a sigmoidal fashion due to interactions with bilayer phospholipids (complex formation) [120, 121, 145]. Theoretical studies have shown that cooperative formation of oligomers of such complexes can further sharpen the sigmoidal change in chemical activity, making it more threshold-like [121, 145]. This simple, intuitive model of complex formation has been extremely useful in accounting for many physical chemical properties of membranes [88, 94, 120, 121, 124, 145], however such complexes have not been isolated. This may not be surprising because molecular complexes in liquids have been described with relatively well-defined structures but very short lifetimes (< 10 picosec) [170]. A well-defined specific structure for phospholipid-cholesterol complexes may be unlikely since sharp changes in chemical activities are observed for a wide variety of phospholipid and sterol structures [88, 108, 145]. Other models that consider non-random arrangements of cholesterol in the bilayer could also result in sharp changes in its chemical activity [2, 109]. Phase separations provide another possible mechanism for triggering sharp changes in the chemical activity of membrane cholesterol, however no liquid phase separations have been observed in the simple DOPC-cholesterol and DPhyPC-cholesterol membranes used here [159, 160]. Whatever the mechanism modulating the chemical activity of cholesterol in membranes, it is clear that a property of the lipid bilayer itself can be a key regulator of cholesterol-sensing proteins.

Disappointingly, there are no high-resolution structures of PFO or ALO bound to cholesterol to test our proposed reaction scheme. However, it is worth examining the structure of cholesterol-bound Osh4, a soluble protein from yeast that is related to the family of mammalian oxysterol-binding protein (OSBP) related proteins (ORPs) that have been implicated in cholesterol homeostasis [81]. The structure of cholesterol-Osh4 shows no direct hydrogen bonds between Osh4 amino acid side chains and the hydroxyl group or any other part of cholesterol,

instead the cholesterol is bound through water-mediated interactions. On the other hand, the crystal structure of cholesterol-bound N-terminal domain of human Niemann Pick C1 (NPC1), a soluble protein involved in cholesterol transport from lysosomes, shows a snug binding pocket and direct close contacts between NPC1 amino acid side chains and the hydroxyl group and tetracyclic steroid nucleus of cholesterol [81]. It remains to be seen whether cholesterol sensors like ALO and PFO employ either one of these strategies for binding to membrane cholesterol.

The chemical activity of membrane cholesterol likely controls its surface accessibility to other soluble molecules such as cholesterol oxidase and cyclodextrin [88, 106, 121]. Of particular interest is a recent study which showed that the cholesterol binding site in Scap, the mammalian cholesterol sensor, is located not in its transmembrane region but in a membrane associated loop that projects into the lumen of the ER [96]. As noted in the Introduction, the binding of PFO to purified ER membranes and the activation of Scap by ER cholesterol both occur at a common threshold concentration of 5 mole% cholesterol. Based on our current understanding of ALO and PFO, it is tempting to speculate that Scap may be binding to a pool of ER cholesterol that exceeds the sequestration capacity of ER phospholipids and projects out of the ER bilayer. Despite the involvement of many proteins, a property of the ER lipid bilayer alone may be a key regulatory element of cholesterol homeostasis [86, 145]. Future studies with purified or reconstituted ER membranes and the tools developed here promise to clarify this issue.

CHAPTER TWO

ULTRASENSITIVE METHOD FOR MEASURING PROTEIN-MEDIATED CHOLESTEROL TRANSPORT BETWEEN FLUID BILAYERS

SUMMARY

A major challenge in membrane biology is to understand how hydrophobic lipids like cholesterol are moved from one lipid bilayer membrane to another through the hydrophilic, aqueous cytoplasm. Regulated cholesterol transport is critical for cellular function and understanding it requires new, robust techniques. Here, we describe a quantitative, label-free method to measure transport of cholesterol between membranes. A cholesterol-rich lipid vesicle suspension (donor) is introduced to a cholesterol-poor supported bilayer membrane on a glass surface (acceptor). Protein-mediated cholesterol transfer from donor to acceptor membrane is measured with a fluorescent sensor that amplifies small changes in cholesterol content of the acceptor membrane, allowing detection of as little as 1 picomole of transferred cholesterol. We measure cholesterol transport by human NPC2 (Niemann Pick C2) and yeast Osh4 (oxysterol-binding protein homolog) proteins, and show that two point mutations in NPC2 that cause cholesterol storage disease also render the protein defective in transporting cholesterol between membranes.

INTRODUCTION

Cholesterol is a critical component of animal cells that is unevenly distributed among cellular membranes. The intracellular gradient of cholesterol is carefully regulated to ensure that the plasma membrane (PM) receives the vast majority (60-90%) of total cell cholesterol [30, 87]. However, the sources of cellular cholesterol are located not in the PM, but in two other organelles, the endoplasmic reticulum (ER, site of cholesterol biosynthesis) and lysosomes (site of cholesterol release from lipoproteins taken up by receptor-mediated endocytosis) [12, 26]. Ferrying hydrophobic cholesterol through the aqueous cytoplasm from ER and lysosomes to PM involves poorly characterized vesicular and/or non-vesicular pathways [63, 82]. A major obstacle to understanding molecular details of these transport pathways and the eventual organization of cholesterol in cells is the lack of quantitative cell-free assays that can be implemented in a high-throughput manner.

Any approach to measure cholesterol transport between membranes faces two critical challenges – i) an efficient way to separate "donor" from "acceptor" membranes so that the cholesterol concentrations in acceptor membranes can be measured after cholesterol transfer from donors; and ii) a sensor that can accurately measure small changes in membrane concentration of label-free cholesterol. Here we describe a method that addresses these challenges and allows the measurement of transfer of as little as 1 picomole of unlabeled cholesterol between membranes. Our approach is compatible with multi-well plate formats and has several distinct advantages over previous attempts – i) the fluorescent sensor that we have developed amplifies small changes in cholesterol levels, allowing for robust detection of transferred cholesterol; ii) the fluorescent sensor detects unlabeled cholesterol, eliminating the

need for membranes with radioactive isotopes of cholesterol [3, 133], which can be cumbersome, or fluorescent versions of cholesterol, which can be misleading [43]; and iii) separation of donor from acceptor membranes does not require centrifugation or incorporation of biotinylated lipids [3, 133].

EXPERIMENTAL PROCEDURES

Materials –We obtained [1,2-^{3}H(N)] cholesterol from American Radiolabeled Chemicals; 1,2-dioleoyl-sn-glycero-3-phosphoethanolamine-N-(cap biotinyl) (Biotin PE) and 1,2-diphytanoyl-sn-glycero-3-phosphocholine (DPhyPC) from Avanti Polar Lipids; Coomassie Brilliant Blue R-250 staining solution from Bio-Rad; hydroxypropyl beta cyclodextrin (HPCD) from CTD Holdings; Alexa Fluor 488 C_5, 546 C_5, 555 C_2, 594 C_5, 647 C_2, and 750 C_5 maleimide, isopropyl-1-thio-β-d-galactopyranoside (IPTG), Oregon Green 488 1,2-dihexadecanoyl-sn-glycero-3-phosphoethanolamine (OG-DHPE) and Texas Red 1,2-dihexadecanoyl-sn-glycero-3-phosphoethanolamine (TR-DHPE), from Life Technologies; 1x FLAG peptide, anti-FLAG M2 antibody, anti-FLAG M2-agarose affinity beads, cholesterol, dithiothreitol (DTT), phenylmethanesulfonyl fluoride (PMSF), reduced L-glutathione, lysozyme, and tris (2-carboxyethyl) phosphine (TCEP) from Sigma-Aldrich; NanoLink streptavidin magnetic beads (0.8 μm) from Solulink (San Diego, CA); epicholesterol from Steraloids; and bovine serum albumin (BSA) and glutathione agarose beads from Thermo Scientific.

Buffers and medium – Buffer A contains 50 mM Tris-HCl (pH 7.5) and 150 mM NaCl. Buffer B is buffer A supplemented with 1 mM DTT. Medium A is a 1:1 mixture of Ham's F-12 medium and Dulbecco's modified Eagle's medium supplemented with 100 units/mL penicillin, 100 μg/mL streptomycin sulfate. Medium B is medium A supplemented with 5% (v/v) fetal calf serum (FCS), and 500 μg/mL G418 (selection antibiotic). Medium C is medium A supplemented with 1% (v/v) ITS (Life Technologies).

Expression plasmids – The following recombinant expression plasmids have been described: pHis$_{10}$-ALO (C472A K46C) encoding His$_{10}$-tagged anthrolysin O (ALO) with the

indicated point mutations in the pRSET B expression vector [40]; pNPC2(WT)-FLAG and pNPC2(V81D)-FLAG encoding the indicated versions of Niemann-Pick C2 (NPC2) with a COOH-terminal FLAG tag [69, 161]; pGST-Osh4 encoding glutathione-S-transferase (GST) fused to Osh4 (amino acids 2-434) with an intervening Tobacco Etch Virus (TEV) protease recognition site in the pGEX-4T expression vector [67]; pHis$_6$-TEV encoding His$_6$-tagged TEV protease [165]. We obtained pNPC2(WT)-His$_{10}$, pNPC2(V81D)-His$_{10}$, and pNPC2(P120S)-His$_{10}$ expression plasmids encoding the indicated versions of NPC2 with COOH-terminal His$_{10}$-tags, all in pFastBac1 expression vectors (Life Technologies), from Genscript Inc. The integrity of all plasmids was verified by DNA sequencing of the entire open reading frame.

Protein Purification and Labeling

ALO – Recombinant ALO was overexpressed, purified, and its lone cysteine was labeled with Alexa Fluor maleimide dyes as described previously (*CHAPTER 1*) [40]. The fluorescently labeled proteins are referred to as fALO-tag, where tag refers to the wavelength specification of the Alexa Fluor label. Degree of labeling was greater than 0.8 in all cases.

NPC2 from insect cells – On day 0, 1 liter cultures of Sf9 cells (5 x 10^5 cells/mL) in Sf-900 SFM medium (Life Technologies) were set up at 27°C. On day 1, cells were infected with NPC2-His$_{10}$ baculovirus produced according to the manufacturer instructions. On day 4, cells were harvested, flash frozen with liquid nitrogen, and stored at -80°C. A cell pellet from a 1L Sf9 cell culture was resuspended in 20 mL of buffer A containing 0.4 mg/ml PMSF and 1 protease inhibitor cocktail tablet (Complete Mini, EDTA-free, Roche). Cells were lysed using a Dounce homogenizer followed by a tip sonicator (Branson Inc) and then subjected to 220,000 x g centrifugation for 1h. The resulting supernatant was loaded on a column packed with nickel-

Sepharose 6 beads (GE Healthcare). The column was sequentially washed with 15 column volumes each of buffer A containing 10 mM, 30 mM and 50 mM imidazole, and bound proteins were eluted with buffer A containing 300 mM imidazole. Fractions containing NPC2 were pooled, concentrated, and subjected to gel filtration chromatography in buffer A using a Tricorn 10/300 Superdex 200 column. Fractions containing NPC2 were pooled, concentrated, and stored at 4°C. Protein concentrations were measured using a BCA kit.

NPC2 from mammalian cells – Procedures for the overexpression and purification of NPC2 from mammalian cells were adapted from previously described protocols [69, 161]. On day 0, CHO-K1 cells stably transfected with NPC2-FLAG plasmids were set up in 850-cm^2 roller bottles (BD Biosciences) containing 100 mL of medium B and cultured at 37°C in 8% CO_2. On day 3, the medium was removed and replaced with 100 mL of medium C. On day 5, media containing secreted NPC2 protein was collected, and fresh medium C was added. Media collection and replacement was repeated every 2 days thereafter until day 13 (5 total collections). After each collection, the media was filtered through a 0.22 μm vacuum filter apparatus (Millipore), concentrated 24-fold using a 10K MWCO Amicon Ultracel Centrifugal Filter device (Millipore), and stored at 4°C for up to 2 weeks. The concentrated media was pooled and loaded onto a column packed with 5 mL anti-FLAG M2-agarose beads (equilibrated with buffer A). After washing with 20 column volumes of buffer A, bound proteins were eluted with buffer A containing 0.1 mg/mL 1x FLAG peptide. Fractions containing NPC2 were pooled, concentrated, and subjected to gel filtration chromatography in buffer A using a Tricorn 10/300 Superdex 200 column (GE Healthcare). Fractions containing NPC2 were pooled, concentrated, and stored at 4°C. Protein concentrations were measured using a BCA kit (Pierce).

Oxysterol binding protein homolog (Osh4) - GST-Osh4 was transformed into BL21 (DE3) pLysS E. coli competent cells (Life Technologies) and protein overexpression was induced with 1 mM IPTG at 30°C for 16 hours. A cell pellet from a 1L bacterial culture was resuspended in 20 mL buffer B containing 1 mg/mL lysozyme, 0.4 mg/mL PMSF, and 1 protease inhibitor tablet, and incubated at 4°C for 3h. The lysozyme-disrupted cells were lysed using a Dounce homogenizer followed by a tip sonicator (Branson, Inc) and then subjected to 220,000 x g centrifugation for 1h. The resulting supernatant was incubated with 1 mL glutathione agarose beads (Thermo Scientific) at 4°C for 16h. The protein-bound glutathione agarose beads were then packed into a column, washed with 20 column volumes buffer B, and bound GST-Osh4 was eluted with buffer B containing 10 mM reduced glutathione. Eluted fractions containing GST-Osh4 were pooled and incubated with His_6-TEV protease (10:1 w/w) for 16h at 4°C. The proteolysis reaction was loaded onto a column packed with nickel-Sepharose 6 beads. Free GST, free Osh4 and residual uncleaved GST-Osh4, but not His_6-TEV protease, were eluted with buffer B containing 50 mM imidazole. This nickel elution was then loaded on a column packed with glutathione agarose beads. The flowthrough containing free Osh4 was concentrated and subjected to gel filtration chromatography in buffer B using a Tricorn 10/300 Superdex 200 Increase column. Fractions containing Osh4 were pooled, concentrated, and stored at 4°C. Protein concentrations were measured using a Nanodrop instrument (Thermo Fisher Scientific).

TEV Protease – Bacterial overexpression and purification of this protease was carried out in the same manner as for ALO. Purified His_6-TEV protease in buffer B containing 20% glycerol was flash frozen in liquid nitrogen and stored at -80°C.

Preparation of supported lipid bilayers in 96-well plates – The glass surface of each well of a 96-well glass-bottom plate (Thermo Scientific) was cleaned and processed by the following steps: i) wells were washed three times with water (350 µL each); ii) wells were treated with isopropanol (300 µL) for 30 min, followed by three washes with water (350 µL each); iii) wells were treated with 1 M NaOH (250 µL) for 1 hour, followed by five washes with water (350 µL each); iv) wells were dried under a stream of compressed air. Plates were then covered with lids, wrapped in aluminum foil, and used within one week. Supported lipid bilayers were generated on the processed glass surfaces of these wells by the following steps: i) wells were filled with water (80 µL) followed by addition of liposomes comprised of DPhyPC and the indicated amounts of sterols (30 µL of 1.6 mM stock), prepared as described previously [40]; ii) after incubation for 1 hour, undeposited liposomes were removed by three successive washing steps, each of which consisted of adding buffer A (200 µL) to each well followed by removing a fraction of the well contents (110 µL of 310 µL total); iii) wells were then treated with a blocking agent (150 µL of 0.5 mg/mL BSA in buffer A) to prevent nonspecific binding; iv) after incubation for 1 hour, unbound BSA was removed by three successive washing steps, each of which consisted of removing a fraction of the well contents (150 µL out of 350 µL total) followed by adding more buffer A (150 µL); v) after the last wash, 200 µL of the well contents was removed, leaving behind a supported lipid bilayer in a total volume of 150 µL of buffer A. All of the preceding steps were carried out at room temperature. Once liposomes were added to wells, caution was exercised to ensure that the glass surface and supported bilayer was not disturbed or exposed to air.

Assay for binding of fALO sensor proteins to sterol-containing liposomes – Each reaction mixture, in a total volume of 20 µL of buffer B in 1.5 mL tubes (Phenix Research Products),

contained 2 µg of fALO labeled with various Alexa Fluor dye and 8 nmoles of liposomes (total lipid) with varying molar ratios of DPhyPC and sterols, 1 mole% biotin-PE, and 0.2 mole% of a fluorescent tracer lipid (TR-DHPE or OG-DHPE). After incubation for 1 h at room temperature, buffer A (230 µL) was added to each reaction. The diluted reaction mixture (250 µL each) was transferred to 1.5 mL low retention tubes (Fisher Scientific) containing 5 µL of 10 mg/mL magnetic streptavidin beads (washed once with buffer A). After incubation for 30 min at room temperature, magnetic beads and bound liposome-fALO complexes were collected on the sides of tubes by placement on a magnetic stand for 2 min, and the unbound supernatant was removed. The beads were resuspended in 250 µL buffer A containing 1% (w/v) SDS, and bound fALO fluorescence from an aliquot (100 µL) was measured using a fluorescence microplate reader (Tecan Inc). Excitation and emission wavelengths ($\lambda_{ex}/\lambda_{em}$) for the various fALO sensor proteins and fluorescent lipids were as follows: fALO-488 (493 nm/516 nm), fALO-546 (554 nm/570 nm), fALO-555 (555 nm/572 nm), fALO-594 (588 nm/614 nm), fALO-647 (651 nm/672 nm), fALO-750 (753 nm/783 nm), TR-DHPE (582 nm/601 nm), and OG-DHPE (501 nm/526 nm).

Assay for binding of fALO-647 to sterol-containing supported lipid bilayers – Binding reactions were carried out in 96-well plates, the well surfaces of which were processed and covered with supported lipid bilayers as described above. Each binding assay, in a total volume of 160 µL of buffer A, contained 1 µg of fALO-647 sensor protein (18 pmoles), produced as described above. After incubation for 30 min, buffer A (190 µL) was added to increase the total reaction volume to 350 µL. Unbound fALO-647 was then removed by serial dilution with ten successive washing steps, each of which consisted of removing a fraction of the well contents (200 µL of 350 µL total) followed by adding more buffer A (200 µL). Membrane-bound fALO-647 was measured using a microplate fluorescence detector (Infinite M1000 Pro; Tecan Inc)

(excitation: 651 nm; emission: 672 nm; band pass: 5 nm). The amount of supported bilayer lipid on glass surfaces was quantified by measuring the fluorescence of a trace indicator lipid (TR-DHPE; excitation: 582 nm; emission: 601 nm; band pass: 5 nm). The ratio of bound fALO-647 fluorescence to TR-DHPE lipid fluorescence provides an estimate of fALO-647 binding per unit membrane surface area (see Figure 2-8 for a detailed description of converting these fluorescence values to cholesterol mass). fALO-647 binding to membrane surfaces was studied at higher spatial resolution using the detector's multi-read mode to measure fluorescence from smaller sub-regions of individual wells in the 96-well plate (Figure 2-1C).

Assay for transfer of cholesterol between membranes – Transfer reactions were carried out in 96-well plates, the well surfaces of which were covered with supported lipid bilayers (acceptor membranes; 0 mole% cholesterol, 99.8 mole% DPhyPC, 0.2 mole% TR-DHPE) as described above. Each transfer reaction, in a total volume of 210 µL, contained 150 µM donor liposomes (30 mole% cholesterol, 69.8 mole% DPhyPC, 0.2 mole% OG-DHPE), and indicated concentrations of transfer agents (HPCD, NPC2, or Osh4). After incubation at 37°C for 1 h, buffer A (140 µL) was added to increase the total reaction volume to 350 µL. Donor liposomes and transfer agents were then removed by serial dilution as described earlier and the new cholesterol content of acceptor membranes was measured using the fALO-647 binding assay described above.

RESULTS

Supported bilayer technology [8, 51, 74] provided a solution to the first challenge of gaining selective access to acceptor membranes in order to measure their cholesterol content after transfer reactions. We deposited lipid bilayers composed of binary mixtures of diphytanoyl-phosphatidylcholine (DPhyPC) and cholesterol (along with 0.2 mole% of TR-DHPE, a fluorescent lipid) on processed glass surfaces of wells in a 96-well glass bottom plate (Figure 2-1A and Figure 2-2). The resulting supported bilayers containing as much as 35 mole% cholesterol were fluid as judged by fluorescence recovery after photobleaching (Figure 2-3). These fluid bilayers served as acceptor membranes to which cholesterol-rich donor membranes and transfer agents could be conveniently added and then washed away. In these initial studies we chose DPhyPC as the bulk phospholipid because of its weak capacity to shield cholesterol from interactions with sensors and transporters [40].

The second challenge of measuring small changes in cholesterol content of acceptor membranes after cholesterol transfer reactions was solved by the use of anthrolysin O (ALO), a soluble bacterial protein that has been recently shown to bind membrane cholesterol with high specificity and sensitivity [40]. When incubated with supported bilayers containing increasing amounts of cholesterol, binding of fluorescently labeled ALO (fALO-647, Figure 2-4) increased 65-fold when the cholesterol content increased by just 3-fold, from 10 mole% to 30 mole% of total lipids (Figure 2-1B). No fALO-647 binding was observed when the supported bilayers contained epicholesterol, a diastereomer of cholesterol (Figure 2-1B). Closer inspection of bound fALO-647 in the supported bilayer-covered wells showed an exact spatial correlation between fluorescence from fALO-647 (*green*) and that from TR-DHPE (*red*), a trace reporter in the

supported bilayer, confirming specific fALO-647 binding to the membrane surface without non-specific adhesion to well edges (Figure 2-1C and Figure 2-5). Equilibrium binding of fALO-647 to supported bilayers was reached after ~30 min and showed a linear dependence on the amount of fALO-647 added to the well (Figure 2-6).

We exploited this specific and amplified fALO-647 response to monitor changes in cholesterol levels of supported bilayer acceptor membranes after transport of cholesterol from donor membranes (Figure 2-7A). To catalyze cholesterol transfer between membranes, we initially used hydroxypropyl β-cyclodextrin (HPCD), a cyclic oligosaccharide that binds cholesterol and is commonly used as a reagent to manipulate cholesterol levels in cell membranes [75, 104]. Acceptor membranes devoid of cholesterol were incubated with cholesterol-rich donor vesicles (30% cholesterol, 70% DPhyPC) in the absence or presence of HPCD for 1h, after which donor vesicles and HPCD were washed away. Newly transferred cholesterol in acceptor membranes was then assayed by fALO-647 binding as described above (Figure 2-1B). We converted the bound fALO-647 fluorescence values into cholesterol mass by using as calibration standards fALO-647 bound to membranes with known amounts of cholesterol (Figure 2-8). To check the fidelity of our calibration method, we conducted a series of HPCD-mediated cholesterol transfer reactions from donor vesicles containing ^{3}H-cholesterol to cholesterol-null acceptor membranes. We measured the transferred ^{3}H-cholesterol directly by scintillation counting and also by fALO-647 binding as described above, and found a strong linear correlation between the two measurements with a best-fit slope of 5.03 (Figure 2-7B). We incorporated this correction factor into our fALO-647-based cholesterol calibration method (Figure 2-8) and used it to quantify HPCD-mediated cholesterol transfer between membranes (Figure 2-7C). In the absence of HPCD, there is no spontaneous transfer of cholesterol from

cholesterol-rich donor membranes to cholesterol-poor acceptor membranes. Addition of HPCD catalyzes the transfer of as much as 100 pmol of cholesterol in a time- and dose-dependent manner. Based on the fluorescence detection limits of our instrument (Infinite M1000 Pro, Tecan Inc.), we estimate that the lowest amount of transferred cholesterol that could be measured in this assay is ~ 1 pmole.

We next applied this fALO-647-based cholesterol transfer assay to characterize human Niemann Pick C2 (NPC2), a soluble glycoprotein that binds cholesterol and moves it between membranes during sperm maturation in epididymal fluid [107] and during the transport of lipoprotein-derived cholesterol from lysosomes to PM and ER [101]. We overexpressed His_{10}-tagged versions of wild-type (WT) NPC2 in insect cells and purified the glycosylated protein using nickel chromatography followed by gel filtration chromatography (Figure 2-9). We also purified a disease-causing mutant version of NPC2 that does not bind cholesterol (P120S) [69], and a mutant version that binds cholesterol but does not catalyze transfer of cholesterol to the N-terminal domain of Niemann Pick C1 (V81D) [161]. When we incubated acceptor membranes with cholesterol-rich donor vesicles in the presence of increasing concentrations of NPC2 proteins for 1 h, we observed saturable transfer of ~400 pmol of cholesterol by NPC2-WT, but not by the cholesterol-binding mutant NPC2-P120S (Figure 2-7D). Interestingly, NPC2-V81D also did not transfer any cholesterol to acceptor membranes, suggesting that the V81D mutation disrupts the interaction of NPC2 not only with NPC1 but also with membrane surfaces. To ensure that the cholesterol transfer deficiency of NPC2-V81D was not due to aberrant glycosylation of this human protein by the insect cell machinery, we overexpressed and purified NPC2-WT and NPC2-V81D from mammalian cells, and observed robust cholesterol transfer by NPC2-WT, but not by NPC2-V81D or by a control protein BSA (Figure 2-10).

Finally, we applied the fALO-647-based cholesterol transfer assay to study yeast oxysterol binding protein homolog (Osh4), a cytoplasmic sterol-binding protein that has been implicated in transporting sterols from ER to PM [41, 67, 133]. We overexpressed Osh4 with a glutathione S-transferase tag (GST-Osh4) in bacterial cells and purified it by GST affinity chromatography. Cleavage of the GST tag by TEV protease, followed by gel filtration chromatography yielded highly purified Osh4 (Figure 2-11). When we incubated acceptor membranes with cholesterol-rich donor vesicles, we observed saturable transfer of ~100 pmol of cholesterol by Osh4, but not by BSA (Figure 2-7E).

FIGURE 2-1

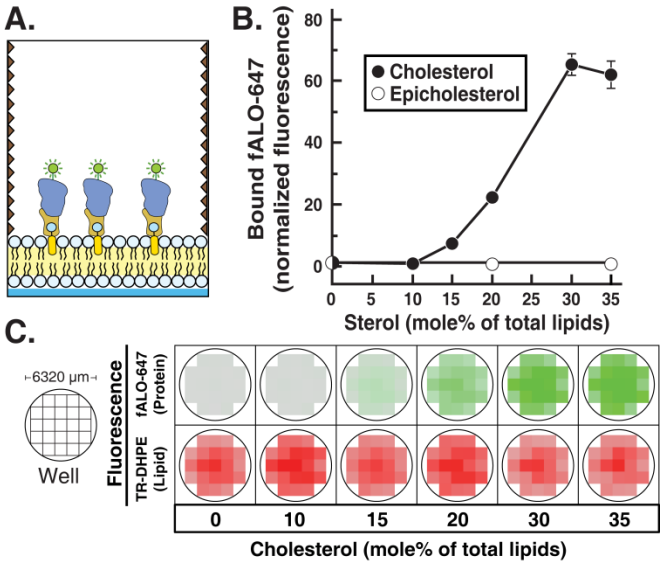

Figure 2-1. Sensitivity and specificity of fALO-647 for membrane cholesterol. (A) Schematic representation of fALO-647 binding to cholesterol-containing fluid supported bilayers in 96-well plates. (B) Supported bilayers composed of DPhyPC, indicated concentrations of cholesterol or epicholesterol, and a trace amount (0.2 mole%) of fluorescent TR-DHPE were generated on processed glass surfaces of 96-well glass-bottom plates and binding of fALO-647 to these membranes was measured (Error bars: n = 6, mean ± s.e.m.). (C) Fluorescence values from 21 sub-regions in single wells of a 96-well plate containing the indicated cholesterol concentration (one of 6 replicates from B) shows exact spatial correlation between bound fALO-647 (green) and supported bilayer lipids (TR-DHPE, red).

FIGURE 2-2

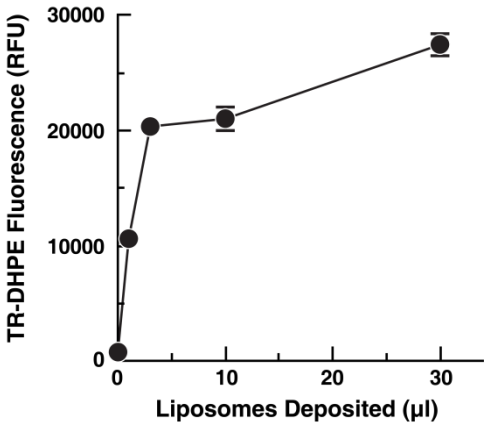

Figure 2-2. Generation of supported bilayer membranes in 96-well glass-bottom plates. Glass surfaces were processed as described (*Experimental Procedures*) and incubated with varying amounts of liposomes composed of DPhyPC (total lipid concentration of liposome stocks: 1.6 mM). After 1 h, unbound liposomes were washed away as described in *Experimental Procedures*, and lipids retained on the glass surface as supported bilayers were quantified by measuring fluorescence of TR-DHPE, a fluorescent lipid incorporated in liposomes at a trace concentration of 0.2 mole% of total lipids (Error bars: n = 3, mean ± s.e.m.). TR-DHPE fluorescence reaches a plateau value when the glass surface is completely covered by a lipid bilayer; further increases may indicate the formation of lipid multilayers.

FIGURE 2-3

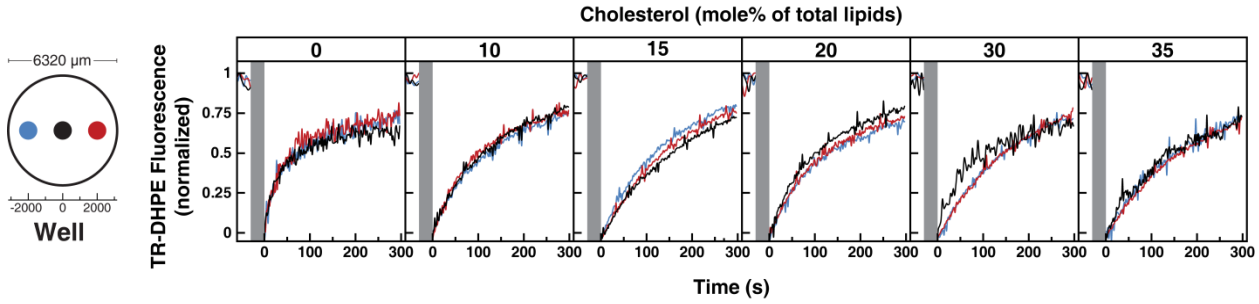

Figure 2-3. Lateral fluidity of supported bilayer membranes in 96-well glass-bottom plates. Supported lipid bilayers composed of DPhyPC and the indicated concentrations of cholesterol were generated on processed glass surfaces of 96-well plates as described in *Experimental Procedures*. All membranes contained a trace amount (0.2 mole% of total lipids) of TR-DHPE, a fluorescent lipid. (*Left*) Schematic diagram of a single well in a 96-well plate (diameter: 6320 µm). A focused beam from a 561 nm laser source (~15 µm in diameter) was used to photobleach TR-DHPE molecules in the three indicated circular regions. (*Right*) Epifluorescence microscopy (Nikon Ti-E microscope, 60x objective) was used to monitor TR-DHPE fluorescence from the three photobleached circular regions over time (fluorescence values 30 s before the photobleaching step are normalized to 1). Recovery of fluorescence, indicative of lateral fluidity of lipid molecules, was observed in all cases, even when the membranes contained 35 mole% cholesterol.

FIGURE 2-4

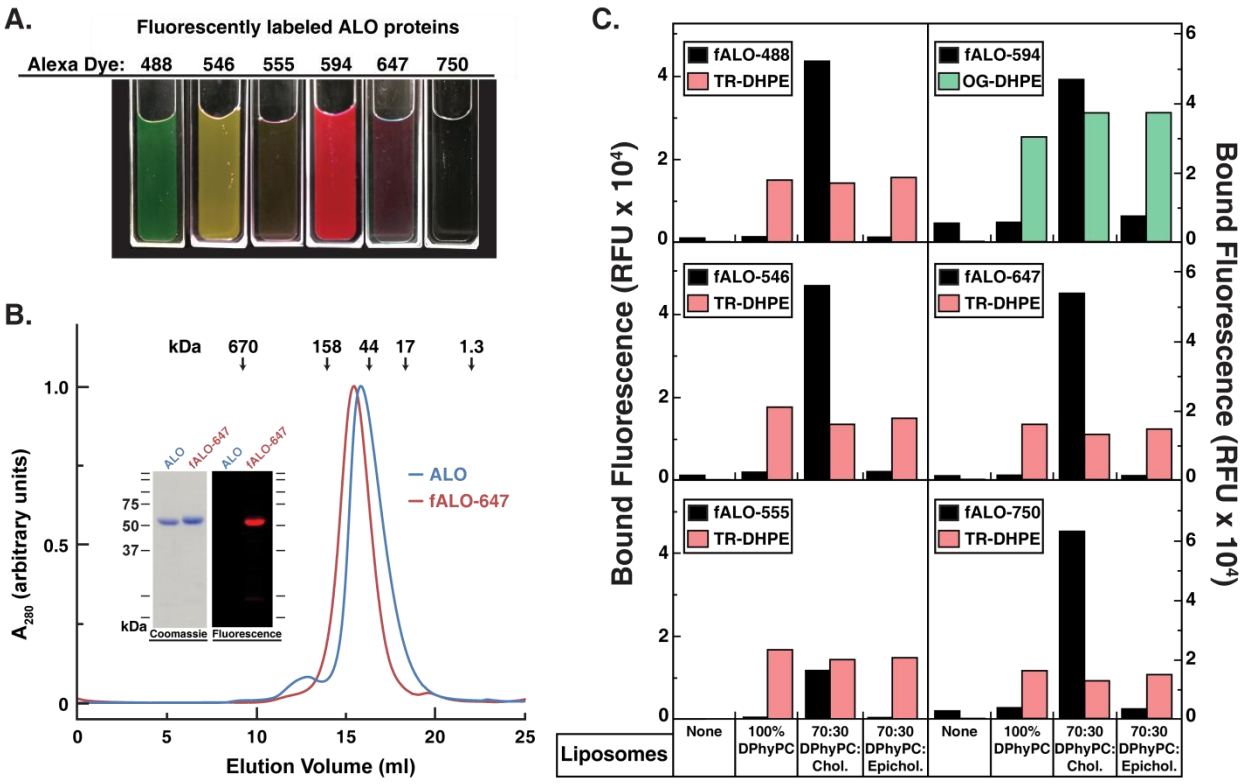

Figure 2-4. Activity of fluorescently labeled ALO sensor proteins. (A) Fluorescently labeled ALO sensor proteins (fALO). Recombinant His_{10}-tagged ALO was purified and labeled with the indicated Alexa Fluor maleimide dyes as described in *Experimental Procedures*. Each cuvette, in a total volume of 100 µL of buffer B, contains 100 µg of fluorescently labeled ALO. (B) Gel filtration chromatography. Samples of ALO (5.8 mg in a total volume of 1 mL) or ALO labeled with Alexa Fluor 647 (fALO-647; 750 µg in a total volume of 1 mL) were loaded on a Superdex 200 column and chromatographed at a flow rate of 0.5 mL/min. fALO-647 eluted as a single sharp peak at a similar volume (15.5 mL) as ALO (15.9 mL). Standard molecular weight markers were chromatographed on the same column under the same conditions (arrows). (*Inset*) An

aliquot of ALO and fALO-647 (3 µg each) was subjected to 10% SDS-PAGE, and proteins were visualized by Coomassie Brilliant Blue R-250 stain or by fluorescence scanning using a LI-COR Odyssey infrared imaging system at 700 nm. (C) Interaction of fALO sensor proteins with sterol-containing liposomes was measured as described in *Experimental Procedures*. All labeled proteins showed binding to cholesterol-containing liposomes, but not to epicholesterol-containing liposomes or to liposomes without sterols.

FIGURE 2-5

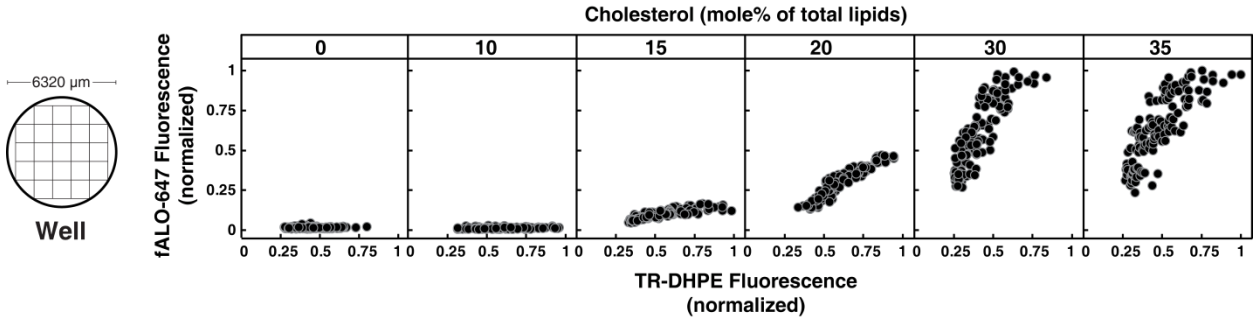

Figure 2-5. Spatial localization of binding of fALO-647 to supported bilayer membrane surfaces in 96-well plates. Supported lipid bilayers composed of DPhyPC and the indicated concentrations of cholesterol were generated on processed glass surfaces of 96-well plates as described (*Experimental Procedures* and Fig. 2-1B). All membranes contained a trace amount (0.2 mole% of total lipids) of TR-DHPE, a fluorescent lipid. Binding of cholesterol-sensing fALO-647 to these membranes was measured as described in *Experimental Procedures*. (*Left*) Schematic diagram of a single well in a 96-well plate (diameter: 6320 μm) with 21 sub-regions from which fluorescence of TR-DHPE lipid or bound fALO-647 was measured. (*Right*) Plots showing spatial correlation of normalized fluorescence values from TR-DHPE (x-axis) and bound fALO-647 (y-axis). Each point represents fluorescence values from one of the 21 sub-regions of 6 replicate wells containing the indicated concentration of cholesterol (126 points/condition).

FIGURE 2-6

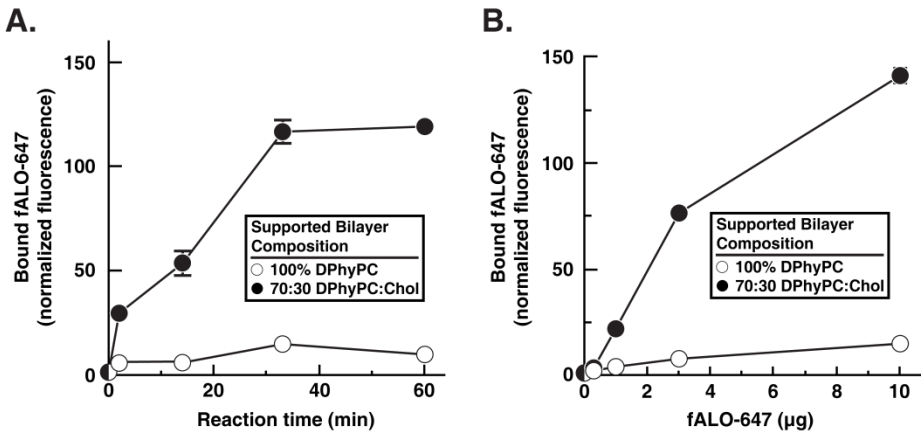

Figure 2-6. Time and concentration dependence for binding of fALO-647 to supported bilayers in 96-well plates. Supported lipid bilayers with the indicated compositions were generated on processed glass surfaces of 96-well plates as described in *Experimental Procedures*. All membranes contained a trace amount (0.2 mole% of total lipids) of TR-DHPE, a fluorescent lipid. Binding of cholesterol-sensing fALO-647 to these membranes was measured as described in *Experimental Procedures*, and expressed as bound fALO-647 fluorescence divided by TR-DHPE fluorescence (an estimate of fALO-647 binding normalized to membrane surface area). Binding assays were carried out with 1 µg fALO-647 for the indicated times (A) or with the indicated amounts of fALO-647 for 1 h (B) (Error bars: $n = 3$, mean ± s.e.m.).

FIGURE 2-7

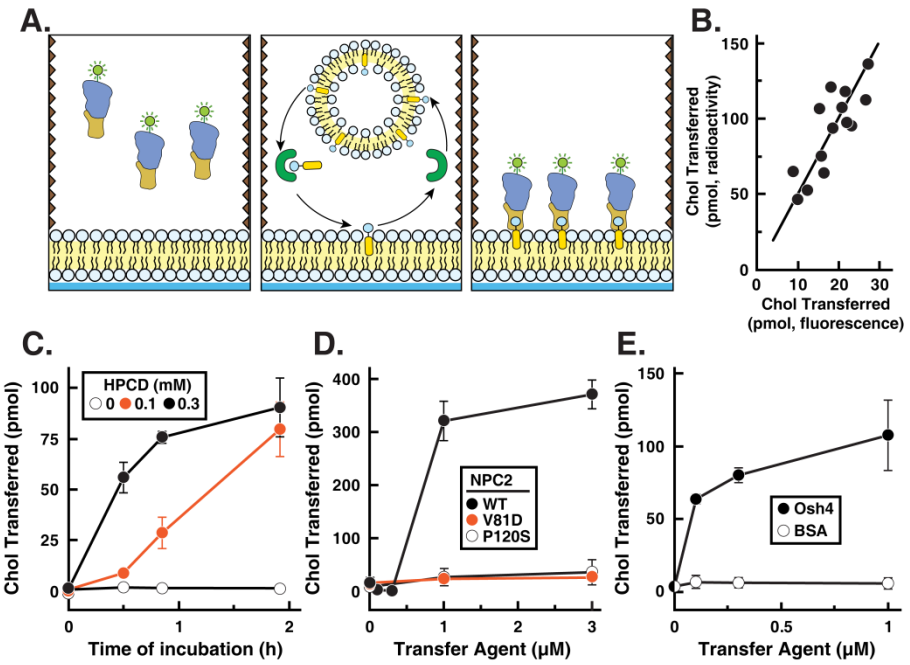

Figure 2-7. Transport of cholesterol between membranes. (A) Schematic representation of movement of cholesterol by transfer agents from donor liposomes containing 30 mole% cholesterol to acceptor supported bilayers devoid of cholesterol. (B) Estimation of transferred cholesterol by fALO-647 sensors is calibrated by carrying out HPCD-catalyzed transfer from ^{3}H-cholesterol-containing donor liposomes and measuring transferred cholesterol in acceptor supported bilayers by scintillation counting and by fALO-647 binding (correction factor is slope of best-fit line: 5.03). c-e) Transfer of cholesterol from cholesterol-containing liposomes (donor) to supported bilayers (acceptor) by indicated transfer agents (Error bars: n = 3, mean ± s.e.m). The transfer agents are HPCD (C), wild-type and mutant versions of NPC2 (D), and Osh4 (E).

FIGURE 2-8

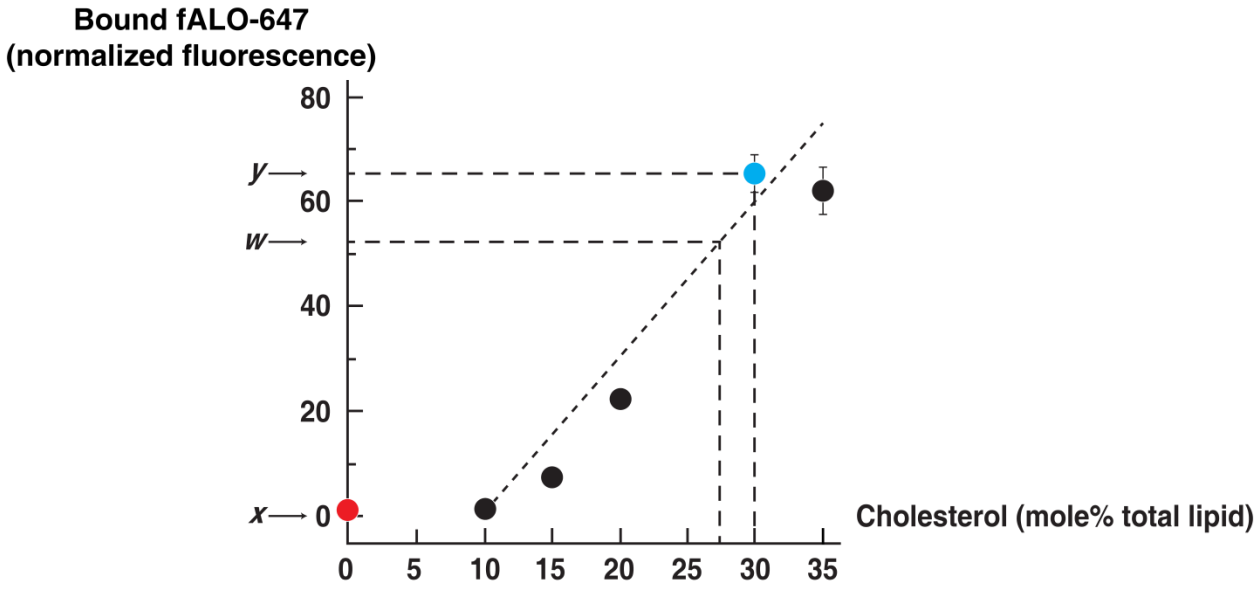

Figure 2-8. Quantification of cholesterol transferred from donor membranes to supported bilayer acceptor membranes using fALO-647 binding assays. As shown above (data replotted from Figure 2-1B), binding of fALO-647 (normalized to supported bilayer membrane area as measured by TR-DHPE fluorescence) shows a linear dependence on the molar percentage of cholesterol in supported bilayers in the composition range of 10-30 mole% cholesterol. In all our cholesterol transfer assays, we measure the normalized fluorescence from fALO-647 bound to supported bilayers containing 0 mole% cholesterol (red circle, *x*) and 30 mole% cholesterol (blue circle, *y*), as described in *Experimental Procedures*. In multiple experiments, we have observed no binding of fALO-647 to supported bilayers until the cholesterol concentration exceeds 10 mole% of total lipids. Therefore, fluorescence values from fALO-647 bound to bilayers without cholesterol are used as an estimate for fALO-647 binding to bilayers containing 10 mole% cholesterol. Using the reported diameter of 6.32 mm for a well in a 96-well plate (Greiner Bio-

One), the moles of cholesterol in wells containing 10 and 30 mole% cholesterol are (5.211/a) and (15.633/a) nanomoles, respectively, where a is the area per lipid molecule in DPhyPC/cholesterol bilayers (units of $Å^2$/molecule). The nanomoles of cholesterol transferred to the supported bilayer, z, corresponding to a normalized bound fALO-647 fluorescence value of w, is easily obtained using linear extrapolation and is expressed as:

$$z = \frac{10.422(w - x)}{a(y - x)}$$

This expression contains only one adjustable parameter, a. Since there are no published values for the area per molecule in DPhyPC/cholesterol bilayers, we estimated this parameter to be 50 $Å^2$/molecule based on values obtained for other lipids and lipid mixtures [66, 111] (we do not take into account the cholesterol-mediated area condensation effects on the value of this parameter). Comparison of this calculated value for transferred cholesterol to direct measurement of ^{3}H-cholesterol transferred from liposomes containing ^{3}H-cholesterol showed a remarkably strong linear correlation, with the slope of 5.03 serving as a correction factor (Figure 2-7B). Incorporation of this correction factor into the above expression allowed for quantification of transferred cholesterol using fALO-647 binding.

FIGURE 2-9

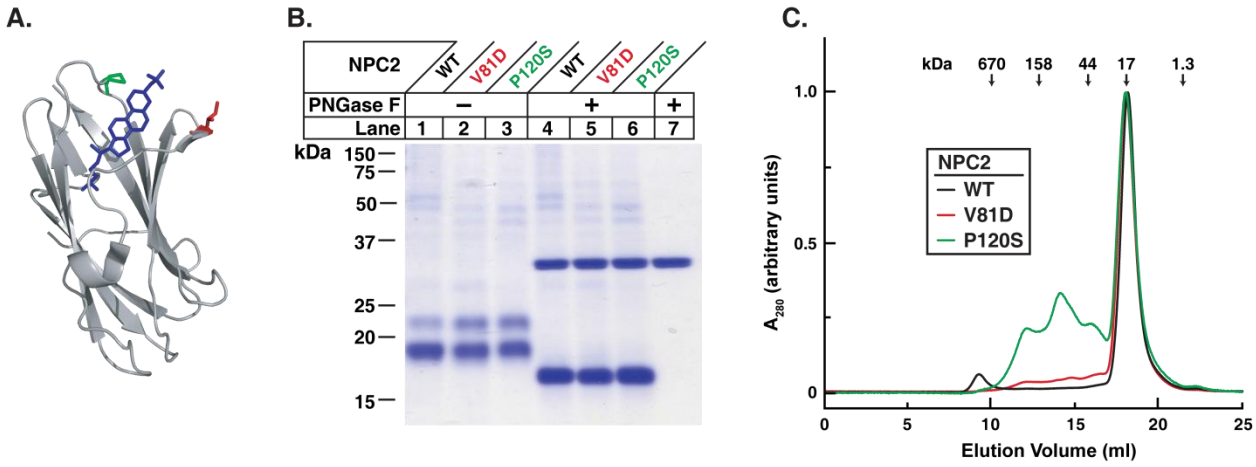

Figure 2-9. Characterization of NPC2 purified from insect cells. (A) Structure of NPC2 bound to cholesterol-3-*O*-sulfate [163]. A ribbon representation of the α-carbon backbone of the crystal structure of bovine NPC2 (gray) is shown with bound cholesterol-3-*O*- sulfate (blue) and locations of two functionally important amino acid residues, Ile 81 (red, Val in human NPC2) and Pro 120 (green, Pro in human NPC2). (B) Purification of glycosylated NPC2 from insect cells. Recombinant wild-type (WT) and mutant versions (V81D and P120S) of His_{10}-tagged human NPC2 were overexpressed in Sf9 insect cells and purified as described in *Experimental Procedures.* Aliquots of purified protein (4 µg) were subjected to 15% SDS-PAGE, and proteins were visualized by Coomassie Brilliant Blue R-250 stain (*lanes 1-3*). Both WT and mutant versions of the protein electrophoresed as a doublet species, due to glycosylation modifications. Treatment of glycosylated NPC2 with PNGase F enzyme (according to manufacturer's instructions, New England Biolabs) resulted in a collapse of both bands into a single homogeneous species at a molecular weight of ~16 kDa, close to the calculated molecular weight of NPC2 (lanes 4-6). (C) Gel filtration chromatography. Samples of purified glycosylated NPC2-

WT, NPC2-V81D, or NPC2-P120S (100 µg in a total volume of 1 mL) were loaded on a Tricorn 10/300 Superdex 200 Increase column and chromatographed at a flow rate of 0.75 mL/min. NPC2-WT and NPC2-V81D eluted as single sharp peaks at similar volumes of 18.2 and 18.1 mL, respectively. NPC2-P120S eluted as a sharp peak as well at 18.1 mL, but a fraction of this protein eluted at earlier volumes. This fast-migrating fraction of NPC2-P120S, likely representing aggregated species, was not included when assaying for cholesterol transfer. Standard molecular weight markers were chromatographed on the same column under the same conditions (*arrows*).

FIGURE 2-10

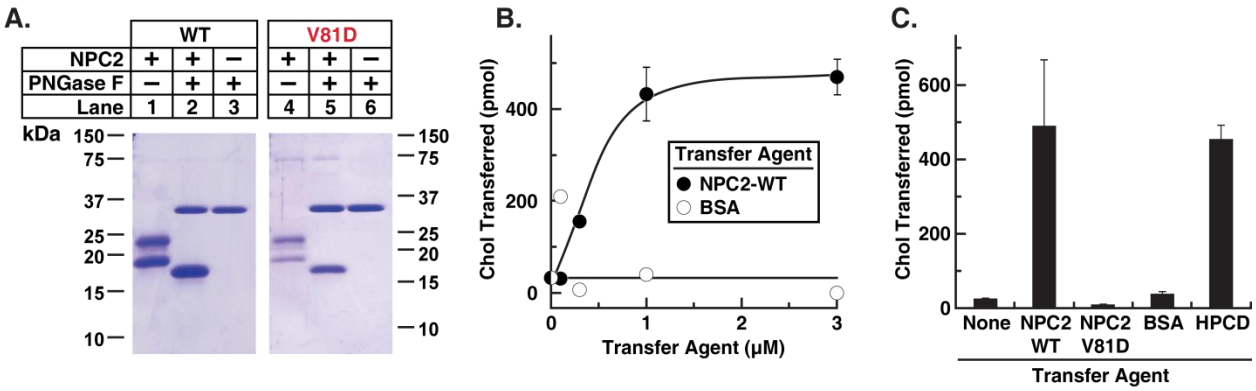

Figure 2-10. Characterization of NPC2 purified from mammalian cells. (A) Purification of glycosylated NPC2 from mammalian cells. Recombinant human NPC2(WT)-FLAG and NPC2(V81D)-FLAG were overexpressed in mammalian cells and purified as described in *Experimental Procedures*. Aliquots of purified protein (3 μg for WT and 0.9 μg for V81D) were subjected to 15% SDS-PAGE, and proteins were visualized by Coomassie Brilliant Blue R-250 stain (*lanes 1 and 4*). Both WT and mutant versions of the protein electrophoresed as a doublet species, due to glycosylation modifications. Treatment of glycosylated NPC2 with PNGase F enzyme (according to manufacturer's instructions, New England Biolabs) resulted in a collapse of both bands into a single homogeneous species at a molecular weight of ~16 kDa, close to the calculated molecular weight of NPC2 (*lanes 2 and 4*). (B and C) Transfer of cholesterol between membranes by NPC2-WT and NPC2-V81D purified from mammalian cells. Supported bilayers composed of DPhyPC (acceptor membrane) were generated on a processed glass surface of 96-well plates as described in *Experimental Procedures*. All membranes contained a trace amount (0.2 mole% of total lipids) of TR-DHPE, a fluorescent lipid. Cholesterol transfer reactions were carried out as described in *Experimental Procedures* using donor liposomes containing 30

mole% cholesterol and the indicated concentrations of NPC2-WT or bovine serum albumin (BSA) for 1 h at 37 °C (B), or the indicated transfer agent (1 μM protein or 1 mM HPCD) for 1 h at 37 °C (C). Newly-transferred cholesterol in acceptor membranes was then assayed by fALO-647 binding as described in *Experimental Procedures* (Error bars: $n = 3$, mean ± s.e.m.).

FIGURE 2-11

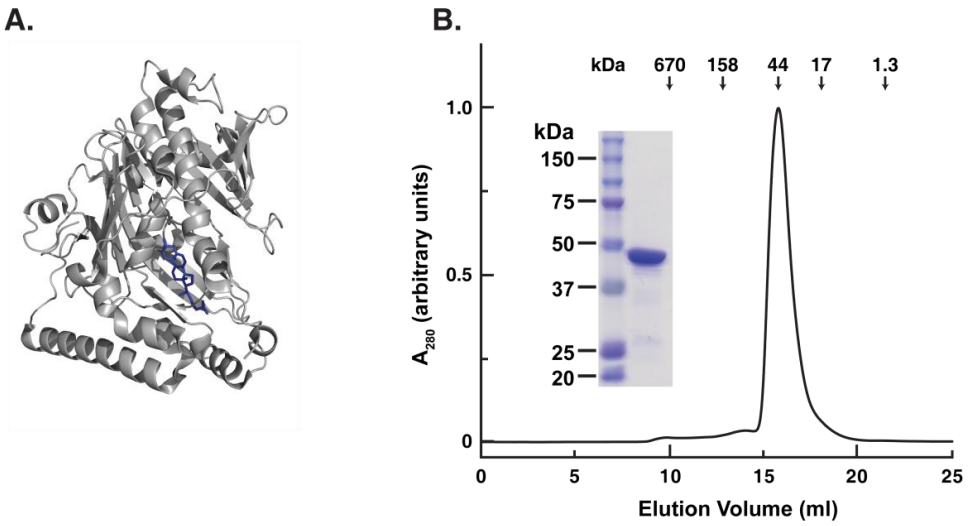

Figure 2-11. Characterization of Osh4. (A) Structure of Osh4 bound to 25-hydroxycholesterol [67]. A ribbon representation of the α-carbon backbone of the crystal structure of yeast Osh4 (gray) with bound 25-hydroxycholesterol (blue). (B) Gel filtration chromatography. Recombinant Osh4 was purified as described in (*Experimental Procedures*) and an aliquot (1 mg in a total volume of 1 mL) was loaded onto a Tricorn 10/300 Superdex 200 Increase column and chromatographed at a flow rate of 0.75 mL/min. Osh4 eluted as a single sharp peak at 15.8 mL. Standard molecular weight markers were chromatographed on the same column under the same conditions (*arrows*). (*Inset*) An aliquot of purified Osh4 (5 µg) was subjected to 10% SDS-PAGE, and proteins were visualized by Coomasie Brilliant Blue R-250 stain.

DISCUSSION

In summary, we report a method that uses a fluorescent cholesterol sensor (fALO-647) to detect cholesterol transfer between fluid lipid membranes. The method does not require labeling of the cholesterol molecule, and can detect as little as 1 pmol of transferred cholesterol, which is 20 times more sensitive than the lower detection limit of cholesterol oxidase, an enzyme commonly used to measure membrane cholesterol (Invitrogen, Inc.). The method also does not require modification of donor and acceptor membranes for separation, allowing for its extension to use vesicles derived from purified cell membranes as donor and acceptors. Finally, the assay can be conveniently carried out in multi-well plates, does not involve any centrifugation steps, and requires no specialized equipment other than a standard fluorescence plate-reader. These features should allow for the rapid adoption of this method to study the mechanistic details of cholesterol transfer proteins such as NPC2 or Osh4, and to screen for as yet unidentified cytosolic proteins that catalyze cholesterol transport between membranes.

CHAPTER THREE

TOOLS FOR PROBING SPHINGOMYELIN-SEQUESTERED CHOLESTEROL IN PLASMA MEMBRANES OF ANIMAL CELLS

INTRODUCTION

While the majority of a cell's total cholesterol resides in the PM (60-90%), cholesterol levels are sensed in the ER, which contains less than 2% of the cell's cholesterol [85, 87]. Roughly one out of two lipid molecules found in the PM are cholesterol; the ER cholesterol concentration teeters around only ~5 mole % total lipid [145]. Interestingly, the binding of soluble bacterial sensors such as PFO or ALO to purified PM and ER does not occur until a threshold cholesterol concentration is exceeded: 40 mole % for PM and 5 mole % for ER [27, 145]. The distinct phospholipid compositions of PM and ER are likely the reasons for the vastly different threshold values for cholesterol accessibility in these membranes. In the ER, the threshold value of 5 mole % cholesterol results in fine-tuning the activation of SREBP [118]. In recent studies, it was proposed that the PM's threshold of 40 mole % cholesterol likely means that cholesterol derived from LDL in lysosomes does not travel to the ER to signal SREBP machinery until the large needs of the PM are satisfied, though this point remains under debate [26]. This ensures that cholesterol uptake and synthesis are not terminated prematurely. In our recent work, we analyzed the PM cholesterol pools in human fibroblasts using cell surface labeling. In this study, a non-lytic ^{125}I-labeled version of PFO, and found that PMs contain three distinct pools of cholesterol [26]. One is a labile pool that declines when cells are deprived of

cholesterol while allowing cells to remain viable. The second pool is inaccessible to 125I-PFO until membranes are treated with sphingomyelinase (SMase), and is referred to as the "sphingomyelin (SM)-sequestered pool" [131]. This pool is constant and does not decline when cells are deprived of cholesterol. The third pool is an "essential pool" and remains intact until cells are treated with powerful cholesterol removing agents like cyclodextrins. Depletion of the essential pool leads to cell death. The physical nature of these pools, especially that of the SM-sequestered pool, is unknown.

Historically, sphingomyelin (SM) has been thought of as an important lipid in cholesterol organization within the membrane; a stoichiometric interaction with defined structure between these two lipids has been proposed [35]. Several studies have postulated that plasma membranes contain distinct microdomains rich in SM and cholesterol, but this remains a controversial idea. Sphingolipid domains in fibroblast PMs are not enriched in cholesterol [10, 38, 39, 79]. The driving force behind this patchy SM distribution is currently under debate. While some support the hypothesis that lipids are able to partially self-organize in biological membranes through lipid-lipid interactions, others propose that this organization is primarily mediated by lipid-protein and protein-protein interactions on the membrane surface and in conjunction with the cytoskeleton [56, 62, 78, 140]. Whether or not lipid rafts form and function as self-assembling entities, SM is an important lipid in cholesterol regulation [98], and understanding its function requires new tools and techniques. Here, I present my preliminary work towards developing novel ways to probe cells for these lipids.

EXPERIMENTAL PROCEDURES

Materials – We obtained 1,2-dioleoyl-sn-glycero-3-phosphocholine (DOPC), egg sphingomyelin, and N-oleoyl-D-erythro-sphingosylphosphorylcholine (18:1 SM) from Avanti Polar Lipids; Coomassie Brilliant Blue R-250 staining solution from Bio-Rad; hydroxypropyl beta cyclodextrin (HPCD) from CTD Holdings; Alexa Fluor 488 C5, and 647 C2 maleimide, isopropyl-1-thio-β-d-galactopyranoside (IPTG), and Texas Red 1,2-dihexadecanoyl-sn-glycero-3-phosphoethanolamine (TR-DHPE) from Life Technologies; cholesterol, dithiothreitol (DTT), phenylmethanesulfonyl fluoride (PMSF), lysozyme, and tris (2-carboxyethyl) phosphine (TCEP) from Sigma-Aldrich; epicholesterol from Steraloids; and bovine serum albumin (BSA) and glutathione agarose beads from Thermo Scientific. Newborn calf lipoprotein-deficient serum (LPDS) was prepared by ultracentrifugation, as described previously [45].

Buffers and medium – Buffer A contains 50 mM Tris-HCl (pH 7.5) and 150 mM NaCl. Buffer B is buffer A supplemented with 1 mM dithiothreitol (DTT). Buffer C is buffer A supplemented with 1 mM TCEP. Buffer D contains 50 mM Tris-HCl (pH 7.5) and 1 mM TCEP. Buffer E is DPBS supplemented with 2% (v/v) LPDS and 1 mM EDTA. Buffer F is 20 mM sodium phosphate (pH 8.0) and 150 mM NaCl. Medium A is a 1:1 mixture of Ham's F-12 medium and Dulbecco's modified Eagle's medium supplemented with 100 U/mL penicillin, and 100 µg/mL streptomycin sulfate. Medium B is medium A supplemented with 5% FCS. Medium C is medium A supplemented with 5% LPDS, 50 µM compactin and 50 µM mevalonate.

Cell culture – CHOK1 cells were grown as monolayer cultures at 37°C in an 8.8% CO_2 incubator and maintained in medium B.

Plasmids – The gene encoding lysenin from *Eisenia fetida* with a COOH-terminal His_6 tag and flanked by *Bam*HI and *Eco*RI restriction sites was synthesized by GenScript with codon selection optimized for bacterial overexpression, and was provided to us in the pUC57 vector. The lysenin gene was then excised and ligated into the pRSET B expression vector. The His_6 tag from the pRSET B vector near the NH_2-terminal active site of lysenin was removed through site-directed mutagenesis. This construct of full-length lysenin with a COOH-terminal His_6 tag is hereafter referred to as lysenin. A plasmid encoding OlyA from *Plurotus ostreatus* with a C-terminal His_6 tag in the pET21c vector was the generous gift of Kristina Sepcić (Department of Biology, University of Ljubljana). Two native cysteines were mutated to serine (C62S, C94S) and a single cysteine was introduced to the COOH-terminus (S151C) through site-directed mutagenesis. This construct is hereafter referred to as OlyA. A plasmid expressing a truncated version of full-length anthrolysin O (Domain 4, amino acids 35-512) from *Bacillus anthracis* (codon-optimized by Genscript for overexpression) in pRSET B with the sole native cysteine mutated to alanine (C472A) and a single cysteine added to the NH_2-terminus (S404C) through site-directed mutagenesis has been described previously and is hereafter referred to as ALO-D4 [40]. All site-directed mutagenesis was carried out using a QuickChange II XL Site-Directed Mutagenesis Kit (Agilent). The integrity of all plasmids was verified by DNA sequencing of the entire open reading frame.

Protein overexpression and purification

All constructs were transformed into BL21 (DE3) pLysS E. coli competent cells (Life Technologies). Protein overexpression was induced with 1 mM IPTG at 25°C for 20 h (lysenin), 0.5 mM IPTG at 37°C for 4 h (OlyA), or 0.5 mM IPTG at 18°C for 16 h (ALO-D4). Each cell

pellet from a 1L bacterial culture was resuspended in 20 mL buffer C (OlyA and ALO-D4) or buffer F (lysenin) containing 1 mg/mL lysozyme, 0.4 mg/mL PMSF, and 1 protease inhibitor cocktail tablet (Roche, cOmplete, Mini, EDTA-free). Cells were disrupted using a Dounce homogenizer, followed by incubation to complete lysozyme treatment for 3 h at 4°C, further Dounce homogenization, and finally tip sonication (Branson, Inc). Homogenate was subjected to centrifugation at 25,000 x g (lysenin) or 220,000 x g for 1 h at 4°C.

Lysenin – Post-spin supernatant was loaded onto a 1 mL nickel-nitrilotriacetic acid (Ni-NTA) column (GE Healthcare) equibibrated in buffer F. The column was washed with 50 column volumes of buffer F containing 30 mM imidazole, and bound lysenin was eluted with buffer F containing a linear gradient of 30-300 mM imidazole. Fractions containing lysenin were pooled and concentrated to 1 mL using an Amicon 10 kDa MWCO concentrator (Millipore) and further purified by gel filtration chromatography on a Tricorn 10/300 Superdex 200 Increase column (GE Healthcare) equilibrated with buffer F.

OlyA – Post-spin supernatant was loaded onto a 1 mL Ni-NTA column equilibrated in buffer C. The column was washed with 40 column volumes of buffer C containing 50 mM imidazole, and bound OlyA was eluted with buffer C containing a linear gradient of 50-300 mM imidazole. Fractions containing OlyA were pooled, diluted fifteen-fold in buffer D, and loaded onto a 1 mL Q Sepharose column (GE Healthcare) equilibrated in buffer D. OlyA did not bind the column under these conditions; the entire flow through was collected and concentrated to 1 mL using an Amicon 10 kDa MWCO concentrator and further purified by gel filtration chromatography on a Tricorn 10/300 Superdex 200 Increase column equilibrated with buffer C.

ALO-D4 – Post-spin supernatant was loaded onto a 4 mL Ni-NTA column equilibrated in buffer C. The column was washed with 50 column volumes of buffer C containing 50 mM

imidazole, and bound proteins were eluted with buffer C containing a linear gradient of 50-300 mM imidazole. Fractions containing ALO-D4 were pooled, diluted four-fold in buffer D, and loaded onto a 1 mL Q Sepharose column equilibrated in buffer D. The column was washed with 5 column volumes of buffer D containing 50 mM NaCl, and bound ALO-D4 was eluted with buffer D containing 500 mM NaCl.

Following chromatography, protein-rich fractions were pooled, concentrated to 1-3 mg/mL and stored at 4°C until use. Protein concentrations were measured using a NanoDrop instrument (Thermo) or by using a 660 nm protein assay (Pierce).

Protein labeling – In a typical 300 µL labeling reaction, 20 nmoles of protein was incubated with 200 nmoles of Alexa Fluor 488 C_5-maleimide (ALO-D4) or 647 C_2-maleimide (OlyA). After incubation for 16 h at 4°C, the reaction was quenched by addition of DTT to a final concentration of 10 mM. Free dye was separated from labeled ALO-D4 by passing the reaction mixture twice through a 7 kDa MWCO Zeba spin desalting column (Pierce) equilibrated in buffer B, followed by gel filtration chromatography on a Tricon 10/300 Superdex 200 column (GE Healthcare) equilibrated in buffer B. Free dye was separated from labeled OlyA by loading the quenched reaction onto a 1 mL Ni-NTA column equilibrated in buffer B. The column was washed with five column volumes of buffer B containing 50 mM imidazole, and bound protein was eluted with buffer B containing 300 mM imidazole. Labeled protein-rich fractions were pooled and concentrated to 0.1-0.5 mg/mL using an Amicon 10 kDa MWCO concentrator, combined with glycerol to a final concentration of 20% (v/v) and stored at -80°C until use.

Preparation of liposomes – All lipids were used without further purification. Mixtures containing the indicated proportions of phospholipids and sterols (from chloroform stock

solutions) were evaporated to dryness under a steady stream of nitrogen gas and stored under vacuum for at least 16 hours. A trace amount (< 0.2 mole%) of a fluorescently labeled phospholipid, TR-DHPE, was included for detection and quantification of liposomes. The dried lipid mixtures were hydrated by adding 500 µL of buffer A (final lipid concentration, 800 µM or 1.6 mM), agitated on a vortexer for 1 hour, and subjected to 3 freeze-thaw cycles (1 cycle = 60 seconds in a liquid nitrogen bath, 3 minutes in a room temperature water bath). The resulting lipid dispersions were placed in a water bath at 37°C and subjected to sonication for 15 min followed by a 15 min pause for cooling (2 cycles). Finally, the lipid mixtures were extruded through a polycarbonate filter (100 nm pore size) 11 times on a heating block set to 37°C to yield homogeneous unilamellar liposomes. Liposomes were stored at 4°C and used within 5 days.

Assays for interaction of purified proteins with artificial liposomes

Lysenin – Reaction mixtures (20 µL) containing 800 µM liposomes (total lipid) from a 1.6 mM liposome stock, and 6 µM protein in buffer A were set up in 1.5 mL tubes (Phenix Research Products). After incubation for 1 h at room temperature, reaction mixtures were mixed with SDS loading buffer, incubated for 10 min at room temperature, and subjected to 10% SDS-PAGE. Proteins were visualized with Coomasie Brilliant Blue R-250 stain (Bio-Rad).

ALO-D4 and OlyA – Reaction mixtures (200 µL) containing 400 µM liposomes (total lipid) from a 1.6 mM liposome stock, and 1 µg protein in buffer A were set up in 1.5 mL tubes (Phenix Research Products). After incubation for 1 h at room temperature, reactions were subjected to centrifugation for 1 h at 100,000 x *g* to pellet lipisomes. The resulting supernatant was collected, and the pellet was resuspended in 50 µL buffer A containing 1% SDS after incubation with the detergent for 30 min. Supernatant and pellet samples were mixed with SDS

loading buffer, boiled for 10 min at 95°C, and subjected to 15% SDS-PAGE. Proteins were transferred to nitrocellulose membranes and visualized by α-His Western Blot.

fOlyA – Reaction mixtures (200 µL) containing 400 µM liposomes (total lipid) from a 1.6 mM liposome stock, and 2.4 µg fluorescently-labeled protein in buffer A were set up in 1.5 mL tubes (Phenix Research Products). After incubation for 1 h at room temperature, reactions were subjected to centrifugation for 1 h at 100,000 x *g* to pellet lipisomes. The resulting pellet was resuspended in 200 µL buffer A containing 1% SDS after incubation with the detergent for 30 min. An aliquot (50% of total) was transferred to a black 96-well plate (Greiner) and fluorescence intensity of each sample was measured (Excitation λ = 651 nm; Emission λ = 672 nm) by microplate reader (Tecan).

Assays for interaction of purified proteins with cell membranes – Experimental details can be found in this chapter's *Results* and *Figure Legends.*

Hemolysis assays – To generate washed erythrocytes with minimal free hemoglobin or dead cells, 4 mL of fresh rabbit blood was centrifuged at 120 x g for 10 min, and the resulting erythrocyte pellet was resuspended in 4 mL of ice-cold buffer E. After gentle mixing by hand, the mixture was centrifuged at 500 x g for 10 min, and the resulting pellet was again resuspended in 4 mL of ice-cold buffer E. After gentle mixing by hand, the mixture was centrifuged at 1000 x g for 20 min, and the resulting pellet was resuspended in 36 mL of ice-cold buffer E. Hemolysis reaction mixtures (500 µL) containing 450 µL of erythrocytes, washed and diluted as described above, and 50 µL of buffer A containing protein (0-300 nM final concentration) were set up in 1.5 mL tubes. After incubation for 10 min at 37°C, the mixtures were centrifuged at 380 x g for 15 min, and a portion of the supernatant (100 µl) was transferred to a 96-well plate (clear, flat-

bottom; Evergreen Scientific). The extent of hemolysis was quantified using a micro-plate reader by measuring absorbance of released hemoglobin at 540 nm.

RESULTS

In order to probe membranes for SM and cholesterol, we cloned, expressed and purified several lipid-sensing proteins. Lysenin, an antimicrobial pore-forming toxin from the earthworm *Eisenia fetida*, has been previously shown to bind and permeabilize sphingomyelin-containing membranes via oligomerization into a membrane-spanning pore [16, 22]. In contrast, Ostreolysin A (OlyA) is a membrane-targeting protein from the fungus *Plurotus ostreatus*, that has been shown to bind only membranes containing both sphingomyelin and cholesterol [134]. Upon membrane binding, OlyA partners with another *Plurotus ostreatus* protein, pleurotolysin B (PlyB), which permeabilizes the membrane [110]. As we have demonstrated previously, ALO-D4 is capable of binding membranes with switch-like sensitivity for cholesterol and high sterol specificity [40]. In order to use these lipid-sensing proteins to probe membranes for SM and cholesterol, we first expressed lysenin, OlyA and ALO-D4 in bacteria. We purified the recombinant proteins to homogeneity, and subsequent SDS-PAGE analysis followed by Coomasie staining confirmed their purity (Figure 3-1).

We next sought to test binding of these proteins to artificial lipid bilayer membranes. We adapted a previously-described assay to use SDS-resistant oligomer formation to assay for membrane binding by lysenin [40]. When lysenin itself or mixtures of lysenin and liposomes comprised of DOPC:cholesterol or DOPC:epicholesterol were subjected to SDS-PAGE, lysenin migrated primarily as a 41 kDa species Figure 3-2A). When lysenin was instead mixed with liposomes containing egg SM (SM:DOPC, SM:cholesterol or SM:epicholesterol), the 41 kDa monomeric form of lysenin was reduced, and a majority of the protein migrated as a slowly-moving species, indicative of a large, SDS-resistant oligomer. Identical results were observed

when a single species of SM (containing an 18:1 acyl chain) or egg-derived SM served as the SM source in liposomes (data not shown).

While OlyA oligomerizes on membranes upon binding, ALO-D4 does not, and neither protein forms SDS-resistant oligomers [20, 40, 110]. Thus, we designed an alternative assay to test binding of these proteins to artificial membranes. We find that when liposomes are subjected to high speed centrifugation, the membranes and bound proteins pellet readily. Presence of liposomes in the post-centrifugation pellet was confirmed by the presence of an incorporated trace fluorescent lipid, TR-DHPE. When mixtures of ALO-D4 and liposomes containing no sterols or epicholesterol were centrifuged, ALO-D4 remained in the supernatant, as measured by α-His Western Blot (Figure 3-2B). When liposomes contained cholesterol, ALO-D4 bound to the membranes and was pelleted. We performed the same experiment using OlyA, and only observed pelleting with liposomes containing both SM and cholesterol. Notably, no OlyA binding was observed using SM:DOPC or SM:epicholesterol liposomes. This confirms that sterol is necessary for OlyA to bind SM-containing membranes in our assay, and that the protein possesses sterol specificity in addition to specificity for SM [126].

The next step in transitioning from artificial bilayers to biological membranes was to ensure that our lipid sensor does not permeabilize cells. Oligomerization of lysenin on lipid bilayer membranes leads to the formation of a transmembrane pore. OlyA has been shown to bind membranes containing SM and sterol, but requires PlyB activity to permeabilize bilayers [110]. We used a hemolysis assay to test whether purified, recombinant lysenin, OlyA and ALO-D4 form transmembrane pores. While lysenin caused complete hemolysis of erythrocytes at a concentration of 30 nM, OlyA and ALO-D4 did not cause hemoglobin release, even at a concentration of 300 nM (Figure 3-3). While certain lysenin mutations that reduce lysis have

been described, we have so far been unable to produce a mutant form of lysenin that does not lyse cells [76]. Therefore, we have focused on OlyA and ALO-D4 as probes for cellular membrane cholesterol and SM. OlyA is especially attractive, since its specificity, may be for the SM-sequestered form of cholesterol.

Previously, we've fluorescently labeled ALO-D4 and used this sensor to label cholesterol-rich cells for the purposes of flow-cytometry, fluorescence microscopy, detecting cholesterol transfer between membranes, and measuring cholesterol accessibility in both biological and artificial membranes. As described previously, we mutated the sole cysteine in ALO-D4 (C472 of the full-length protein) to alanine and introduced a single cysteine near the NH_2-terminus of cysteine-less ALO-D4 (K46C) [40]. We then covalently attached Alexa Fluor 488 to the sulfhydryl group of this cysteine. This fluorescently-labeled protein is hereafter referred to as fALO-D4. We then adapted our labeling procedure for use with OlyA. We mutated the two native cysteines in OlyA (C62 and C94) to serine, introduced a single cysteine near the COOH-terminus of cysteine-less OlyA (S151C), and covalently attached Alexa Fluor 647 to the sulfhydryl group of this cysteine. This fluorescently labeled protein is hereafter referred to as fOlyA (Figure3-4A).

We have previously used fALO-D4 to label cholesterol-rich cells, and were confident in the utility of this sensor. To ensure that the attached fluorophore did not interfere with fOlyA binding to SM:cholesterol- containing membranes, we repeated the liposome pelleting assay performed on the unlabeled protein. In this experiment, fOlyA binding was measured by fluorescence rather than Western blot, to ensure that the actual labeled protein is functional and our result does not reflect a remaining unlabeled portion of OlyA. When mixtures of liposomes and fOlyA were centrifuged, fOlyA only pelleted with membranes containing both SM and

cholesterol, just like the unlabeled protein (Figure 3-4B). The labeled protein retains phospholipid specificity for SM over DOPC, and sterol specificity for cholesterol over epicholesterol.

Given that fOlyA and fALO-D4 bind to particular membranes depending on lipid composition, do not lyse membrane upon binding, and remain active after fluorescent labeling, we next sought to test their binding to mammalian cells under various lipid treatment conditions. CHOK1 cells cultured in a 24-well plate were treated with either compactin in the presence of LPDS or cholesterol:HPCD complex in the presence of FCS to generate cholesterol-depleted and cholesterol-enriched cells, respectively. Cells were then chilled in PBS and incubated with either fOlyA or fALO-D4. After washing away unbound sensor, cell membranes were solubilized using SDS to relieve potential quenching effects, and total fluorescence was measured by microplate reader (Tecan) scanner directly in the plate. Total cellular protein was then measured for each well using a BCA assay (Pierce). By loading a known amount of fOlyA and fALO-D4 into the wells of an identical 24-well plate with the same concentration of SDS, we generated a standard curve such that fluorescence signals from fOlyA and fALO-D4 could be converted to protein amount. By using this estimate and normalizing to total cellular protein, we are able to compare the amount of sensor binding between experiments.

When fOlyA or fALO-D4 were incubated with cholesterol-depleted cells, we observed little binding compared to when these fluorescent probes were incubated with cholesterol-enriched cells (Figure 3-5A and Figure 3-5C). This is not surprising, given that fOlyA requires cholesterol in addition to SM, and fALO-D4 requires cholesterol. When we treated cholesterol-enriched cells with SMase, we observed decreased binding of fOlyA, but increased binding of fALO-D4 (Figure 3-5B and Figure 3-5D). Cholesterol-depleted cells treated with SMase bound

marginally more fALO-binding compared to cholesterol-depleted cells without SMase (data not shown). These data are in line with fOlyA being a SM:cholesterol sensor, and fALO-D4 being a sensor of only accessible membrane cholesterol. Our model is that SM sequesters cholesterol, and that depleting SM from cells frees up additional cholesterol to be sensed by fALO-D4.

FIGURE 3-1

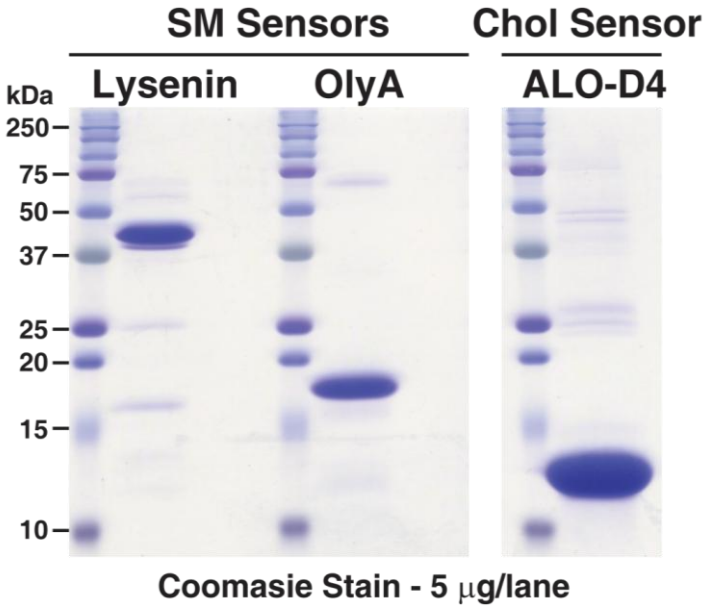

Figure 3-1. Isolation of recombinant lipid-sensing proteins. Protein overexpression and purification was carried out as described in *Experimental Procedures*. An aliquot of each protein (5 μg) was subjected to SDS-PAGE (10% for lysenin, 15% for OlyA and ALO-D4). Proteins were visualized by Coomassie Brilliant Blue R-250 stain.

FIGURE 3-2

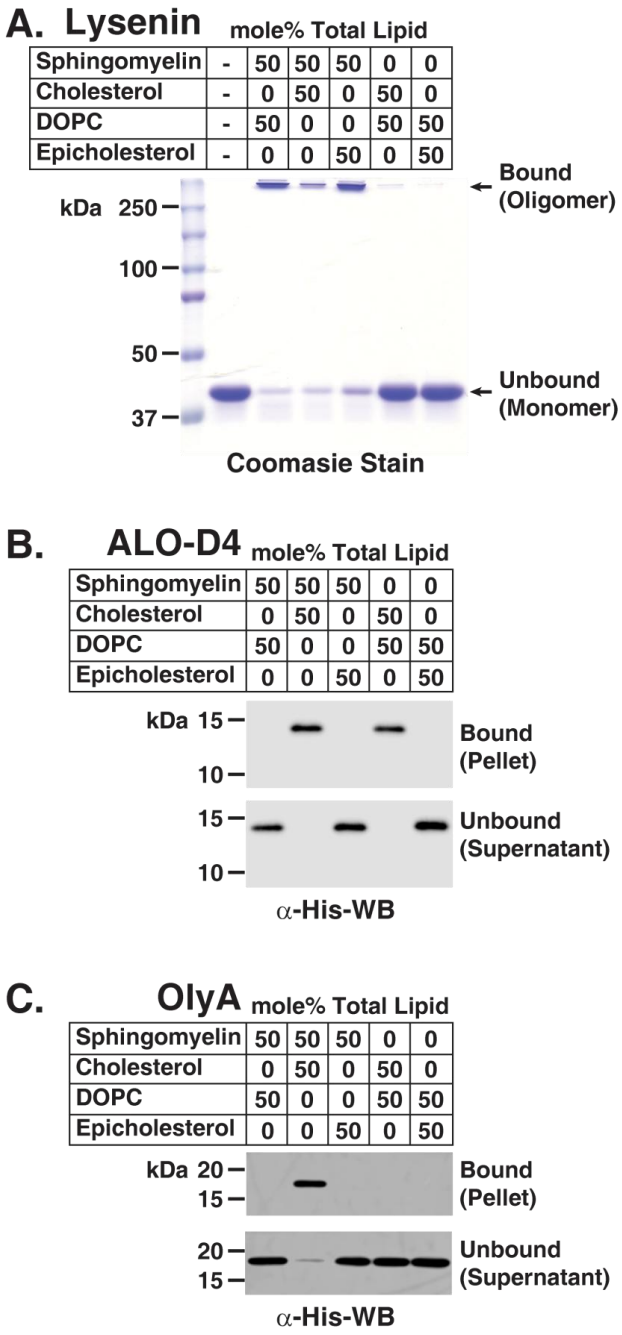
A. Lysenin
mole% Total Lipid
Sphingomyelin - 50 50 50 0 0
Cholesterol - 0 50 0 50 0
DOPC - 50 0 0 50 50
Epicholesterol - 0 0 50 0 50
kDa 250
100
50
37
Bound (Oligomer)
Unbound (Monomer)
Coomasie Stain
B. ALO-D4
mole% Total Lipid
Sphingomyelin 50 50 50 0 0
Cholesterol 0 50 0 50 0
DOPC 50 0 0 50 50
Epicholesterol 0 0 50 0 50
kDa 15
10
15
10
Bound (Pellet)
Unbound (Supernatant)
α-His-WB
C. OlyA
mole% Total Lipid
Sphingomyelin 50 50 50 0 0
Cholesterol 0 50 0 50 0
DOPC 50 0 0 50 50
Epicholesterol 0 0 50 0 50
kDa 20
15
20
15
Bound (Pellet)
Unbound (Supernatant)
α-His-WB

Figure 3-2. Binding of lipid-sensing proteins to artificial liposomes. (A) Binding and oligomerization of lysenin on liposome membranes. Each reaction mixture, in a total volume of 20 µL of buffer A, contained 6 µM lysenin and 800 nmoles liposomes (total lipid) with the indicated molar ratios of lipids. After incubation for 1 h at room temperature, samples were subjected 10% SDS-PAGE. Proteins were visualized with Coomasie Brilliant Blue R-250 stain. (B-C) Binding of ALO-D4 and OlyA to pelleted liposomes. Each reaction mixture, in a total volume of 200 µL, contained 1 µg of ALO-D4 (B) or OlyA (C), and 400 nmoles liposomes (total lipid) with the indicated molar ratios of lipids. After incubation for 1 h at room temperature, samples were subjected to centrifugation for 1 h at 100,000 x g. The post-spin supernatant was collected, and the pelleted liposomes were resuspended in 50 µL buffer A with 1% SDS. An aliquot of each sample was subjected to 15% SDS-PAGE, and proteins were visualized by .α-His Western blot. The molecular masses of protein standards are indicated.

FIGURE 3-3

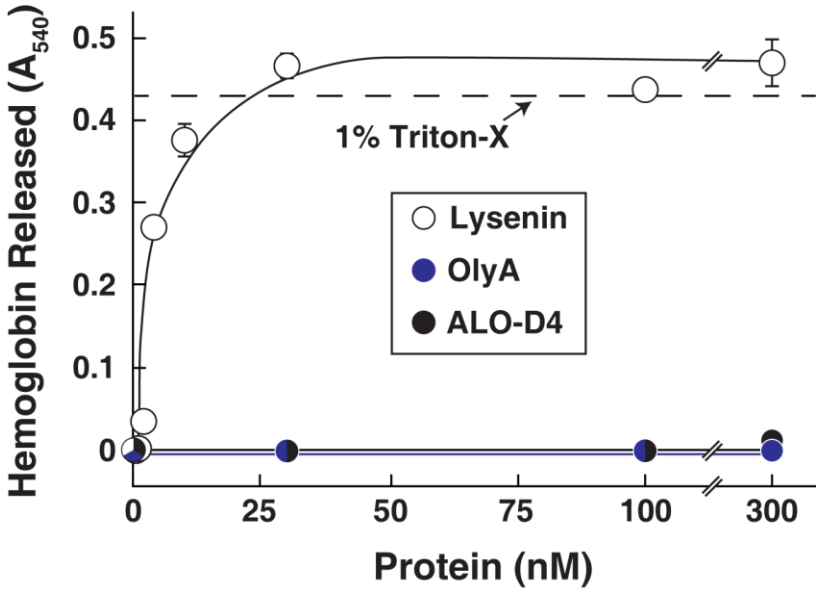

Figure 3-3. Hemolysis by lipid-sensing proteins. Each reaction mixture, in a final volume of 500 µL, contained varying amounts of Lysenin, OlyA or ALO-D4, and 450 µL rabbit erythrocytes that had been washed and diluted as described in *Experimental Procedures*. After incubation for 10 min at 37°C, the extent of hemolysis was quantified by measuring the release of hemoglobin (absorbance at 540 nm). The dashed line represents the absorbance of hemoglobin released after treatment with 1% (w/v) Triton-X 100 detergent. The data represents the mean ± SEM calculated from three independent assays.

FIGURE 3-4

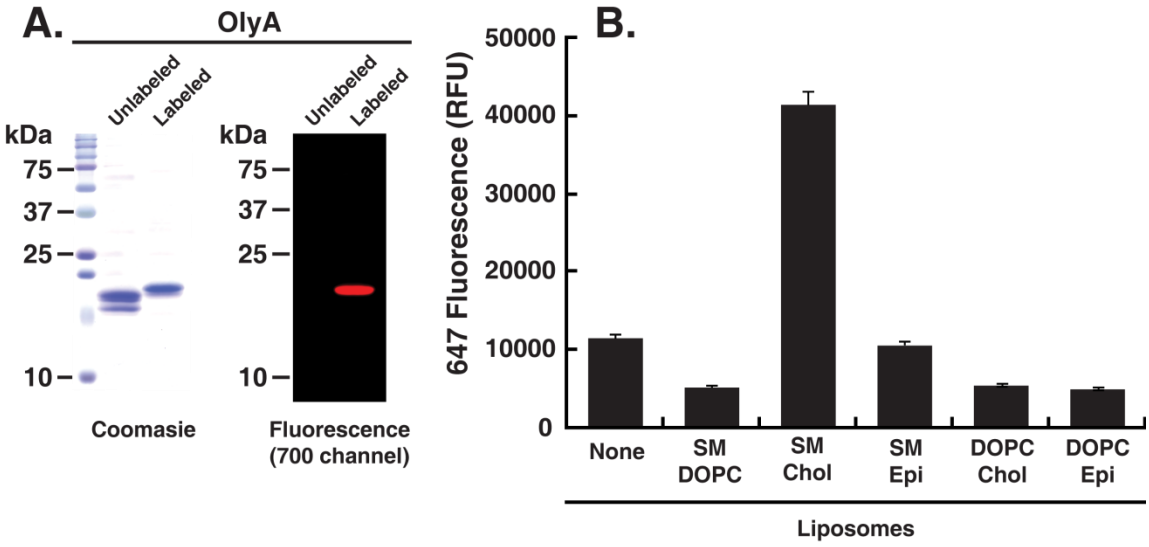

Figure 3-4. Specificity of fluorescently labeled OlyA. (A) SDS-PAGE of OlyA and fOlyA. An aliquot of OlyA and fOlyA (5.5 µg each) were subjected to 15% SDS-PAGE and visualized by Coomasie Brilliant Blue R-250 stain or by fluorescence scanning using a LI-COR Odyssey infrared imaging system at 700 nm. The molecular masses of proteins standards are indicated. (B) Lipid dependence of fOlyA binding to artificial liposomes. Each reaction mixture, in a final volume of 200 µL, contained 2.4 µg fOlyA and 400 nmoles liposomes (total lipid). After incubation for 1 h at room temperature, reactions were subjected to centrifugation for 1 h at 100,000 x *g*. The pelleted liposomes were resuspended in 200 µL, and fluorescence from an aliquot (100 µL) was measured by microplate reader (Tecan). The data represents the mean ± SEM calculated from three independent assays.

FIGURE 3-5

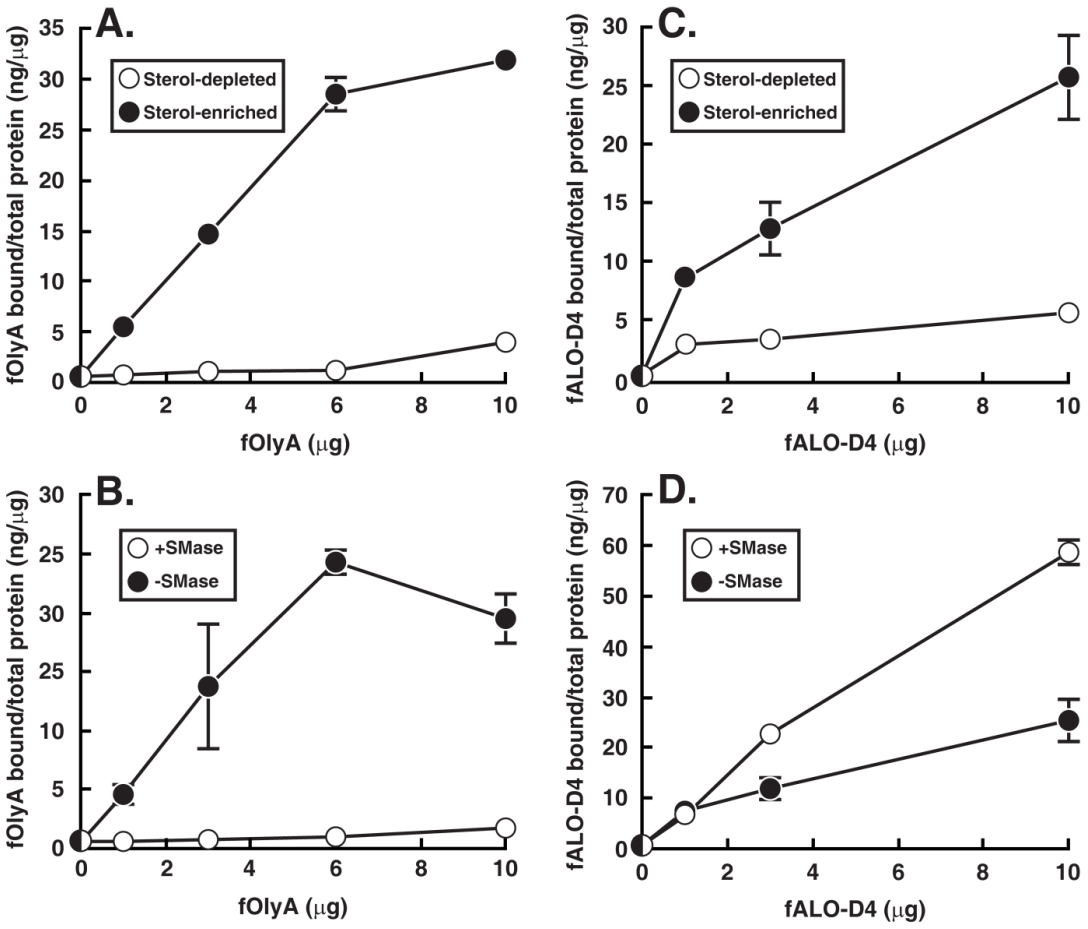

Figure 3-5. Binding of fOlyA and fALO-D4 to CHOK1 cells. On day 0, CHOK1 cells were set up in medium B at 50K cells per well of a 24-well tissue culture plate. On day 1, cells were washed once with PBS and switched to either fresh medium B (high cholesterol) or medium C (low cholesterol) and incubated for 16 h at 37°C. On day 2, cholesterol treatment was continued by switching cells to either fresh medium B supplemented with 50 µM cholesterol:HPCD complex (high cholesterol) or medium C supplemented with 1% (w/v) HPCD (low cholesterol) (A and C), or medium B supplemented with 50 µM cholesterol:HPCD complex with or without

20 mU/mL SMase (B and D). After incubation for 1 h at 37°C, the cells were washed twice with PBS at room temperature, followed by one 10 minute wash with ice-cold PBS at 4°C. Cells were then treated with 250 µL PBS containing the indicated amount of fluorescently labeled lipid-sensing protein. After incubation for 2 h at 4°C, cells were washed with ice-cold PBS. Each well then received 500 µL PBS and 100 µL 10% SDS plus protease inhibitors. Cells were subjected to platform shaking at room temperature for 1 hour, and fOlyA fluorescence (A and B) (excitation wavelength, 651 nm; emission wavelength, 672 nm) or fALO-D4 fluorescence (C and D) (excitation wavelength, 495 nm; emission wavelength, 517 nm) was measured. Solubilized cells were further disrupted by freezing at -20°C for 16 h, after which cellular protein concentrations were calculated by BCA assay. The graphs show the amount of fluorescent lipid-sensor bound to the cell surface, normalized to total cellular protein, as a function of fluorescent lipid-sensor added. The data represents the mean ± SEM calculated from three independent assays.

DISCUSSION

Our characterization of fOlyA and fALO-D4 membrane interactions is a first step towards a better understanding of the nature of cholesterol's relationship with SM. It has been proposed that SM:cholesterol complexes with defined structures exist in biological membranes due to hydrogen bonding [105]. Such a complex could potentially be captured in the binding pocket of a protein that requires both SM and cholesterol to bind membranes, such as OlyA. Alternatively, OlyA could induce a complex between these two lipids that did not previously exist in the membrane.

Unfortunately, there are no high-resolution structures of OlyA. OlyA's binding partner, PlyB, shares structural homology with lysenin and the CDC family of proteins, and has been shown to lyse membranes using a similar mechanism [29, 110, 150]. We are currently expressing and testing high-stability OlyA constructs for crystallography studies. We are also testing solution binding of OlyA to SM and cholesterol in preparation for obtaining crystals of both the free and lipid-bound forms of OlyA. It is worth nothing that there are no structures of ALO bound to cholesterol. The structure of ALO in absence of cholesterol ligand has been solved, but there is no obvious cholesterol-binding pocket in this structure [7].

Our ultimate goal is to use the fOlyA and fALO-D4 tools and the methods described here to understand the organization of cholesterol in PM. We plan to vary the cholesterol and SM content of cells using the techniques described in *Results*. We will then measure the binding of fALO-D4 and fOlyA to the PM of these cells as described. We will also use a modified version of a previously-described method of purifying PM in order to quantify the SM and cholesterol levels in the PM [26]. Briefly, cells will be treated with a membrane-impermeable biotinylation

reagent, lysed and then incubated with streptavidin beads to isolate biotinylated PM transmembrane proteins and the surrounding PM lipid bilayers. Following lipid extraction from the membranes, samples will be analyzed by mass spectrometry to determine the amount of total lipid and the relative ratio of SM and cholesterol. We expect that as SM levels decrease, free cholesterol will increase, thus increasing fALO-D4 binding to membranes. In the case of fOlyA, we might observe maximal binding at an intermediate ratio of SM:cholesterol, with reduced binding to membranes dominated by one lipid or the other. This ratio might indicate the stoichiometry of putative SM:cholesterol complexes. We have already performed several preliminary experiments towards this goal, and hope to finish these studies soon. These tools and studies will let us ask new questions regarding SM and cholesterol regulation in the cell.

CONCLUSION AND PERSPECTIVE

I began this project to learn more about the switch-like activation of cholesterol binding proteins such as Scap, using the CDC family of toxins as a proxy. A simple answer to this question was provided by studying domains of PFO and ALO; the availability of membrane cholesterol itself is switch-like due to lipid-lipid interactions. While protein-protein interactions certainly accentuate the sensitivity of these cholesterol detectors, they are not absolutely required for this non-linear response. Cells maintain membrane cholesterol near specific threshold concentrations: ~40 mole % in PM and 5 mole % in ER. Cholesterol accessibility sharply rises when these thresholds are exceeded; and cells likely exploit this property to prime amplified responses from proteins such as Scap. While the PM contains >70% of total cellular cholesterol, detection occurs in the ER [30, 84]. It is tempting to speculate that the cell measures cholesterol in the ER as opposed to the PM because small changes in cholesterol concentration lead to comparatively larger changes in cholesterol accessibility. It is also likely that membrane fluidity and integrity are optimal near this switch-point and that cholesterol transport or disposal by proteins such as ACAT occurs when cholesterol concentrations rise past this same point in order to preserve membrane function.

After demonstrating that protein-protein interactions were not strictly necessary for switch-like responses to cholesterol, it quickly became apparent that these lipid-sensing proteins were valuable tools in answering many other open questions in cholesterol homeostasis. Cholesterol transport through the cytosol was our next target, as there was unmet need for high-throughput, in vitro assays that measure cholesterol transport between membranes. I created a novel assay by generating a supported lipid bilayer devoid of cholesterol on a glass surface,

adding sterol-containing donor liposomes, and incubating the reaction with putative cholesterol transfer factors. I then removed the donor liposomes and transfer factors. Transfer of cholesterol was then measured with a sensitive, switch-like probe that I had previously developed. This assay can measure transfer of as little as 1 pmole of cholesterol, and is optimized for a 96-well plate format. Using this assay, I have found that whole cytosol has cholesterol-transfer ability, and am currently working to fractionate this activity and identify unknown cholesterol transfer proteins.

I became interested in adapting our methods to other proteins that sense lipids in order to study the relationship between cholesterol and other components of the membrane. One such protein is OlyA, which only binds to membranes containing both cholesterol and SM. OlyA and ALO-D4 are thus ideal tools for studying the organization of the membrane and the mutual regulation of SM and cholesterol [65]. In my ongoing work, I will manipulate the lipid levels of live cells, measure binding of these probes to the PM, purify the PM through biotinylation of surface proteins followed by streptavidin pull-down, extract the PM lipids and measure their lipid content by mass spectrometry. The relationship between binding of ALO and OlyA probes and SM:cholesterol ratios should provide new insight into the relationship between these important lipids. We are also currently working to solve the NMR and X-ray crystal structures of ALO-D4 and OlyA bound to their respective ligands. Binding of ALO to membrane cholesterol would give insight into how proteins bind to cholesterol in lipid bilayers. Since OlyA binds only to membranes containing both SM and cholesterol, a solved crystal structure of the lipid-bound proteins may reveal the structure of long-hypothesized SM:cholesterol complexes.

While basic insights into how proteins sense lipids in membrane lead to better understanding of human disease, we are also working directly to translate our new tools towards

clinical application. There is great interest in modifying Scap binding to cholesterol for research and healthcare purposes. Screening for potential inhibitors of Scap has thus far been problematic due to technical challenges. What is missing is a robust, high-throughput assay for protein binding to sterols that can be applied to Scap. We reasoned that the CDC family proteins would be a suitable proxy for Scap in such an assay. As described in *CHAPTER 1*, CDCs and Scap share common sterol specificity [145]. We have since tested many other sterols against Scap and ALO binding, and find that this holds true for all sterols tested (Figure 3). Because Scap, PFO-D4 and ALO-D4 also share identical, switch-like responses to membrane cholesterol, they may be sensing cholesterol in mechanistically-similar ways. Therefore, finding an inhibitor of CDC binding may present leads towards modulators of mammalian sterol-sensing domains in proteins such as Scap [49]. In an ongoing project, we are screening a large chemical library (~200,000 compounds) at UT Southwestern's High Throughput Screening Core for molecules that bind ALO and prevent its sensing of membrane cholesterol. We are using an assay that I developed for this high-throughput screen (Figure 1-5D) [40]. Briefly, ALO protein is incubated with cholesterol or epicholesterol in 384-well plates. Washed erythrocytes are then added, and hemolysis by ALO is quantified by measuring the absorbance of released hemoglobin. Preincubating ALO with cholesterol inhibits hemolysis, while epicholesterol does not (Figure 4A). Our pilot screen of a subset of the UT Southwestern library has unearthed a candidate that binds to ALO and blocks SREBP-2 processing, just like cholesterol (Figure 4B-C). This candidate is a fraction from Dr. John MacMillan's natural product library. We are currently working to further fractionate this sample and identify the single active compound as a potential drug candidate.

Another potential application for a fluorescently-labeled lipid sensor is as a diagnostic tool in humans. We are currently adapting our lipid sensing proteins for use in live animals in collaboration with the lab of Dr. Daniel Siegwart. While we and other groups have used modified CDCs to probe sterol pools in live cells, moving into living animals has faced several hurdles [43, 141]. First, detecting fluorescence emission *in vivo* through tissue is more effective using long wavelength, near-infrared (NIR) fluorophores due to less background autofluorescence in the so-called NIR "imaging window" [37]. Second, our initial attempts using a small molecule Alexa Fluor-labeled version of ALO-D4 showed that the labeled protein had a very short blood circulation time. To correct these issues, the Siegwart lab synthesized a NIR-labeled, long-circulating hydrophilic polymer modified ALO-D4. Cyanine 5.5 *N*-hydroxy succinimide ester was reacted with the primary amine end terminus of a heterobifunctional poly(ethylene glycol) (PEG) (average M_n = 5,000). The other functional chain end of the PEG (malemide) was then used for bioconjugation with a free cysteine on ALO-D4 to prepare the NIR dye-labeled and PEGylated protein-based cholesterol sensor. PEG polymers are often attached to intravenously administered probes and drugs in order to extend blood circulation time [168]. This is due to the high molecular weight, hydrophilicity (water solubility), and non-specific protein repulsion (non-fouling) properties of PEG. Switching from a small molecule Alexa Fluor dye to the high molecular weight PEG increased the blood half-life of our probe from less than five minutes to more than an hour. We are currently working to compare the tissue binding of our WT probe with that of a non-binding mutant. Since ALO binds membranes on the basis of cholesterol accessibility rather than outright concentration, this probe may provide new information on which tissues contain the most active pools of cholesterol [26]. Additionally, the

fluorescent probe could be used to visualize sites of cholesterol buildup in the vasculature, or as a targeting factor for cholesterol-modifying drugs or proteins.

FIGURE 3

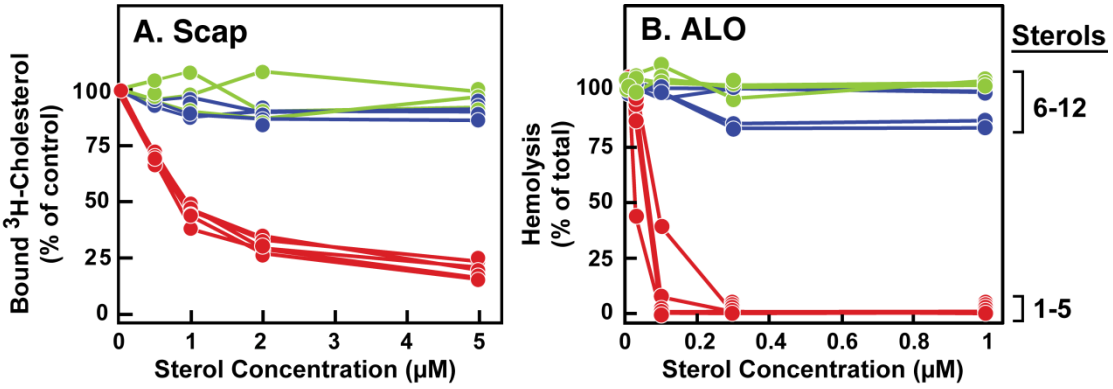

Figure 3. Identical sterol specificity for Scap binding and inhibition of erythrocyte lysis by ALO. (A) Scap binding data from [122] in which 30 pmol of purified Scap transmembrane helices 1-8 were incubated with 100 nM [^{3}H]cholesterol in absence or presence of indicated unlabeled competitor sterol. Each value represents amount of [^{3}H]cholesterol bound in presence of unlabeled sterol relative to control (no unlabeled sterol). (B) Each 50 µL reaction ALO binding reaction contained 50 fmol of ALO and indicated sterols solubilized in DMSO. After 1 h at 24°C, 450 µl of washed rabbit erythrocytes (see *CHAPTER 3 Experimental Procedures*) were added to each reaction. After incubation for 10 min at 37°C, the extent of hemolysis was quantified by measuring the release of hemoglobin (absorbance at 540 nm). 100% of control represents the absorbance of hemoglobin released after treatment with 1% (w/v) Triton-X 100 detergent. (A and B) Sterols tested: 1, cholesterol; 2, dihydrocholesterol; 3, desmosterol; 4, 25-fluorocholesterol; 5, sitosterol; 6, 25-hydroxycholesterol; 7, 22-R-hydroxycholesterol; 8, 27-hydroxycholesterol; 9, 24-25-epoxycholesterol; 10, 19-hydroxycholesterol; 11, epicholesterol; 12, lanosterol.

FIGURE 4

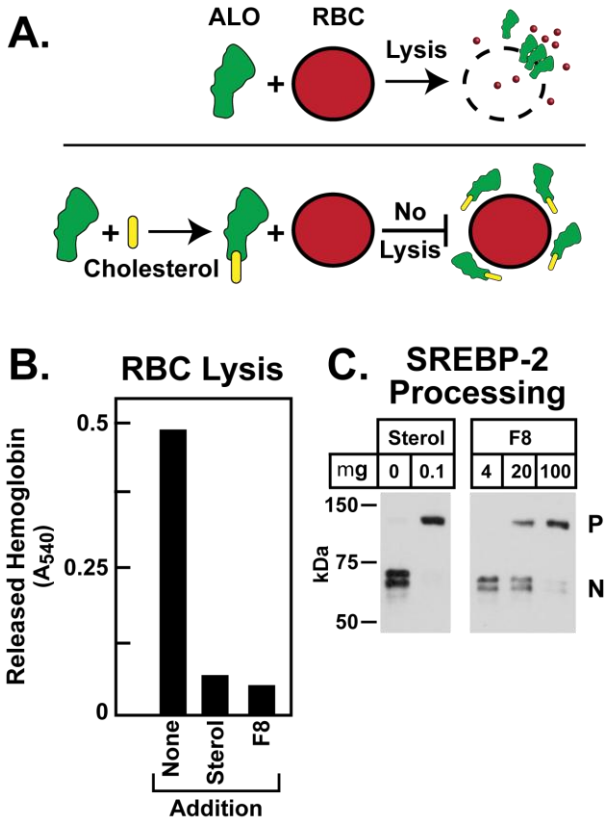

Figure 4. Screen for inhibitors of membrane cholesterol binding. (A) Schematic of hemolysis inhibition assay. When incubated with RBCs, ALO binds to membrane cholesterol and forms pores, resulting in hemolysis and release of hemoglobin (top). Pre-incubation of ALO with cholesterol blocks hemolysis, indicating cholesterol binding (bottom). (B and C) Isolation of compounds from *Streptomyces variabilis* that bind to ALO and inhibit SREBP-2 processing. Nonpolar small molecules were isolated from SNB047 cultures and fractionated by reversed phase chromatography. Fraction 8 (F8) was active in the ALO binding assay (B) and in inhibition of SREBP-2 processing in SV-589 cells (C). P, membrane precursor form of SREBP-2; N, processed nuclear form.

BIBLIOGRAPHY

1. *Global, regional, and national age-sex specific all-cause and cause-specific mortality for 240 causes of death, 1990-2013: a systematic analysis for the Global Burden of Disease Study 2013.* Lancet, 2015. **385**(9963): p. 117-71.
2. Ali, M.R., K.H. Cheng, and J. Huang, *Assess the nature of cholesterol-lipid interactions through the chemical potential of cholesterol in phosphatidylcholine bilayers.* PNAS, 2007. **104**(13): p. 5372-5377.
3. Babalola, J.O., et al., *Development of an assay for the intermembrane transfer of cholesterol by Niemann-Pick C2 protein.* Biol Chem, 2007. **388**(6): p. 617-26.
4. Beisiegel, U., W. Weber, and G. Bengtsson-Olivecrona, *Lipoprotein lipase enhances the binding of chylomicrons to low density lipoprotein receptor-related protein.* Proceedings of the National Academy of Sciences of the United States of America, 1991. **88**(19): p. 8342-8346.
5. Bilheimer, D.W., S. Eisenberg, and R.I. Levy, *The metabolism of very low density lipoprotein proteins I. Preliminary in vitro and in vivo observations.* Biochimica et Biophysica Acta (BBA) - Lipids and Lipid Metabolism, 1972. **260**(2): p. 212-221.
6. Bloch, K., *The biological synthesis of cholesterol.* Science, 1965. **150**(3692): p. 19-28.
7. Bourdeau, R.W., et al., *Cellular functions and X-ray structure of anthrolysin O, a cholesterol-dependent cytolysin secreted by Bacillus anthracis.* J Biol Chem, 2009. **284**(21): p. 14645-56.
8. Brian, A.A. and H.M. McConnell, *Allogeneic stimulation of cytotoxic T cells by supported planar membranes.* Proc Natl Acad Sci U S A, 1984. **81**(19): p. 6159-63.

9. Brown, A.J., et al., *Cholesterol addition to ER membranes alters conformation of SCAP, the SREBP escort protein that regulates cholesterol metabolism.* Mol. Cell, 2002. **10**(2): p. 237-245.

10. Brown, D.A. and E. London, *Functions of lipid rafts in biological membranes.* Annu Rev Cell Dev Biol, 1998. **14**: p. 111-36.

11. Brown, M.S. and J.L. Goldstein, *Lipoprotein receptors in the liver. Control signals for plasma cholesterol traffic.* Journal of Clinical Investigation, 1983. **72**(3): p. 743-747.

12. Brown, M.S. and J.L. Goldstein, *A receptor-mediated pathway for cholesterol homeostasis.* Science, 1986. **232**(4746): p. 34-47.

13. Brown, M.S. and J.L. Goldstein, *The SREBP pathway: regulation of cholesterol metabolism by proteolysis of a membrane-bound transcription factor.* Cell, 1997. **89**: p. 331-340.

14. Brown, M.S. and J.L. Goldstein, *Cholesterol feedback: from Schoenheimer's bottle to Scap's MELADL.* J Lipid Res, 2009. **50 Suppl**: p. S15-27.

15. Brown, M.S., et al., *Regulated intramembrane proteolysis: A control mechanism conserved from bacteria to humans.* Cell, 2000. **100**(4): p. 391-398.

16. Bruhn, H., et al., *Dissection of the mechanisms of cytolytic and antibacterial activity of lysenin, a defence protein of the annelid Eisenia fetida.* Dev Comp Immunol, 2006. **30**(7): p. 597-606.

17. Carstea, E.D., et al., *Niemann-Pick C1 disease gene: homology to mediators of cholesterol homeostasis.* Science, 1997. **277**(5323): p. 228-31.

18. Casey, P.J., *Protein lipidation in cell signaling.* Science, 1995. **268**(5208): p. 221-5.

19. Chatterjee, S., et al., *Identification of Novel Genes and Pathways Regulating SREBP Transcriptional Activity.* PLoS ONE, 2009. **4**(4): p. e5197.

20. Cocklin, S., et al., *Real-time monitoring of the membrane-binding and insertion properties of the cholesterol-dependent cytolysin anthrolysin O from Bacillus anthracis.* J Mol Recognit, 2006. **19**(4): p. 354-62.

21. Cook, R.P., et al., *Cholesterol metabolism. 6. The fate of ingested cholesterol in the intact rat.* Biochemical Journal, 1955. **61**(4): p. 676-681.

22. Cooper, E.L., E. Kauschke, and A. Cossarizza, *Annelid humoral immunity: cell lysis in earthworms.* Adv Exp Med Biol, 2001. **484**: p. 169-83.

23. Cooper, R.A., *Influence of increased membrane cholesterol on membrane fluidity and cell function in human red blood cells.* J Supramol Struct, 1978. **8**(4): p. 413-30.

24. Cryer, A., *Tissue lipoprotein lipase activity and its action in lipoprotein metabolism.* International Journal of Biochemistry, 1981. **13**(5): p. 525-541.

25. Cui, Q. and M. Karplus, *Allostery and cooperativity revisited.* Protein Science : A Publication of the Protein Society, 2008. **17**(8): p. 1295-1307.

26. Das, A., et al., *Three pools of plasma membrane cholesterol and their relation to cholesterol homeostasis.* Elife (Cambridge), 2014: p. e02882.

27. Das, A., et al., *Use of mutant 125I-perfringolysin O to probe transport and organization of cholesterol in membranes of animal cells.* Proc Natl Acad Sci U S A, 2013. **110**(26): p. 10580-5.

28. Dawson, P.A. and L.L. Rudel, *Intestinal cholesterol absorption.* Current Opinion in Lipidology, 1999. **10**(4): p. 315-320.

29. De Colibus, L., et al., *Structures of lysenin reveal a shared evolutionary origin for pore-forming proteins and its mode of sphingomyelin recognition.* Structure, 2012. **20**(9): p. 1498-507.

30. De Duve, C., *Tissue fractionation. Past and present.* J Cell Biol, 1971. **50**(1): p. 20d-55d.

31. Dietschy, J.M., S.D. Turley, and D.K. Spady, *Role of liver in the maintenance of cholesterol and low density lipoprotein homeostasis in different animal species, including humans.* Journal of Lipid Research, 1993. **34**(10): p. 1637-59.

32. Dubland, J.A. and G.A. Francis, *Lysosomal acid lipase: at the crossroads of normal and atherogenic cholesterol metabolism.* Frontiers in Cell and Developmental Biology, 2015. **3**: p. 3.

33. Farrand, A.J., et al., *Only two amino acids are essential for cytolytic toxin recognition of cholesterol at the membrane surface.* PNAS, 2010. **107**(9): p. 4341-4346.

34. Feil, S.C., et al., *Structural studies of Streptococcus pyogenes streptolysin O provide insights into the early steps of membrane penetration.* J Mol Biol, 2014. **426**(4): p. 785-92.

35. Finean, J.B., *Phospholipid-cholesterol complex in the structure of myelin.* Experientia, 1953. **9**(1): p. 17-9.

36. Flanagan, J.J., et al., *Cholesterol exposure at the membrane surface is necessary and sufficient to trigger perfringolysin O binding.* Biochemistry, 2009. **48**(18): p. 3977-3987.

37. Frangioni, J.V., *In vivo near-infrared fluorescence imaging.* Current Opinion in Chemical Biology, 2003. **7**(5): p. 626-634.

38. Frisz, J.F., et al., *Sphingolipid Domains in the Plasma Membranes of Fibroblasts Are Not Enriched with Cholesterol.* The Journal of Biological Chemistry, 2013. **288**(23): p. 16855-16861.

39. Frisz, J.F., et al., *Direct chemical evidence for sphingolipid domains in the plasma membranes of fibroblasts.* Proceedings of the National Academy of Sciences of the United States of America, 2013. **110**(8): p. E613-E622.

40. Gay, A., D. Rye, and A. Radhakrishnan, *Switch-like Responses of Two Cholesterol Sensors Do Not Require Protein Oligomerization in Membranes.* Biophys J, 2015. **108**(6): p. 1459-69.

41. Georgiev, A.G., et al., *Osh proteins regulate membrane sterol organization but are not required for sterol movement between the ER and PM.* Traffic, 2011. **12**(10): p. 1341-55.

42. Gil, G., et al., *Membrane-bound domain of HMG CoA reductase is required for sterol-enhanced degradation of the enzyme.* Cell, 1985. **41**(1): p. 249-58.

43. Gimpl, G. and K. Gehrig-Burger, *Probes for studying cholesterol binding and cell biology.* Steroids, 2011. **76**(3): p. 216-231.

44. Ginsberg, H.N., Y.-L. Zhang, and A. Hernandez-Ono, *Regulation of Plasma Triglycerides in Insulin Resistance and Diabetes.* Archives of Medical Research, 2005. **36**(3): p. 232-240.

45. Goldstein, J.L., S.K. Basu, and M.S. Brown, *Receptor-mediated endocytosis of low-density lipoprotein in cultured cells.* Meth. Enzymology, 1983. **98**: p. 241-260.

46. Goldstein, J.L. and M.S. Brown, *The low-density lipoprotein pathway and its relation to atherosclerosis.* Annu Rev Biochem, 1977. **46**: p. 897-930.

47. Goldstein, J.L. and M.S. Brown, *The LDL receptor.* Arterioscler Thromb Vasc Biol, 2009. **29**(4): p. 431-8.

48. Goldstein, J.L. and M.S. Brown, *A Century of Cholesterol and Coronaries: From Plaques to Genes to Statins.* Cell, 2015. **161**(1): p. 161-172.

49. Goldstein, J.L., R.A. Debose-Boyd, and M.S. Brown, *Protein sensors for membrane sterols.* Cell, 2006. **124**: p. 35-46.

50. Gould, R.G., et al., *Cholesterol metabolism. I. Effect of dietary cholesterol on the synthesis of cholesterol in dog tissue in vitro.* J Biol Chem, 1953. **201**(2): p. 519-28.

51. Groves, J.T., S.G. Boxer, and H.M. McConnell, *Electric field-induced reorganization of two-component supported bilayer membranes.* Proc Natl Acad Sci U S A, 1997. **94**(25): p. 13390-5.

52. Grundy, S.M., *Absorption and metabolism of dietary cholesterol.* Annu Rev Nutr, 1983. **3**: p. 71-96.

53. Hacke, M., et al., *Inhibition of Ebola virus glycoprotein-mediated cytotoxicity by targeting its transmembrane domain and cholesterol.* Nat Commun, 2015. **6**: p. 7688.

54. Hannaoui, S., et al., *Cholesterol Balance in Prion Diseases and Alzheimer's Disease.* Viruses, 2014. **6**(11): p. 4505-4535.

55. Hanukoglu, I., *Steroidogenic enzymes: structure, function, and role in regulation of steroid hormone biosynthesis.* J Steroid Biochem Mol Biol, 1992. **43**(8): p. 779-804.

56. Harder, T., et al., *Lipid Domain Structure of the Plasma Membrane Revealed by Patching of Membrane Components.* The Journal of Cell Biology, 1998. **141**(4): p. 929-942.

57. Herbert, A.S., et al., *Niemann-pick C1 is essential for ebolavirus replication and pathogenesis in vivo.* MBio, 2015. **6**(3): p. e00565-15.

58. Heron, M., *Deaths: Leading Causes for 2013.* Natl Vital Stat Rep, 2016. **65**(2): p. 1-14.

59. Heuck, A.P., et al., *Mechanism of membrane insertion of a multimeric b-barrel protein: Perfringolysin O creates a pore using ordered and coupled conformational changes.* Mol. Cell, 2000. **6**: p. 1233-1242.

60. Heuck, A.P., P.C. Moe, and B.B. Johnson, *The cholesterol-dependent cytolysin family of gram-positive bacterial toxins.* Subcell Biochem, 2010. **51**: p. 551-77.

61. Hofmann, A.F., *The function of bile salts in fat absorption. The solvent properties of dilute micellar solutions of conjugated bile salts.* Biochemical Journal, 1963. **89**(1): p. 57-68.

62. Holopainen, J.M., et al., *Evidence for the Lack of a Specific Interaction between Cholesterol and Sphingomyelin.* Biophysical Journal, 2004. **86**(3): p. 1510-1520.

63. Holthuis, J.C. and A.K. Menon, *Lipid landscapes and pipelines in membrane homeostasis.* Nature, 2014. **510**(7503): p. 48-57.

64. Horton, J.D., J.L. Goldstein, and M.S. Brown, *SREBPs: activators of the complete program of cholesterol and fatty acid synthesis in the liver.* Journal of Clinical Investigation, 2002. **109**(9): p. 1125-1131.

65. Hullin-Matsuda, F., et al., *Imaging lipid membrane domains with lipid-specific probes.* Methods Mol Biol, 2009. **580**: p. 203-20.

66. Hung, W.C., F.Y. Chen, and H.W. Huang, *Order-disorder transition in bilayers of diphytanoyl phosphatidylcholine.* Biochim Biophys Acta, 2000. **1467**(1): p. 198-206.

67. Im, Y.J., et al., *Structural mechanism for sterol sensing and transport by OSBP-related proteins.* Nature, 2005. **437**(7055): p. 154-8.

68. Infante, R.E., et al., *Purified NPC1 protein. I. Binding of cholesterol and oxysterols to a 1278-amino acid membrane protein.* J Biol Chem, 2008. **283**(2): p. 1052-63.

69. Infante, R.E., et al., *NPC2 facilitates bidirectional transfer of cholesterol between NPC1 and lipid bilayers, a step in cholesterol egress from lysosomes.* Proc Natl Acad Sci U S A, 2008. **105**(40): p. 15287-92.

70. Ishitsuka, R., et al., *Fluorescence image screening for chemical compounds modifying cholesterol metabolism and distribution.* J Lipid Res, 2011. **52**(11): p. 2084-94.

71. Jeong, J. and A.P. McMahon, *Cholesterol modification of Hedgehog family proteins.* The Journal of Clinical Investigation, 2002. **110**(5): p. 591-596.

72. Johnson, B.B., et al., *Modifications in perfringolysin O domain 4 alter the cholesterol concentration threshold required for binding.* Biochemistry, 2012. **51**(16): p. 3373-82.

73. Keller, S.L., A. Radhakrishnan, and H.M. McConnell, *Saturated phospholipids with high melting temperatures form complexes with cholesterol in monolayers.* Journal of Physical Chemistry B, 2000. **104**(31): p. 7522-7527.

74. Kiessling, V., S.T. Yang, and L.K. Tamm, *Supported lipid bilayers as models for studying membrane domains.* Curr Top Membr, 2015. **75**: p. 1-23.

75. Kilsdonk, E.P.C., et al., *Cellular cholesterol efflux mediated by cyclodextrins.* J. Biol. Chem., 1995. **270**: p. 17250-17256.

76. Kiyokawa, E., et al., *Spatial and functional heterogeneity of sphingolipid-rich membrane domains.* J Biol Chem, 2005. **280**(25): p. 24072-84.

77. Koster, S., et al., *Crystallization and X-ray crystallographic analysis of the cholesterol-dependent cytolysin listeriolysin O from Listeria monocytogenes.* Acta Crystallogr Sect F Struct Biol Cryst Commun, 2013. **69**(Pt 11): p. 1212-5.

78. Kraft, M.L., *Plasma membrane organization and function: moving past lipid rafts.* Mol Biol Cell, 2013. **24**(18): p. 2765-8.

79. Kraft, M.L. and H.A. Klitzing, *Imaging lipids with secondary ion mass spectrometry.* Biochim Biophys Acta, 2014. **1841**(8): p. 1108-19.

80. Kwiterovich Jr, P.O., *The metabolic pathways of high-density lipoprotein, low-density lipoprotein, and triglycerides: a current review.* The American Journal of Cardiology, 2000. **86**(12, Supplement 1): p. 5-10.

81. Kwon, H.J., et al., *Structure of N-terminal domain of NPC1 reveals distinct subdomains for binding and transfer of cholesterol.* Cell, 2009. **137**(7): p. 1213-24.

82. Lahiri, S., A. Toulmay, and W.A. Prinz, *Membrane contact sites, gateways for lipid homeostasis.* Curr Opin Cell Biol, 2015. **33**: p. 82-87.

83. Langdon, R.G. and K. Bloch, *The effect of some dietary additions on the synthesis of cholesterol from acetate in vitro.* J Biol Chem, 1953. **202**(1): p. 77-81.

84. Lange, Y. and B.V. Ramos, *Analysis of the distribution of cholesterol in the intact cell.* J Biol Chem, 1983. **258**(24): p. 15130-4.

85. Lange, Y. and T.L. Steck, *Quantitation of the pool of cholesterol associated with acyl-CoA:cholesterol acyltransferase in human fibroblasts.* J. Biol. Chem., 1997. **272**: p. 13103-13108.

86. Lange, Y. and T.L. Steck, *Cholesterol homeostasis and the escape tendency (activity) of plasma membrane cholesterol.* Prog. Lipid Res., 2008. **47**: p. 319-332.

87. Lange, Y., et al., *Plasma membranes contain half the phospholipid and 90% of the cholesterol and sphingomyelin in cultured human fibroblasts.* J Biol Chem, 1989. **264**(7): p. 3786-93.

88. Lange, Y., et al., *Stability and stoichiometry of bilayer phospholipid-cholesterol complexes: relationship to cellular sterol distribution and homeostasis.* Biochemistry, 2013. **52**(40): p. 6950-9.

89. Lange, Y., J. Ye, and T.L. Steck, *Circulation of cholesterol between lysosomes and the plasma membrane.* J. Biol. Chem., 1998. **273**(30): p. 18915-18922.

90. Liscum, L. and J.R. Faust, *Low density lipoprotein (LDL)-mediated suppression of cholesterol synthesis and LDL uptake is defective in Niemann-Pick type C fibroblasts.* Journal of Biological Chemistry, 1987. **262**(35): p. 17002-17008.

91. Lu, F., et al., *Identification of NPC1 as the target of U18666A, an inhibitor of lysosomal cholesterol export and Ebola infection.* Elife, 2015. **4**.

92. Mahmood Hussain, M., *A proposed model for the assembly of chylomicrons.* Atherosclerosis, 2000. **148**(1): p. 1-15.

93. Mansbach, C.M. and S.A. Siddiqi, *The biogenesis of chylomicrons.* Annu Rev Physiol, 2010. **72**: p. 315-33.

94. McConnell, H. and A. Radhakrishnan, *Theory of the deuterium NMR of sterol-phospholipid membranes.* Proc Natl Acad Sci U S A, 2006. **103**(5): p. 1184-9.

95. Monod, J., J. Wyman, and J.P. Changeux, *ON THE NATURE OF ALLOSTERIC TRANSITIONS: A PLAUSIBLE MODEL.* J Mol Biol, 1965. **12**: p. 88-118.

96. Motamed, M., et al., *Identification of luminal Loop 1 of Scap protein as the sterol sensor that maintains cholesterol homeostasis.* J Biol Chem, 2011. **286**(20): p. 18002-18012.

97. Mouritsen, O.G. and M.J. Zuckermann, *What's so special about cholesterol?* Lipids, 2004. **39**(11): p. 1101-13.

98. Munro, S., *Lipid rafts: elusive or illusive ?* Cell, 2003. **115**: p. 377-388.

99. Nakamura, M., et al., *Interaction of Theta-toxin (Perfringolysin O), a cholesterol-binding cytolysin, with liposomal membranes: change in the aromatic side chains upon binding and insertion.* Biochemistry, 1995. **34**: p. 6513-6520.

100. Nakanishi, M., J.L. Goldstein, and M.S. Brown, *Multivalent control of 3-hydroxy-3-methylglutaryl coenzyme A reductase. Mevalonate-derived product inhibits translation of mRNA and accelerates degradation of enzyme.* J Biol Chem, 1988. **263**(18): p. 8929-37.

101. Naureckiene, S., et al., *Identification of HE1 as the second gene of Niemann-Pick C disease.* Science, 2000. **290**(5500): p. 2298-301.

102. Nelson, L.D., A.E. Johnson, and E. London, *How interaction of perfringolysin O with membranes is controlled by sterol structure, lipid structure, and physiological low pH.* J. Biol. Chem., 2008. **283**(8): p. 4632-4642.

103. Neufeld, E.B., et al., *Intracellular trafficking of cholesterol monitored with a cyclodextrin.* J Biol Chem, 1996. **271**(35): p. 21604-13.

104. Ohtani, Y., et al., *Differential effects of a-, b- and g-cyclodextrins on human erythrocytes.* Eur. J. Biochem., 1989. **186**: p. 17-22.

105. Ohvo-Rekilä, H., et al., *Cholesterol interactions with phospholipids in membranes.* Progress in Lipid Research, 2002. **41**(1): p. 66-97.

106. Ohvo, H. and J.P. Slotte, *Cyclodextrin-mediated removal of sterols from monolayers: Effects of sterol structure and phospholipids on desorption rate.* Biochemistry, 1996. **35**: p. 8018-8024.

107. Okamura, N., et al., *A porcine homolog of the major secretory protein of human epididymis, HE1, specifically binds cholesterol.* Biochim Biophys Acta, 1999. **1438**(3): p. 377-87.

108. Okonogi, T.M., A. Radhakrishnan, and H.M. McConnell, *Two fatty acids can replace one phospholipid in condensed complexes with cholesterol.* Biochim Biophys Acta, 2002. **1564**(1): p. 1-4.

109. Olsen, B.N., et al., *The structural basis of cholesterol accessibility in membranes.* Biophys J, 2013. **105**(8): p. 1838-47.

110. Ota, K., et al., *Membrane cholesterol and sphingomyelin, and ostreolysin A are obligatory for pore-formation by a MACPF/CDC-like pore-forming protein, pleurotolysin B.* Biochimie, 2013. **95**(10): p. 1855-64.

111. Pan, J.J., S. Tristram-Nagle, and J.F. Nagle, *Effect of cholesterol on structural and mechanical properties of membranes depends on lipid chain saturation.* Physical Review E, 2009. **80**(2): p. 12.

112. Pani, A., A. Mandas, and S. Dessi, *Cholesterol, Alzheimer's disease, prion disorders: a menage a trois?* Curr Drug Targets, 2010. **11**(8): p. 1018-31.

113. Pannu, P.S., S. Allahverdian, and G.A. Francis, *Oxysterol generation and liver X receptor-dependent reverse cholesterol transport: not all roads lead to Rome.* Mol Cell Endocrinol, 2013. **368**(1-2): p. 99-107.

114. Peters, C., et al., *The cholesterol membrane anchor of the Hedgehog protein confers stable membrane association to lipid-modified proteins.* Proc Natl Acad Sci U S A, 2004. **101**(23): p. 8531-6.

115. Phillips, M.C., W.J. Johnson, and G.H. Rothblat, *Mechanisms and consequences of cellular cholesterol exchange and transfer.* Biochim Biophys Acta, 1987. **906**(2): p. 223-76.

116. Polekhina, G., et al., *Insights into the action of the superfamily of cholesterol-dependent cytolysins from studies of intermedilysin.* Proc Natl Acad Sci U S A, 2005. **102**(3): p. 600-5.

117. Porter, J.A., K.E. Young, and P.A. Beachy, *Cholesterol modification of hedgehog signaling proteins in animal development.* Science, 1996. **274**(5285): p. 255-9.

118. Radhakrishnan, A., et al., *Switch-like control of SREBP-2 transport triggered by small changes in ER cholesterol: a delicate balance.* Cell Metab, 2008. **8**(6): p. 512-21.

119. Radhakrishnan, A., et al., *Sterol-regulated transport of SREBPs from endoplasmic reticulum to Golgi: oxysterols block transport by binding to Insig.* Proc Natl Acad Sci U S A, 2007. **104**(16): p. 6511-8.

120. Radhakrishnan, A. and H. McConnell, *Condensed complexes in vesicles containing cholesterol and phospholipids.* Proc Natl Acad Sci U S A, 2005. **102**(36): p. 12662-6.

121. Radhakrishnan, A. and H.M. McConnell, *Chemical activity of cholesterol in membranes.* Biochemistry, 2000. **39**(28): p. 8119-24.

122. Radhakrishnan, A., et al., *Direct binding of cholesterol to the purified membrane region of SCAP: mechanism for a sterol-sensing domain.* Mol Cell, 2004. **15**(2): p. 259-68.

123. Ramachandran, R., R.K. Tweten, and A.E. Johnson, *The domains of a cholesterol-dependent cytolysin undergo a major FRET-detected rearrangement during pore formation.* Proc Natl Acad Sci U S A, 2005. **102**(20): p. 7139-44.

124. Ratajczak, M.K., et al., *Ordered nanoclusters in lipid-cholesterol membranes.* Phys. Rev. Lett., 2009. **103**: p. 028103.

125. Rawson, R.B., et al., *Complementation Cloning of S2P, a Gene Encoding a Putative Metalloprotease Required for Intramembrane Cleavage of SREBPs.* Molecular Cell, 1997. **1**(1): p. 47-57.

126. Rebolj, K., et al., *Steroid structural requirements for interaction of ostreolysin, a lipid-raft binding cytolysin, with lipid monolayers and bilayers.* Biochimica et Biophysica Acta (BBA) - Biomembranes, 2006. **1758**(10): p. 1662-1670.

127. Redgrave, T., *Formation and metabolism of chylomicrons.* International review of physiology, 1982. **28**: p. 103-130.

128. Rossjohn, J., et al., *Structure of a cholesterol-binding, thiol-activated cytolysin and a model of its membrane form.* Cell, 1997. **89**: p. 685-692.

129. Russell, D.W., *Fifty years of advances in bile acid synthesis and metabolism.* J Lipid Res, 2009. **50 Suppl**: p. S120-5.

130. Sato, T.K., R.K. Tweten, and A.E. Johnson, *Disulfide-bond scanning reveals assembly state and beta-strand tilt angle of the PFO beta-barrel.* Nat Chem Biol, 2013. **9**(6): p. 383-9.

131. Scheek, S., M.S. Brown, and J.L. Goldstein, *Sphingomyelin depletion in cultured cells blocks proteolysis of sterol regulatory element binding proteins at site 1.* PNAS, 1997. **94**: p. 11179-11183.

132. Schoenheimer, R. and F. Breusch, *SYNTHESIS AND DESTRUCTION OF CHOLESTEROL IN THE ORGANISM.* Journal of Biological Chemistry, 1933. **103**(2): p. 439-448.

133. Schulz, T.A., et al., *Lipid-regulated sterol transfer between closely apposed membranes by oxysterol-binding protein homologues.* J Cell Biol, 2009. **187**(6): p. 889-903.

134. Sepcic, K., et al., *Ostreolysin, a pore-forming protein from the oyster mushroom, interacts specifically with membrane cholesterol-rich lipid domains.* FEBS Lett, 2004. **575**(1-3): p. 81-5.

135. Sever, N., et al., *Insig-dependent ubiquitination and degradation of mammalian 3-hydroxy-3-methylglutaryl-CoA reductase stimulated by sterols and geranylgeraniol.* J Biol Chem, 2003. **278**(52): p. 52479-90.

136. Sever, N., et al., *Accelerated degradation of HMG CoA reductase mediated by binding of insig-1 to its sterol-sensing domain.* Mol Cell, 2003. **11**(1): p. 25-33.

137. Sherrill, B.C. and J.M. Dietschy, *Characterization of the sinusoidal transport process responsible for uptake of chylomicrons by the liver.* Journal of Biological Chemistry, 1978. **253**(6): p. 1859-1867.

138. Shimada, Y., et al., *The C-terminal domain of perfringolysin O is an essential cholesterol-binding unit targeting to cholesterol-rich microdomains.* Eur J Biochem, 2002. **269**(24): p. 6195-203.

139. Silvius, J.R. and F. l'Heureux, *Fluorimetric evaluation of the affinities of isoprenylated peptides for lipid bilayers.* Biochemistry, 1994. **33**(10): p. 3014-22.

140. Simons, K. and J.L. Sampaio, *Membrane organization and lipid rafts.* Cold Spring Harb Perspect Biol, 2011. **3**(10): p. a004697.

141. Skocaj, M., et al., *Tracking cholesterol/sphingomyelin-rich membrane domains with the ostreolysin A-mCherry protein.* PLoS One, 2014. **9**(3): p. e92783.

142. Smith, J.R., et al., *Multiple sterol regulatory elements in promoter for hamster 3-hydroxy-3-methylglutaryl-coenzyme A synthase.* J Biol Chem, 1988. **263**(34): p. 18480-7.

143. Smith, J.R., et al., *Identification of nucleotides responsible for enhancer activity of sterol regulatory element in low density lipoprotein receptor gene.* J Biol Chem, 1990. **265**(4): p. 2306-10.

144. Sokol, J., et al., *Type C Niemann-Pick disease. Lysosomal accumulation and defective intracellular mobilization of low density lipoprotein cholesterol.* Journal of Biological Chemistry, 1988. **263**(7): p. 3411-3417.

145. Sokolov, A. and A. Radhakrishnan, *Accessibility of cholesterol in endoplasmic reticulum membranes and activation of SREBP-2 switch abruptly at a common cholesterol threshold.* J Biol Chem, 2010. **285**(38): p. 29480-90.

146. Song, Y., A.K. Kenworthy, and C.R. Sanders, *Cholesterol as a co-solvent and a ligand for membrane proteins.* Protein Science : A Publication of the Protein Society, 2014. **23**(1): p. 1-22.

147. Steinberg, D., *Hypercholesterolemia and inflammation in atherogenesis: two sides of the same coin.* Mol Nutr Food Res, 2005. **49**(11): p. 995-8.

148. Steinberg, D., *Thematic review series: the pathogenesis of atherosclerosis. An interpretive history of the cholesterol controversy, part V: the discovery of the statins and the end of the controversy.* J Lipid Res, 2006. **47**(7): p. 1339-51.

149. Sun, L.P., et al., *Sterol-regulated transport of SREBPs from endoplasmic reticulum to Golgi: Insig renders sorting signal in Scap inaccessible to COPII proteins.* PNAS, 2007. **104**(16): p. 6519-6526.

150. Szczesny, P., et al., *Extending the aerolysin family: from bacteria to vertebrates.* PLoS One, 2011. **6**(6): p. e20349.

151. Tilley, S.J., et al., *Structural basis of pore formation by the bacterial toxin pneumolysin.* Cell, 2005. **121**(2): p. 247-56.

152. Traversari, C., et al., *LXR-dependent and -independent effects of oxysterols on immunity and tumor growth.* Eur J Immunol, 2014. **44**(7): p. 1896-903.

153. Tso, P., M.B. Lindström, and B. Borgström, *Factors regulating the formation of chylomicrons and very-low-density lipoproteins by the rat small intestine.* Biochimica et Biophysica Acta (BBA) - Lipids and Lipid Metabolism, 1987. **922**(3): p. 304-313.

154. Tweten, R.K., *Cholesterol-dependent cytolysins, a family of versatile pore-forming toxins.* Infect Immun, 2005. **73**(10): p. 6199-209.

155. Umetani, M., *Re-adopting classical nuclear receptors by cholesterol metabolites.* J Steroid Biochem Mol Biol, 2016. **157**: p. 20-6.

156. Underwood, K.W., et al., *Evidence for a cholesterol transport pathway from lysosomes to endoplasmic reticulum that is independent of the plasma membrane.* J Biol Chem, 1998. **273**(7): p. 4266-74.

157. Van Blitterswijk, W.J., B.W. Van der Meer, and H. Hilkmann, *Quantitative contributions of cholesterol and the individual classes of phospholipids and their degree of fatty acyl (un)saturation to membrane fluidity measured by fluorescence polarization.* Biochemistry, 1987. **26**(6): p. 1746-1756.

158. Vanier, M.T., *Niemann-Pick disease type C.* Orphanet Journal of Rare Diseases, 2010. **5**: p. 16-16.

159. Veatch, S.L., K. Gawrisch, and S.L. Keller, *Closed-loop miscibility gap and quantitative tie-lines in ternary membranes containing diphytanoyl PC.* Biophys. J., 2006. **90**: p. 4428-4436.

160. Veatch, S.L., et al., *Liquid domains in vesicles investigated by NMR and fluorescence microscopy.* Biophys. J., 2004. **86**: p. 2910-2922.

161. Wang, M.L., et al., *Identification of surface residues on Niemann-Pick C2 essential for hydrophobic handoff of cholesterol to NPC1 in lysosomes.* Cell Metab, 2010. **12**(2): p. 166-73.

162. Xu, L., et al., *Crystal structure of cytotoxin protein suilysin from Streptococcus suis.* Protein Cell, 2010. **1**(1): p. 96-105.

163. Xu, S., et al., *Structural basis of sterol binding by NPC2, a lysosomal protein deficient in Niemann-Pick type C2 disease.* J Biol Chem, 2007. **282**(32): p. 23525-31.

164. Yabe, D., M.S. Brown, and J.L. Goldstein, *Insig-2, a second endoplasmic reticulum protein that binds SCAP and blocks export of sterol regulatory element-binding proteins.* Proc Natl Acad Sci U S A, 2002. **99**(20): p. 12753-8.

165. Yang, J., et al., *Identification of the acyltransferase that octanoylates ghrelin, an appetite-stimulating peptide hormone.* Cell, 2008. **132**(3): p. 387-396.

166. Yang, T., et al., *Crucial Step in Cholesterol Homeostasis: Sterols Promote Binding of SCAP to INSIG-1, a Membrane Protein that Facilitates Retention of SREBPs in ER.* Cell, 2002. **110**(4): p. 489-500.

167. Yang, T., J.L. Goldstein, and M.S. Brown, *Overexpression of membrane domain of SCAP prevents sterols from inhibiting SCAP.SREBP exit from endoplasmic reticulum.* J Biol Chem, 2000. **275**(38): p. 29881-6.

168. Zalipsky, S., *Chemistry of polyethylene glycol conjugates with biologically active molecules.* Advanced Drug Delivery Reviews, 1995. **16**(2–3): p. 157-182.

169. Zeng, X., et al., *A freely diffusible form of Sonic hedgehog mediates long-range signalling.* Nature, 2001. **411**(6838): p. 716-20.

170. Zheng, J., et al., *Ultrafast dynamics of solute-solvent complexation observed at thermal equilibrium in real time.* Science, 2005. **309**: p. 1338-1343.